

University of Texas at Arlington

MavMatrix

Bioengineering Dissertations

Department of Bioengineering

2022

An In vitro 3D Model to Investigate IOL: Posterior Lens Capsule Interactions on Lens Epithelial Cell Responses

Joyita Roy

Follow this and additional works at: https://mavmatrix.uta.edu/bioengineering_dissertations



Part of the [Biomedical Engineering and Bioengineering Commons](#)

Recommended Citation

Roy, Joyita, "An In vitro 3D Model to Investigate IOL: Posterior Lens Capsule Interactions on Lens Epithelial Cell Responses" (2022). *Bioengineering Dissertations*. 153.

https://mavmatrix.uta.edu/bioengineering_dissertations/153

This Dissertation is brought to you for free and open access by the Department of Bioengineering at MavMatrix. It has been accepted for inclusion in Bioengineering Dissertations by an authorized administrator of MavMatrix. For more information, please contact leah.mccurdy@uta.edu, erica.rousseau@uta.edu, vanessa.garrett@uta.edu.

An In vitro 3D Model to Investigate IOL: Posterior Lens Capsule
Interactions on Lens Epithelial Cell Responses

By Joyita Roy

A Dissertation Submitted to the Graduate School of the University of
Texas at Arlington in Partial Fulfillment of the Requirements for the
Degree of Doctor of Philosophy

Arlington, Texas

December 2022

Copyright © by Joyita Roy

All Rights Reserved

2022

The University of Texas at Arlington
DISSERTATION DEFENSE REPORT (DDR)

This report must be submitted to the Office of the Registrar, via email to gradteam@uta.edu, after the examination is administered regardless of the outcome of the defense. Students & advisors should consult the current Graduate Catalog for deadline dates applicable to the administration & report of the exam. The student must be enrolled in the term in which he/she takes the Dissertation Defense. An unconditional pass is required before degree can be conferred. In order to update a student from "passed with conditions" the Milestone Conditions Update form will need to be submitted.

Student: Roy Joyita Date of Examination: 12/01/2022
Last Name First Name

UTA ID: 1001644159 Program: PhD College/School: College of Engineering Dept: Bioengineering

Title of Dissertation: An in vitro 3D model to investigate IOL:posterior lens capsule interactions on lens epithelial cell responses

This is to report that the above-named student, under the direction of their committee, completed the Dissertation Defense with the following results

- Passed Unconditionally, the dissertation document and defense fully satisfy requirements for the doctoral degree.
- Passed, with following conditions that must be satisfied
- Failed, with permission to retake with these stipulations
- Failed, dismissed from the program

Name (typed)	Signature	Date (mm/dd/yyyy)
<u>Liping Tang</u> <small>Supervisor/Chair</small>	<u>Liping Tang</u> <small>Digitally signed by Liping Tang Date: 2022.12.01 12:26:46 -06'00'</small>	<u>12/1/2022</u>
<u>Ali Akinay</u> <small>Committee Member</small>	<u>Akinay, Ali</u> <small>Digitally signed by Akinay, Ali Date: 2022.12.01 13:55:32 -06'00'</small>	<u>12/1/2022</u>
<u>Chi-Chun Tsai</u> <small>Committee Member</small>	<u>Tsai, Chi-Chun</u> <small>Digitally signed by Tsai, Chi-Chun DN: cn=Tsai, Chi-Chun, o=PDF Internal Signing, ou=Alcon Vision, LLC Date: 2022.12.01 14:31:39 -06'00' Adobe Acrobat version: 2021.011.20039</small>	<u>12/1/2022</u>
<u>Kytai Nguyen</u> <small>Committee Member</small>	<u>Kytai T. Nguyen</u> <small>Digitally signed by Kytai T. Nguyen Date: 2022.12.01 15:45:38 -06'00'</small>	<u>12/1/2022</u>
<u>Jun Liao</u> <small>Committee Member</small>	<u>Jun Liao</u> <small>Digitally signed by Jun Liao DN: cn=Jun Liao, o=UTA, ou=gradteam@uta.edu, c=US Date: 2022.12.11 14:52:18 -06'00'</small>	<u>12/1/2022</u>
<u>George Alexandrakis</u> <small>Advisor/Coordinator</small>	<u>George Alexandrakis</u> <small>Digitally signed by George Alexandrakis Date: 2022.12.13 08:13:38 -06'00'</small>	<u>12/13/2022</u>
<u>Joyita Roy</u> <small>Student</small>	<u>Joyita Roy</u> <small>Digitally signed by Joyita Roy Date: 2022.12.12 19:50:13 -06'00'</small>	<u>12/1/2022</u>

DEDICATION

This dissertation is dedicated to my parents, who have always motivated and supported me to achieve my goals. Their blessings have been a source of constant encouragement to fulfill all my dreams.

ACKNOWLEDGEMENTS

First, I would like to thank my advisor and mentor, Dr. Liping Tang, for his invaluable support and guidance throughout the four years of my journey as a PhD student. From the very beginning, he taught me how to lead a project independently, while ensuring I had the support I needed to make constant progress. His immense knowledge in the field of tissue engineering and his excellent problem-solving skills were instrumental in helping me move forward and accomplish my goals. I would also like to thank all my committee members- Dr. Jun Liao, Dr. Kytai Nguyen, Dr. Ali Akinay, and Dr. Chi-Chun Tsai, for their key insights on my thesis. Their suggestions and guidance were essential in improving my research work and successfully completing my dissertation.

Next, I would like to extend my sincere appreciation for my entire project team and lab mates. I would specially like to thank Samira Izuagbe for her help with cell culture during the later years of my research. I will always be grateful to her for her dedication to the project and all the hard work she put in, without which this project would not have been the same. A special thanks to my undergraduate volunteer Sambriddhi Ghimire, for helping me with capsule fabrication and most of the groundwork. I would also like to thank the other members of my lab- Cynthia, Bhavya, Amjad, and Le, who have all helped me with my work at some point during my time in Dr. Tang's lab.

Last but not the least, I would like to acknowledge the immense support I got from my fiancé, Sidhartha, who understood my commitment to the project and patiently waited for me to finish my research.

TABLE OF CONTENTS

DEDICATION	iv
ACKNOWLEDGEMENTS	v
LIST OF FIGURES AND TABLES	ix
ABSTRACT	1
CHAPTER 1	4
Introduction and Rationales for Dissertation Research	5
1.1. Cataracts and PCO	5
1.2. Clinical PCO Performance of IOLs	5
1.3. Role of Lens Capsule	6
1.4. Role of IOL design and material properties	7
1.5. Role of ECM proteins affecting PCO potential	8
1.6. Lack of a suitable in vitro model	8
1.7. Rationale and Scientific Premise for Dissertation Research	10
CHAPTER 2	13
Effect of Time and Temperature-Dependent Changes of IOL Material Properties on IOL: Lens Capsule Interactions	14
2.1. Introduction	14
2.2. Materials and Methods	17
2.2.1. Intraocular Lenses	17
2.2.2. Fabrication of Simulated Lens Capsule	18
2.2.3. Characterization of simulated lens capsule	19
2.2.4. Adhesion force measurements	20
2.2.5. Surface hydrophilicity and roughness measurements	21
2.2.6. Visualize “cell” infiltration at the space between IOL and LC	22
2.2.7. Statistical Analyses	24
2.3. Results	25
2.3.1. Effect of temperature and incubation time on IOL: LC Adhesion Force....	25

2.3.2. Effect of temperature and hydration time on surface hydrophobicity	26
2.3.3. Effect of temperature and hydration time on surface roughness	28
2.3.4. Examination of “no space no cell” hypothesis in vitro.....	29
2.4. Discussion	30
2.5. Conclusions	36
CHAPTER 3	38
Role of Fibronectin and IOL surface modification in IOL: Lens Capsule Interactions	39
3.1. Introduction	39
3.2. Materials and Methods	42
3.2.1. Intraocular Lenses	42
3.2.2. Surface modification of acrylic foldable IOLs	43
3.2.3. Preparation of Simulated Lens Capsules	43
3.2.4. Surface characterization of various treated IOLs	44
3.2.5. Surface coating and Fibronectin adsorption	44
3.2.6. Statistical analyses	45
3.3. Results	
3.3.1. Effect of FN on IOL:LC adhesion force for acrylic foldable IOLs	46
3.3.2. Effect of FN on IOL:LC adhesion for different materials	47
3.3.3. Simulated cell infiltration for different IOL materials in presence of FN ..	49
3.3.4. Influence of surface coatings and FN on surface hydrophilicity	50
3.3.5. Effect of Surface Coatings on IOL: LC adhesion force	52
3.3.6. Simulated cell infiltration for acrylic foldable-DG IOLs	54
3.3.7. Relationship between IOL materials, adhesion force cell infiltration	55
3.4. Discussion	56
3.5. Conclusions	59
CHAPTER 4	61
A 3D In vitro Model for Assessing Intraocular Lens: Posterior Lens Capsule Interactions and their Influence on Lens Epithelial Cell Responses	62
4.1. Introduction	62

4.2. Materials and Methods	67
4.2.1. Intraocular Lenses	67
4.2.2. Fabrication and characterization of 3D simulated PLC	67
4.2.3. Adhesion Force Measurements.....	68
4.2.4. OCT Imaging of IOL: PLC Closure Mechanism	68
4.2.5. IOL: PLC Interface Barrier Testing	68
4.2.6. Assessment of IOL: PLC affinity on simulated LEC infiltration	69
4.2.7. Assessment of IOL: PLC affinity on LEC infiltration	69
4.2.8. Assessment of IOL: PLC affinity on LEC proliferation	70
4.2.9. Assessment of LEC metabolic activity at IOL: PLC interface.....	70
4.2.10. Statistical Analyses	70
4.3. Results	71
4.3.1. Physical interactions between IOLs and simulated PLC	71
4.3.2. The influence of IOL: PLC affinity on simulated cell infiltration	73
4.3.3. The influence of IOL: PLC affinity on LEC infiltration	73
4.3.4. The influence of IOL: PLC affinity on LEC proliferation	75
4.3.5. The influence of IOL: PLC affinity on LEC metabolic activity	76
4.4. Discussion	77
4.5. Conclusion	80
CHAPTER 5	81
Conclusions and Future Direction	82
5.1. Conclusions	82
5.2. Future Direction	83
REFERENCES	86
BIOGRAPHICAL INFORMATION	98

LIST OF FIGURES AND TABLES

Table 2.1. Comparison of material properties of the simulated lens capsule and the human lens capsule.

Figure 2.1. Mechanical Apparatus System Schematic (A) and Test Process Schematic (B).

Figure 2.2. Front view (A) and side view (B) photographs of the imaging system.

Figure 2.3. Imaging Test Process Schematic (A) of blue dextran dye occupying posterior side of IOL and on the periphery of the IOL: LC interface (B). The collected image(s) was analyzed to calculate the % of dye penetration in ImageJ software as shown below (C).

Figure 2.4. IOL: LC adhesion force for PMMA, silicone and acrylic foldable IOLs at different incubation time (0, 4 and 24 hours) and temperatures (21 °C and 37°C) (n = 10).

Figure 2.5. Change in surface contact angle as a function of incubation time and temperature. Contact angle measurements for PMMA, silicone and acrylic foldable test IOLs were carried out at 0 and 24 hours post hydration in BSS at different temperatures (21 °C and 37 °C) (n=10).

Figure 2.6. Change in surface Roughness as a function of incubation time and temperature in BSS. Surface Roughness measurement on PMMA, silicone and acrylic foldable test IOLs was carried out at 0 and 24 h post hydration in BSS at 21 °C and 37 °C for (n=10).

Figure 2.7. Photographs collected using the IOL: LC imaging system depicting visualization of dye penetration at IOL: LC interface at 37°C. (A) Representative images and percentage of dye coverage at IOL: LC interface for PMMA, silicone and acrylic foldable IOLs. (n = 10) (B) Paired t-test analysis of changes in dye penetration percentages by compared with 0 hour of the same IOL materials.

Figure 2.8. Percentage change in average IOL: LC adhesion force, contact angle, surface roughness and dye penetration for PMMA, silicone and acrylic foldable IOLs at 37°C.

Figure 3.1. IOL: PC adhesion force as a function of fibronectin concentration after incubation of acrylic foldable IOLs @ 37°C for 24 hours. Data presented as mean \pm SD (N=10).

Figure 3.2. IOL: PC adhesion force of different IOL materials – Acrylic foldable, PMMA and Silicone - with either BSS (as control) or fibronectin (FN) solution (2 uL of 1 mg/mL FN in BSS) at IOL: PC interface and then incubated at 37°C for 24 hours. Data presented as mean \pm SD (N=10).

Figure 3.3. Simulated cell infiltration study for different IOL materials with either BSS (as control) or fibronectin (FN) solution (2 uL of 1 mg/mL FN in BSS) at IOL: PC interface and then incubated at 37°C for 24 hours. Data presented as mean \pm SD (N=10). (A) Representative images of simulated cell free regions for PMMA, silicone and acrylic foldable IOLs. (B) Paired t-test analysis of changes in simulated cell free areas at IOL: PC interface with and without the presence of FN (N=10).

Figure 3.4. Surface contact angle of acrylic foldable and diglyme modified acrylic foldable (DG-acrylic foldable) incubated with either BSS (as control) or fibronectin (FN) solution (2 uL of 1 mg/mL FN in BSS) at IOL: PC interface for 24 hours @ 37°C. Data presented as mean \pm SD (N=10).

Figure 3.5. Influence of surface coatings on IOL: PC adhesion force of acrylic foldable and DG-modified acrylic foldable IOLs after incubated for different periods of time (0 and 24 hours) @ 37 °C.

Figure 3.6. IOL: PC adhesion force of acrylic foldable and DG-modified acrylic foldable IOLs with or without the presence of FN (2 uL of 1 mg/mL FN in BSS vs. BSS) at IOL: PC interface @ 37°C for 24 hours.

Figure 3.7. (A) Extent of simulated cell infiltration at IOL: PC interface with or without the presence of FN (2 uL of 1 mg/mL FN in BSS vs. BSS) at IOL: PC interface incubated for 24 hours. Data presented as mean \pm SD (N=10). (B) Paired t-test analysis of changes in the extent of simulated cell (dye) infiltration in different conditions.

Figure 3.8. Relationship between the IOL: PC adhesion force and cell infiltration at IOL: PC interface among all tested IOLs, including PMMA, silicone, acrylic foldable and DG-acrylic foldable with and without the presence of fibronectin (FN) after 24h of incubation at 37°C.

Figure 4.1. A schematic for “No Space, No Cell” hypothesis.

Table 4.1. Quantitative evidence supporting the “No space, no cell” hypothesis. Distance at IOL: PLC interface is directly proportional to PCO incidence.

Table 4.2. Dimensions of the native posterior lens capsule.

Table 4.3. Potential Curvatures for simulated PLC and their dimensions measured using OCT.

Figure 4.2. Physical interactions between IOL and simulated PLCs. A) Adhesion force of different IOLs to the simulated PLC. B) The distance between the IOL and simulated PLC.

Figure 4.3. The rate of IOL: PLC closure. A) Distance of IOLs from simulated PLC. B) Percent of IOLs in direct contact with simulated PLC. C) Area between IOLs and simulated PLC. Statistical analysis was done using One-way ANOVA at each timepoint with Tukey’s post-hoc test and an alpha of 0.05. ‘*’ represents statistical significance of Acrylic vs PMMA, ‘#’

represents statistical significance of Acrylic vs Silicone, '\$' represents statistical significance of Silicone vs PMMA.

Figure 4.4. Evaluation of IOL: PLC closure by infiltration of a contrast enhancer. A) Images of contrast agent infiltration in Acrylic, PMMA and silicone IOLs. B) Percentage area at IOL: PLC interface infiltrated by contrast agent.

Figure 4.5. Evaluation of IOL: PLC closure's influence on LEC infiltration. A) OCT images showing LEC's attempt to infiltrate the IOL: PLC interface. B) Quantitative representation of LEC infiltration from the simulated PLC to the IOL: PLC interface. (Dotted box represents area covered by IOL).

Figure 4.6. Evaluation of LEC proliferation at IOL: PLC interface. Cell density at IOL: PLC interface over time with microscope images of ROIs of LECs in Acrylic, PMMA and Silicone groups at day 5.

Figure 4.7. Metabolic activity of LECs at the IOL: PLC interface. A) Images of LECs stained with ki-67 antibody and counterstained with DAPI B) Percentage of metabolically active cells.

ABSTRACT

Posterior Capsule Opacification (PCO) is the most common complication associated with Intraocular Lens (IOL) implantation. The disease is caused by the infiltration and proliferation of Lens Epithelial Cells (LEC) into the interface between the IOL and Posterior Lens Capsule (PLC). The severity of these cell responses depends on a lot of factors like the IOL design, IOL material, and interaction between the IOL and the posterior lens capsule. While some studies have also shown that adsorption of certain proteins present in the PLC, like fibronectin, may affect IOL-induced PCO in the clinical setting, the mechanism governing such interactions is not totally understood. Based on the assumption that the interactions between an IOL and the PLC, along with the aforementioned factors, may influence the extent of PCO formation, a new *in vitro* model was developed to quantify the adhesion force of an IOL to simulated PLC using a custom-designed micro-force tester.

For Aim 1, using the micro-force testing system, we examined the influence of temperature (room temperature vs. body temperature) and incubation time (0 vs. 24 hours) on the adhesion force between IOLs and PLCs. The results show that, in line with clinical observations of PCO incidence, the adhesion force increased at body temperature and with increase in incubation time in the following order, Acrylic foldable IOLs > Silicone IOLs > PMMA IOLs. By examining the changes of surface properties as a function of temperature and incubation time, we found that acrylic foldable IOLs showed the largest increase in their hydrophilicity and reported the lowest surface roughness in comparison to other IOL groups. Coincidentally, using a newly established macromolecular dye imaging system to simulate cell migration between IOLs and PLC, we observed that the amount of macromolecular dye infiltration between IOLs and PLCs was in the following order: PMMA IOLs > Silicone IOLs > Acrylic foldable IOLs. These results support a

new potential mechanism that body temperature, incubation time, surface hydrophilicity and smoothness of IOLs greatly contribute to their tight binding to PLCs and such tight binding may lead to reduced IOL: PLC space, cell infiltration, and thus PCO formation.

In Aim 2, a study was designed to assess whether fibronectin adsorption and IOL material properties would impact the IOL: PLC adhesion force and cell infiltration using a PCO predictive *in vitro* model and a macromolecular dye imaging model, respectively. Our results showed that fibronectin adsorption significantly increased the adhesion forces and reduced simulated cell infiltration between acrylic foldable IOLs and the PLC at physiological temperature in comparison to fibronectin-free controls. This fibronectin mediated strong IOL: PLC bond may be contributing to low PCO rates in the clinic for acrylic foldable IOLs. In addition, acrylic foldable IOLs coated with Di(ethylene glycol) (Diglyme), a hydrophilic coating known to reduce protein adsorption, was tested for its ability to alter adhesion force and cell infiltration. We observed that IOLs coated with Diglyme coating greatly reduced surface hydrophobicity and fibronectin adsorption of acrylic foldable IOLs. Furthermore, Diglyme coated IOLs showed significantly reduced adhesion force and increased simulated cell infiltration at the IOL: PLC interface. The overall results support the hypothesis that IOL surface properties and their ability to adsorb fibronectin may have great impact on the IOL: PLC adhesion force. A tight binding between IOLs and PLC may contribute to the reduction of cell infiltration and thus the PCO incidence rate in the clinic.

For Aim 3, the “No space, no cell” hypothesis was studied, which states that an IOL with maximum contact with the PLC will leave no space for LEC infiltration and proliferation, has been used to explain this phenomenon. Although this hypothesis has been indirectly supported by *in vivo* studies, it has not been directly tested because current *in vitro* models lack the

appropriate geometry to mimic the in vivo IOL and human PLC closure mechanism. Therefore, a 3D simulated PLC with similar geometry to the human PLC was developed to test the “No space, no cell” hypothesis. Optical Coherence Tomography (OCT) imaging showed the simulated PLC was able to reproduce in vivo closure mechanism. In addition, the “No space, no cell” hypothesis was directly tested by monitoring the infiltration and proliferation of LECs at the IOL: PLC interface. As expected, Acrylic IOL prevented the infiltration and proliferation of LECs while PMMA and Silicone IOLs permitted LEC infiltration and proliferation. Additionally, Acrylic IOL’s strong affinity for the simulated PLC induced the contact inhibition of LECs present at the interface. Overall, the simulated PLC was able to mimic IOL and human PLC interactions and the results supported the “No space, no cell” hypothesis.

Keywords: Intraocular lens, posterior lens capsule, posterior capsule opacification, adhesion force, 3D in vitro model, gelatin, lens epithelial cells, fibronectin, optical coherence tomography.

CHAPTER 1

Introduction and Rationales for Dissertation Research

1.1 Cataracts and PCO

Cataract is the second most common cause of blindness in the world after age-related macular degeneration affecting ~ 27 million people in the United States alone (Pérez-Vives, 2018a). Currently, cataracts are usually treated using surgical methods, which involves removal of the cataractous lens, followed by implantation of an artificial intraocular lens (IOL) (Eldred et al., 2019a). This surgery initially improves impaired vision, but postoperative complications is commonly seen in some patients due to development of Posterior Capsule Opacification (PCO) which often leads to secondary vision loss over time (Konopińska et al., 2021a). PCO not only reduces the quality of vision, but also causes quantitative visual disturbances, which further leads to a reduced contrast sensitivity and halo effect in vision (J Gonzalez-Martin-Moro and J J Gonzalez-Lopez, 2015). It is believed that the interaction between the posterior surface of the IOL with the posterior lens capsule plays a crucial role in the pathogenesis of PCO (Jaitli et al., 2021b; Katayama et al., 2007b; Linnola, 1997a; Linnola et al., 2003a, 2000a; Oshika et al., 1998a; Pérez-Vives, 2018a; Versura, 1999a; I. M. Wormstone et al., 2021). Over the last two decades, numerous research efforts have been made to study the interaction between the IOL and the human posterior capsule to reduce the progression of PCO, but the mechanism of PCO occurrence is not clearly understood, which makes it difficult for the leading IOL manufacturing companies like Alcon Research LLC, Hoya Corporation, Allergan, Abbott Medical Optics, etc. to develop biocompatible IOLs which might inhibit the development of PCO post cataract surgery.

1.2 Clinical PCO performance of IOLs

Several research attempts have been conducted to study the clinical PCO performance of IOLs (Oshika et al., 1996; Rönbeck et al., 2009a; Rönbeck and Kugelberg, 2014a; Ursell et al., 1998a; Wejde et al., 2003a). Some of the early studies date back to the nineties which focused on assessing the PCO potential in different IOL materials and designs like plate-haptic silicone (Artaria et al., 1994), three-piece prolene (Cumming and Ritter, 1994), sulcus-fixated silicone (Shepherd, 1989), hydrogels (Noble et al., 1990), and soft acrylics (Oshika et al., 1996). The data collected from these clinical studies showed that the lowest incidence of PCO was found in plate-haptic silicone IOLs (~ 1.1 % at 23 months) followed by PMMA (~7.9% at 24 months), hydrogels (~8% at 20 months) and then soft acrylics (~11.1 % @ 24 months) (Chehade and Elder, 1997). As the technology in cataract surgery improved, the small incision technique influenced the development of foldable IOL materials, which led to the launch of foldable hydrophobic acrylic materials in the mid-nineties (Ursell et al., 1998a, 1997). Acrylics, along with silicone and PMMA materials became one of the most widely used IOLs and extensive research began to assess the clinical PCO performance of those IOL materials.

1.3 Role of Lens Capsule

The human lens capsule is a thick basement membrane comprising collagen type IV-laminin networks bound by nidogen, perlecan, collagen type XVIII, and other proteoglycans (Danysh and Duncan, 2009a). The lens capsule surrounds the eye lens to provide structure and protection, while its individual ECM components interact with LECs to partake in signaling pathways governing LEC growth, migration, and proliferation. Upon interaction with matrix metalloproteinases (MMPs), the lens capsule releases growth factors, such as TGF- β , FGF-2, and PDGF, to help remodel the capsule's ECM composition and ensure normal signaling activity and

development of the lens (FW, 1996). In a diseased state, such as a cataract, unregulated release of growth factors may alter the normal ECM composition of the capsule and lead to excessive signaling activity, and subsequently, activation of previously dormant LECs at the anterior and equator of the capsule. Excess LECs may then immigrate, proliferate, and produce ECM under the IOL, resulting in PCO formation (Saika et al., 1995).

1.4 Role of IOL design and material properties

The material, shape, haptic design, and surface chemistry of IOLs affect its performance after implantation (Bellucci, 2013; Cooksley et al., 2021a; Li et al., 2013a). PMMA IOLs were first used to replace diseased lenses with tolerable results. However, over time, its susceptibility to PCO formation and rigidity outweighed its advantages and soon other materials such as silicone and acrylic were preferred (Bellucci, 2013; Cooksley et al., 2021a). Acrylic IOLs are desirable for their good flexibility, biocompatibility, and adhesion to the capsular bag. Although studies have shown they promote cell adhesion, PCO occurrence is still the lowest among the three major materials (PMMA, silicone, acrylic) (Jaitli et al., 2021b). Silicone IOLs have better performance than PMMA for its low cell deposition and flexibility but because of its low adhesion to the capsular bag, it cannot achieve a barrier effect and thus impede its ability at reducing PCO formation (Cooksley et al., 2021a).

Studies have shown that IOLs with square edges can prevent cell infiltration because of the creation of a barrier and, for some square shaped IOLs, a capsular bend. However, round IOLs produce poor results regardless of the material used to create the IOL (Cooksley et al., 2021a). Besides material and shape, the surface chemistry, specifically wettability also influences PCO formation. While there is controversy on whether hydrophobic or hydrophilic IOLs have better

clinical outcomes, a study carried out with square edge IOLs shows that hydrophobic IOLs developed less PCO occurrence in 1-yr and 2-yr follow-ups than hydrophilic ones (Li et al., 2013a). Another factor of IOL design with an influence on PCO formation is the design of the haptics. Studies show that although one-piece IOLs have greater stability in the capsular bag, they have a slightly higher PCO occurrence (Bellucci, 2013).

1.5 Role of ECM proteins affecting PCO potential

ECM proteins can act as mediators of IOL adhesion, accumulate between the PC and IOL, and play an important role in PCO formation (Saika et al., 1993a; S. Saika, 1997a). Different ECM components present in the lens capsule include laminin, vitronectin, fibronectin and perlecan. A study showed that laminin and vitronectin only present near the fibrotic tissue, mostly on the anterior surface of the lens capsule, whereas fibronectin was present on the PC, which contributed to the sandwich theory (Linnola, 1997a; Linnola et al., 2003a, 2000e, 2000a). Fibronectin, one of the major components of ECM in the PC, has been observed on the posterior surface of IOLs post cataract surgery(Linnola et al., 2000a). It has been suggested that the accumulation of fibronectin is responsible for the immigration and proliferation of LECs and then PCO formation at the interface between IOL and PC (Shimizu et al., 1997b; Sottile et al., 2007b). It has been suggested that adding fibronectin to the lens capsule prior to implanting the IOL may improve IOL: PC binding, leaving no space for the LECs to grow and produce more ECM (Linnola et al., 2000a). However, the potential influence of ECM proteins on IOL: PLC interactions is not totally understood.

1.6 Lack of a suitable in vitro model

For the past 40 years, intensive research efforts have been placed on the development of IOLs with low PCO potential by changing the IOL design, including material, surface modification, optic edge design, and haptic design. Despite of early success, significant improvement of IOL outcome in recent years is limited. The lack of suitable *in vitro* and *in vivo* models to simulate IOL: PC interactions and to assess PCO potential is at least partially responsible for such a slow evolvement. Briefly, cell culture *in vitro* models are commonly used to assess the extent of LEC proliferation, collagenous tissue growth and ECM production on both the IOL and the capsule (Linnola et al., 2000a; Oshika et al., 1996). The growth of LECs, and adhesion of various ECM proteins on different IOL materials have also been conducted to assess the influence of material properties on PCO (Linnola et al., 2003a; Oshika et al., 1998a). However, such models have many drawbacks. First, the current *in vitro* models are established on a flat platform, such as culture plates, collagen membrane, or PDMS films (Kwon et al., 2017). These models cannot be used to test real IOLs with different physical design and to simulate 3D interactions between IOLs and lens capsule. In one study to investigate the “no space, no cell” hypothesis, they placed weights on the IOL to achieve an adhesion of the IOL to the *in vitro* PC like *in vivo* conditions (Mencucci et al., 2015a). This may skew results because of external forces that are not present *in vivo*. Rabbit *in vivo* model has widely been used to analyze the PCO performance of IOL material (Aliancy et al., 2018; Wormstone and Eldred, 2016a). Although such a model can assess the extent of foreign body reactions and IOL-mediated PCO formation (Aliancy et al., 2018), these models have many limitations. First, the model is expensive, time consuming and cannot successfully predict the IOL performance in human. Second, the surgical techniques involving a cataract surgery also create variability, and the observed capsular bag shrinking and PCO rates in rabbit models do not match the human response (Raj et al., 2007). Third, rabbits often trigger

significantly stronger proliferation of residual LECs and foreign body reactions to IOL implantation than human patients (Wormstone and Eldred, 2016a), which makes the model less suitable for simulating differential PCO responses to different lens materials. On the other hand, rabbit LECs are more resistant to stress compared to human LECs, i.e., rabbit models are prone to greater PCO formation (Werner et al., 2004). Fourth, since treatments that may not significantly reduce PCO in the rabbit model could still reduce PCO in humans, treatments that are effective for humans might be overlooked. Last, because of inherent variability associated with surgical technique and post-op care, the observed PCO rate & bag shrinking/wrinkling may differ, leading to confounding results (M et al., 2007). These drawbacks significantly limit the potential of using the rabbit in vivo model to predict PCO responses in human. Therefore, the focus of this investigation is on the development of an in vitro model to simulate IOL: PC interactions and to assess IOL's PCO potential.

1.7. Rationale and Scientific Premise for Dissertation Research

Several hypotheses have been proposed to show the causative effect of IOL characteristics on PCO occurrence. IOL surface chemistry is believed to play a major role in PCO formation, by altering cell and protein adhesion (Lin et al., 2017; Mareo and Rotner, 1989; Xia et al., 2021). IOL shape and edge are believed to influence cell migration between the IOL-PC interface. For example, 360° sharp edge IOLs have been shown to inhibit cell infiltration by creating a capsular bend on the PC, whereas cells freely immigrate into IOLs with round edges (Nishi et al., 2004a). The 'no space, no cell' hypothesis suggests that strong adhesion between the IOL and PC would reduce the space available for buildup of LECs and ECM proteins, hence reducing the incidence of PCO (Linnola, 1997a; Pearlstein et al., 1988a). Coincidentally, IOLs with low PCO

incidence—such as hydrophobic acrylic IOLs (Ursell et al., 1998a; Wejde et al., 2003a) have tight binding to the capsular bag (Katayama et al., 2007b; Oshika et al., 1998a, 1996) while IOLs with high PCO incidence—such as PMMA IOLs (Ursell et al., 1998a; Wejde et al., 2003a) have poor binding to the lens capsule *in vitro* (Linnola et al., 2003a).

To extensively study the effect of characteristics of different IOLs affecting the occurrence of PCO, we developed an *in vitro* 3D model to allow investigation of IOL: PC interactions to 1) uncover how PC physical and biological properties would influence their interactions with IOLs, 2) analyze how PC:IOL interactions would influence on LEC behavior and responses; 3) study how IOL physical and chemical properties would influence the PC:IOL adhesion force and LEC reactions; and 4) provide an effective *in vitro* model to simulate IOL:LEC:PC interactions and to assess IOLs' PCO potential. Specifically, simulated PCs were be fabricated to mimic PC properties. By correlating the results from this 3D system and clinical findings, this work has helped to determine the critical factor(s) and microenvironment essential for developing IOL-mediated PCO.

In **Aim 1**, the effect of time and temperature dependent IOL material properties was observed in IOL: PC interactions, using the *in vitro* model. The simulated PC was fabricated using denatured collagen (gelatin) cross-linked with glutaraldehyde and was optimized to mimic the physical and mechanical properties of the human PC (Jaitli and Roy et al., 2021a). The simulated PC was created using the posterior surface of IOL, resulting in a capsule having the exact same geometry of the IOL's posterior curvature.

In **Aim 2**, using the same micro-force tester system, the role of fibronectin and IOL surface modifications were observed by testing the adhesion force between the IOL and the simulated PC. This study showed that fibronectin, as an important ECM protein in the human PC, might

affect cell adhesion, proliferation and the overall PCO performance in the gelatin based simulated capsules (Jaitli and Roy et al., 2022a).

In **Aim 3**, the 3D model was further improved by incorporating lens epithelial cells, which allowed us to decipher the processes governing the pathogenesis of PCO. The movement of LECs into the IOL: PC interface was deeply studied by analyzing the cell proliferation and infiltration over time and the IOL: PC interaction in the presence of cells gave us a better outlook at understanding the PCO occurrence clinically.

CHAPTER 2

Effect of Time and Temperature-Dependent Changes of IOL Material Properties on IOL: Lens Capsule Interactions

2.1 Introduction

Cataract is the second most common cause of blindness in the world after age-related macular degeneration affecting ~ 27 million people in the United States alone (Pérez-Vives, 2018b). At present, cataract induced visual impairment is treated by surgical removal of the cataractous lens and implantation of an artificial Intraocular Lens (IOL) (Eldred et al., 2019b). While surgical intervention followed by IOL implantation initially restores vision in patients, some patients develop Posterior Capsule Opacification (PCO) leading to secondary vision loss. It is generally believed that the interaction of an implanted IOL with the lens capsule plays a pivotal role in affecting the path of PCO progression (Jaitli et al., 2021; Nibourg et al., 2015; Oshika et al., 1998a; Pérez-Vives, 2018; Wormstone, 2020). While the adherence and then proliferation of residual lens epithelial cells (LECs) onto the implanted IOL may proliferate at the IOL: Lens capsule (LC) interface and eventually determine the extent of PCO formation (Eldred et al., 2019b; Huang et al., 2010; Linnola, 1997b; Nibourg et al., 2015; Nishi et al., 2004b; Oshika et al., 1998c; Pérez-Vives, 2018b; Vasavada and Praveen, 2014; Versura, 1999b; Wormstone, 2020; Wormstone and Eldred, 2016b), the influence of IOL properties and their interactions with LCs on PCO pathogenesis are still not clearly understood (Cheng et al., 2007; Findl et al., 2010; Hyeon et al., 2007; Pérez-Vives, 2018b) .

To find the answer, many *in vitro* models have been established. Specifically, several cell culture models have been used to access the extent of LEC proliferation, collagenous tissue growth and ECM components on both the IOL and the capsule ECM coated surfaces (Linnola et al., 2000b). While these studies have produced a lot of useful information, these models cannot be used to simulate the 3D interactions between the lens capsule and IOLs. While *in vitro* studies have been able to study the influence of IOL material chemical, physical, and adhesion

properties on their PCO performance, such models and predications are often unreliable. For instance, Oshika et al's study to measure adhesion forces of PMMA, silicone and acrylic foldable IOLs with flat bovine collagen sheets *in vitro* provided useful information about the adhesion characteristics of these biomaterials (Oshika et al., 1998b). However, the absence of a LC (or a simulated mold) that mimics the mechanical geometry of the capsule questions the validity of the data to draw clinically relevant conclusions. To fill the gap, a human capsular bag model, which uses lens capsule isolated from human cadaver eyes, has been used to study the interactions between IOLs and lens capsule during the shrink wrapping process (Dawes et al., 2012a; Eldred et al., 2019b, 2014; I. Michael Wormstone et al., 2021a; Wormstone, 2020; Wormstone and Eldred, 2016c). The capsular bag model offers a valuable clinically relevant tool to assess IOL capsule interactions (Dawes et al., 2012; Eldred et al., 2019, 2014; Wormstone, 2020; Wormstone and Eldred, 2016b). Despite its strengths, the human capsular bag model is still limited by tissue availability. Also to the best of our knowledge, the quantitative assessment of adhesion force/interactions has not been performed in the capsular bag model. To overcome such limitations, we have recently created a new *in vitro* 3D system to assess the adhesion force between an IOL and a simulated LC. This *in vitro* model utilized simulated LCs that were fabricated by imprinting IOLs onto molten gelatin to create simulated three dimensional (3D) LCs with curvature resembling the bag-like structure that collapses on the IOL post implantation (Jaitli et al., 2021c). This model may serve as a new and alternative system to evaluate the interactions between IOLs and LCs.

Several physical and chemical properties of IOLs, such as surface hydrophobicity, adhesiveness and posterior edge geometry, have been known to influence the rate of PCO formation (Boulton and Saxby, 1998)(Katayama et al., 2007c)(Kim et al., 2001)(Linnola et al., 2003, 2003, 2000b, 2000a)(Linnola et al., 2003, 2000a) (Oshika et al., 1998c)(Ursell et al., 1998) (Versura, 1999b)(Xu et al., 2016a, 2016b). For example, a study found that the PCO rate of three different

acrylic IOL materials was inversely proportional to their adhesiveness (Katayama et al., 2007c). Studies have also shown that a sharp posterior optic edge may create a barrier effect to suppress the migration of LECs and thus the pathogenesis of IOL induced PCO (Buehl et al., 2005) (Buehl et al., 2005; Haripriya et al., 2017; Nishi, 1999a; Nishi et al., 2000; Wormstone, 2020; Wormstone and Eldred, 2016c). Furthermore, the adhesiveness or “tackiness” of IOL materials has also been shown to influence the rate of PCO formation. Results have found that IOLs with high adhesiveness may bind tightly to lens capsule and indirectly suppress the migration of lens epithelial cells and thus reduce the rate of PCO formation (Oshika et al., 1998c). In an attempt to answer some of the above questions, intensive research efforts have been placed in this field. Unfortunately, many of these results are contradicting with each other. Coincidentally, many of these studies were carried out at different conditions, such as study temperature and incubation time. For example, Nagata conducted a study to measure the adhesive force of both Acrysof and PMMA IOLs at 37 °C but only tested adhesion of these IOLs after 1 minute incubation with a collagen film (Nagata et al., 1998). Further, Oshika’s *in vitro* study to assess adhesion of different IOL materials with collagen was conducted at 22 °C with adhesion force measured after 30 seconds of incubation (Oshika et al., 1998a). Predicate studies aimed at characterizing the glistening formation and optical properties of IOLs have shown a strong relationship with temperature and environmental conditions. Shiba et al. observed different rates of glistening formation in the Acrysof lens as a function of temperature and soak times (Shiba et al., 2003). Further, it is well established that the optical properties of IOLs such as spherical power, astigmatism and spherical aberration vary as a function of material temperature and surrounding medium (Walker et al., 2014). Thus, to assess the influence of experimental conditions on the interaction between IOLs and LCs, this study was carried out to examine the influence of

incubation time (0 vs 24 hours) and temperature (21 °C vs. 37 °C) on the adhesion force between LCs and three commonly used IOLs (hydrophobic acrylic foldable, PMMA and Silicone IOLs). We also examined whether and how body temperature may affect the surface properties of different IOL materials by conducting hydrophilicity and surface roughness measurements of these IOLs. Last, to indirectly test the “No space, No cell” hypothesis (Ursell et al., 1998b), a novel imaging technique was developed to determine whether the high adhesion force would lead to reduced macromolecule dye infiltration between the LC and IOLs.

2.2 Materials and Methods

2.2.1. Intraocular Lenses

IOLs fabricated from three types of materials – Hydrophobic acrylic foldable (hereafter referred to as ‘acrylic foldable’), PMMA and Silicone were utilized in this study. The single piece acrylic foldable IOLs had a 6.0 mm biconvex optic, a sharp rectangular posterior edge and planar haptics with an overall length of 13.0 mm (Alcon’s SN60WF, Alcon Research, Fort Worth, Texas) with a dioptric power of 21.0D. The PMMA group were single piece IOLs with a 5.5 mm PMMA optic, round posterior edge and multiflex haptics with an overall length of 13.0 mm (Alcon’s MTA4U0, Alcon Research, Fort Worth, Texas) with a dioptric power of 23.5D. The Silicone group comprised of three-piece posterior chamber biconvex silicone 6.0 mm optics that had a round edged profile and blue PMMA mod C haptics with an overall length of 13.0 mm (Allergan’s AMO Array SA40N, Allergan Inc, Irvine, California) with dioptric powers between 10.0 D and 26.0 D. ‘Mod C Haptics’ is the term that describes the haptic configuration of the IOL which is listed as ‘Modified-C’ in the technical specifications of this IOL. This information can be found on the package document and its directions for use (DFU) of this commercially

available IOL product. The term ‘Mod C’ is an acronym used by the manufacturer to describe the configuration of the haptic portion of this IOL that the authors assume refers to the shape of the haptic loop which looks similar to the alphabet ‘C’. These haptics were fabricated from blue polypropylene monofilament or blue core polymethylmethacrylate (PMMA) monofilament material.

2.2.2 Fabrication of simulated lens capsule

Simulated LCs were created to possess a spherical cup shaped structure that closely mimics the morphology, structure and mechanical integrity of the human capsular bag (Jaitli et al, 2021). To better mimic the mechanical strength of the LCs, simulated LCs were gently crosslinked with glutaraldehyde using previously published crosslinking method (Dardelle et al., 2011a). The modified procedure is described as follows. Briefly, simulated LCs were fabricated using high strength gelatin from porcine skin (Sigma-Aldrich, #48724, 240-270 g Bloom gel strength). A 10% gelatin solution was dissolved and stirred in de-ionized water at 40 °C for 10 minutes. To simulate real LCs which possess high mechanical strength and withstand high temperature, the solution was then crosslinked with 0.25% w/v glutaraldehyde solution (Sigma Aldrich, #G6257, grade II, 25% in water) as established earlier (Dardelle et al., 2011). The prepared solution was poured into acrylic petri-dishes immediately prior to the placement of IOLs. Next, IOLs with haptics intact were taped onto small thin circular lightweight support materials to ensure the IOL stayed afloat through the solidification process at 4 °C for 1 hour. By gently peeling the IOLs from the gelatin surfaces with the help of thin forceps, a simulated lens capsule mold with a geometry identical to the posterior surface of the lens was created. To minimize variability potentially resulting from different IOL geometries, every capsule was custom built using the test IOL itself. Further, the concentration of cross-linker was optimized by assessing the potential

influence of different concentrations on the surface adhesiveness and the stability of the simulated capsules at body temperatures.

2.2.3. Characterization of simulated lens capsule

Uniaxial testing was performed on the crosslinked gelatin mold specimens that were dissected into 10 thin rectangular strips with Length: 35mm, Width: 6mm, and Thickness: 5.15-6.37 mm. All uniaxial tensile testing was performed using a universal mechanical testing system (TestResources, MN) as described earlier (Weed et al., 2012). Briefly, uniaxial testing was performed at a ramping speed of 25 mm/min until fracture was observed. The stress-strain curve showed an overall linear trend and the elastic modulus was estimated using linear regression. For all samples, engineering stress was calculated by normalizing the applied force to the original cross-sectional area, and engineering strain was calculated by normalizing the amount of specimen deformation to the initial gauge length. To verify that the simulated lens capsules possessed material properties similar to the human capsule, the gelatin capsule's material properties were characterized and compared to the properties of the human capsule (Danysh and Duncan, 2009b); (Ziebarth et al., 2011). The average elastic modulus of the specimens was observed to be 0.023 ± 0.005 N/mm² and their average ultimate strength was observed to be 0.021 ± 0.002 N/mm². A comparison of the material and mechanical properties of the simulated capsules and the human lens capsule has been summarized in Table 2.1.

Properties	Human Lens capsule	Simulated Lens Capsule
Protein composition	Collagen (type IV), Laminin, Nidogen/Entactin, Heparan Sulfate Proteoglycans, Perlecan, Collagen XVIII, Fibronectin, SPARC (osteonectin)	Collagen (type I) crosslinked with 0.25 % w/v Glutaraldehyde
Surface hydrophobicity	Hydrophilic	Hydrophilic with a contact angle of < 20 Deg
Physical property	Thin membrane around the natural lens	Cross-linked gel containing an adhesive IOL contact surface with curvature equal to test IOL posterior surface. Enhanced stability to hold mechanical integrity at physiological temperatures for 24 – 48 h.
Elastic Modulus	~ 0.02 N/mm ²	0.023 N/mm ²
Ultimate Stress	1.5 N/mm ²	0.021 N/mm ²
Interaction with IOL	Shrink wrap around IOL	Custom made to fit test IOL

Table 2.1. Comparison of material properties of the simulated lens capsule and the human lens capsule.

2.2.4. Adhesion force measurements

All test samples (Acrylic foldable, PMMA and Silicone) and LC assemblies were incubated in a temperature-controlled chamber at 21±1 °C and 37±1 °C for 4 hours and 24 hours to assess the influence of incubation time and temperature on IOL: LC adhesion force for all materials. A 3-D printed pinhole structure with a flat circular 3-mm disk head was attached to the anterior surface of the IOL optic and placed carefully at the gelatin capsule. The IOL: LC assemblies were then placed in an airtight container to minimize the change in concentration of the 3D LC molds resulting from evaporation of water at elevated temperatures and placed inside the incubation chamber for predefined time points. Adhesion force was measured at the predefined time points and analyzed to calculate the differences in the forces observed at the different time points. After incubation at 4 and 24 hours, the adhesion force between the IOLs and LCs was determined

using previously established custom-made adhesion force apparatus (Jaitli et al, 2021). Figure 1 shows a 3-D model of the system apparatus (Fig. 2.1, A) and the test process (Fig. 2.1, B).

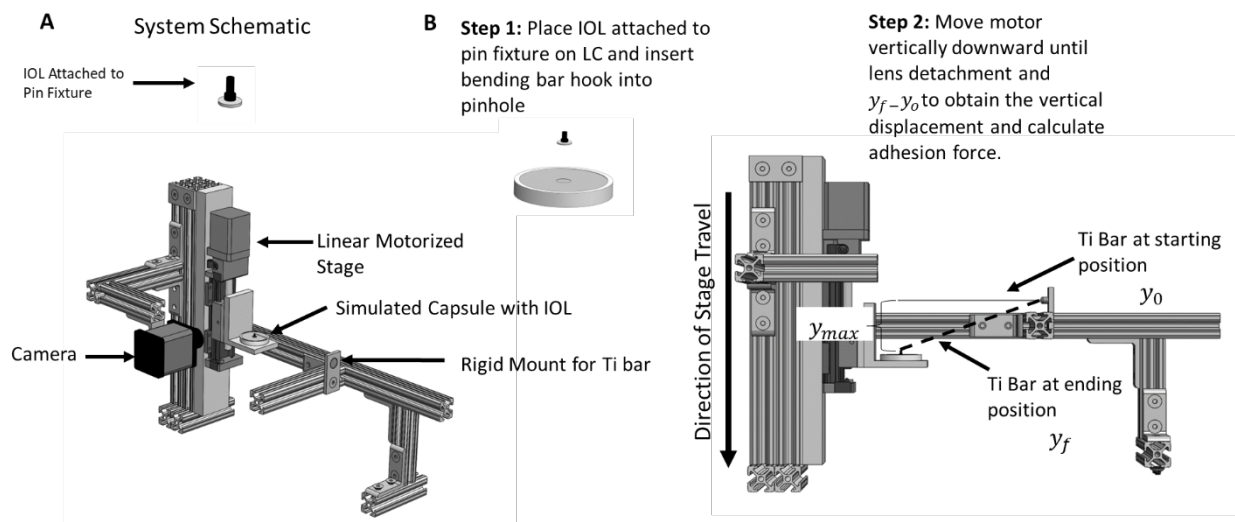


Figure 2.1. Mechanical Apparatus System Schematic (A) and Test Process Schematic (B).

2.2.5. Surface hydrophilicity and roughness measurements

Material surface properties play a critical role in its adhesion to a biological substrate such as the lens capsule and influence biological responses post implantation (Jung et al., 2017a). To assess the influence of temperature and hydration, surface properties of the test IOL materials before and after incubation in Balanced Salt Solution (BSS) at 21 °C and 37 °C for 24 hours were characterized by contact angle measurements to determine the surface hydrophobicity and by white light interferometry (WLI) to measure their surface roughness. Both measurements were made on acrylic foldable, PMMA, and silicone IOLs. Contact angle measurements of all IOLs were made using the Video Contact Angle (VCA) Optima system (AST Product Inc., Billerica, MA) by following manufacturer's instructions. The contact angle was calculated using the Sessile Drop method with an accuracy of $\pm 0.5^\circ$ as described earlier (Cunanan et al., 1998; Jung et al., 2017b). The surface roughness, morphology and topology of test IOL materials were

characterized using a Taylor Hobson Coherence Correlation Interferometry (CCI) instrument (Model # CCI MPHS, Taylor Hobson, Leicester, United Kingdom). All data was acquired using a TalySurf CCI software and post processed in TalyMap Platinum. To avoid discrepancies in surface roughness results caused by debris/particulate on the test samples, the lens surface was cleaned with a fine Q-tip soaked in DI water. The “Sloped or Curved” measurement mode was utilized for all scans in the study for surface roughness characterization. Raw data comprised of 2D maps and 3D surface morphology and topology information and was processed using a 4th degree polynomial function to remove the general form of the test surface i.e. the curvature of the lens. Resulting data consisted of peaks and valleys that were utilized to collect surface roughness of the test surface. The surface roughness parameters investigated in this study was *Sa* (mean surface roughness or arithmetic mean of the absolute value of the height within a sampling area) as shown in the equation provided below.

$$Sa = \frac{1}{A} \iint_A |z(x, y)| dx dy$$

where *A* refers to the sampling area and *z(x, y)* is the surface departure.

2.2.6. Visualize “cell” infiltration at the space between IOL and LC

To test the “No space, No cell” hypothesis (Pearlstein et al., 1988; Ursell et al., 1998), a novel imaging system was established to assess the available space between IOLs and LC using a macromolecule dye solution to simulate cell infiltration. Briefly, the imaging set-up consisted of a 3.2 MP color camera with a 2048 x 1536 resolution (GS3-U3-32S4C-C, Wilsonville, OR) paired with an Edmund Optics telecentric lens (54-798, Tucson, AZ) mounted vertically utilizing Edmund Optics mounting clamp (56-024, Tucson, AZ) to maximize the field of view capturing the lens and LC. A diffused white light (LND2-200SW, Japan) was used to fully illuminate the

mold and lens. The imaging assembly was mounted on the following opto-mechanical hardware: Newport optical rail carrier (PRC-3, Irvine, CA), Newport precision optical rail (PRL-12, Irvine, California), with a 3D printed part to interface with mounting clamp and carrier. The rail was mounted to an optical bread board (MB612F, Newton, NJ) held by two right angle brackets (VB01, Newton, NJ) mounted to another optical breadboard (MB12, Newton, NJ). Figure 2.2 shows photographs of the imaging bench in frontview (Fig. 2.2, A) and sideview (Fig 2.2, B) orientations. Blue Dextran dye (Sigma-Aldrich D575) at 5 mg/mL concentration was used to simulate cell infiltration and provide a visual cue on the space between IOLs and LCs. The studies were carried out as follows. IOLs were placed inside the gelatin molds which were then placed in $37\pm 1^\circ\text{C}$ incubator for 24 hours (Fig. 2.3, A). The dye solution ($10\mu\text{L}$) was then injected at the edge of IOL-filled molds (Fig. 2.3, A) and the molds were then imaged (Fig. 2.3, A). The extent of dye penetration in the space between IOL and LC was then calculated by analyzing the images (Fig. 2.3, B) using NIH ImageJ software (Fig. 2.3, C).

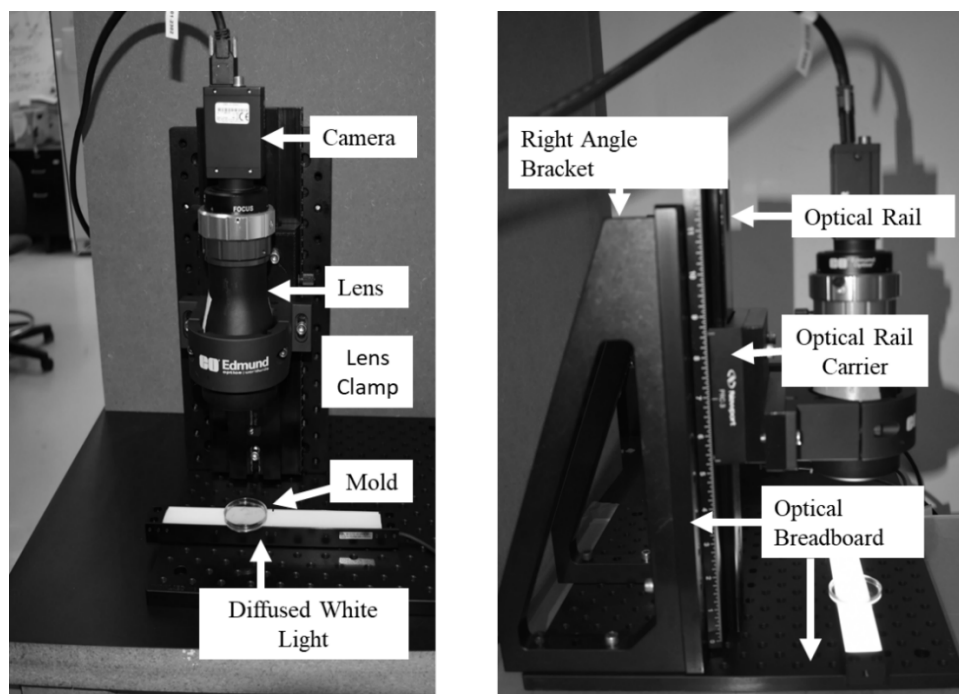


Figure 2.2. Front view (A) and side view (B) photographs of the imaging system.

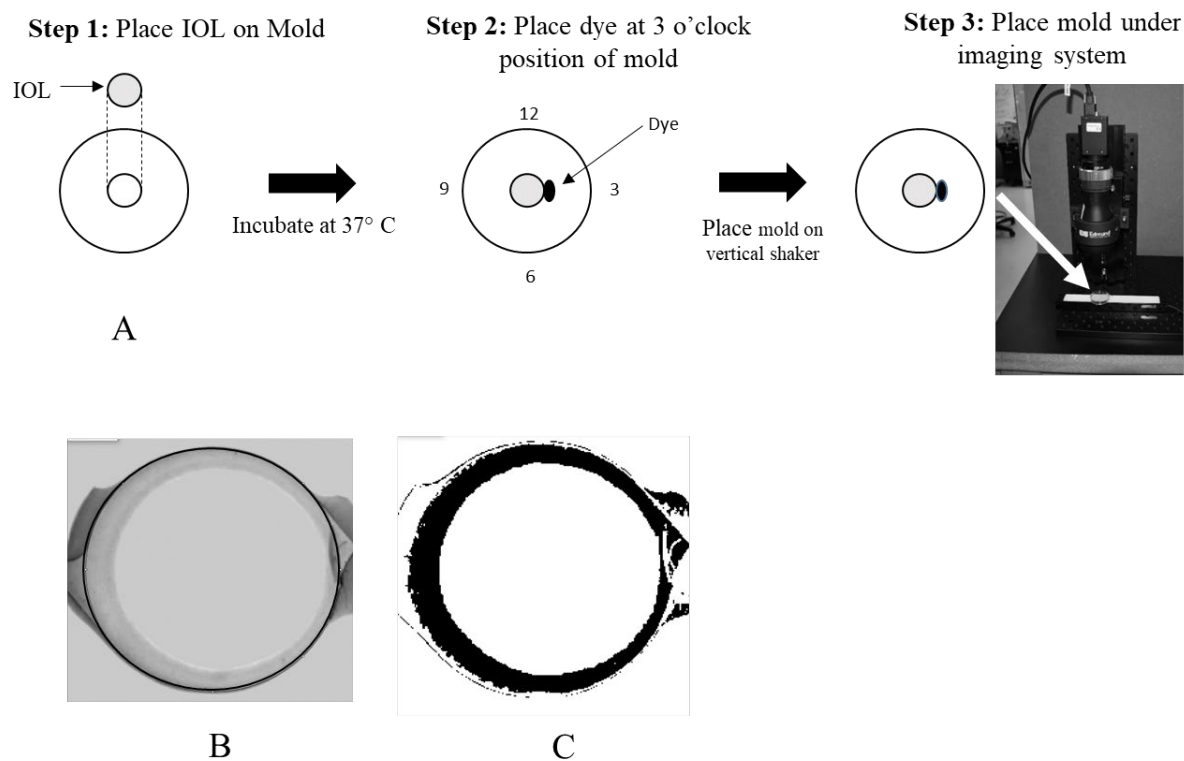


Figure 2.3. Imaging Test Process Schematic (A) of blue dextran dye occupying posterior side of IOL and on the periphery of the IOL: LC interface (B). The collected image(s) was analyzed to calculate the % of dye penetration in ImageJ software as shown below (C).

2.2.7. Statistical analyses

All statistical data analysis was conducted utilizing the Minitab 19 Statistical Software Package. Two-way ANOVA test with replicates @ 95% Confidence Interval (CI) were conducted to determine statistically significant differences between the IOL materials and incubation time at specific temperature conditions. Furthermore, two-sample t tests @ 95% CI were also conducted to determine statistically significant differences between the IOL materials at specific time and temperature conditions. Intragroup differences for each material resulting as a function of time and/or temperature were determined by paired t-tests @ 95% CI.

2.3 Results

2.3.1. Effect of temperature and incubation time on IOL: LC Adhesion Force

To study the effect of temperature and incubation time on IOL: LC interaction and also simulate true clinical phenomena, it was imperative to study the IOL: LC adhesion forces at different temperatures (ambient temperature $\sim 21^{\circ}\text{C}$ and body temperature $\sim 37^{\circ}\text{C}$) and incubation time (0, 4, and 24 hours). At 0 hour, the adhesion forces of 0.757 ± 0.111 mN, 0.473 ± 0.075 mN, 0.377 ± 0.111 mN were observed for acrylic foldable, silicone and PMMA IOLs, respectively (Fig. 2.4). A paired t-test showed that the average force observed for each group was statistically different from each other. After incubation for 4 and 24 hours, we found that the adhesion forces among all IOLs were in the following order: acrylic foldable > Silicone > PMMA. However, the change in adhesion force for all groups over time at 21°C was insignificant with a paired t-test at 95% CI. On the other hand, at 37°C , there was substantial increase of adhesion forces with increasing incubation time among all three IOLs in the following order: acrylic foldable > Silicone > PMMA (Fig. 2.4). Further, paired t-tests at a 95% CI showed statistically significant difference in average forces between T0, T4, and T24 time points for each group. It should be noted that the difference between average forces reported for T4 and T24 time points was statistically insignificant for PMMA and silicone groups at 37°C . These results suggest that the adhesion force between IOL and LCs for PMMA and silicone IOLs achieve plateau at or before 4 hours for these groups. The acrylic foldable group, however, reported further increase in adhesion force after 4 hours (Fig. 2.4). These results show that there is a much stronger interaction between the IOL and LC at 37°C in comparison to 21°C . Two-way ANOVA with replicates (95% CI) was used to compare the adhesion forces of different IOL materials with

different incubation time. Significant differences of adhesion forces between different IOL materials were found at both 21°C and 37°C. On the other hand, significant differences were found at 37°C, but not 21°C. These results support that, at body temperature - 37 °C, both IOL materials and incubation time play an important role on affecting IOL:LC adhesion forces.

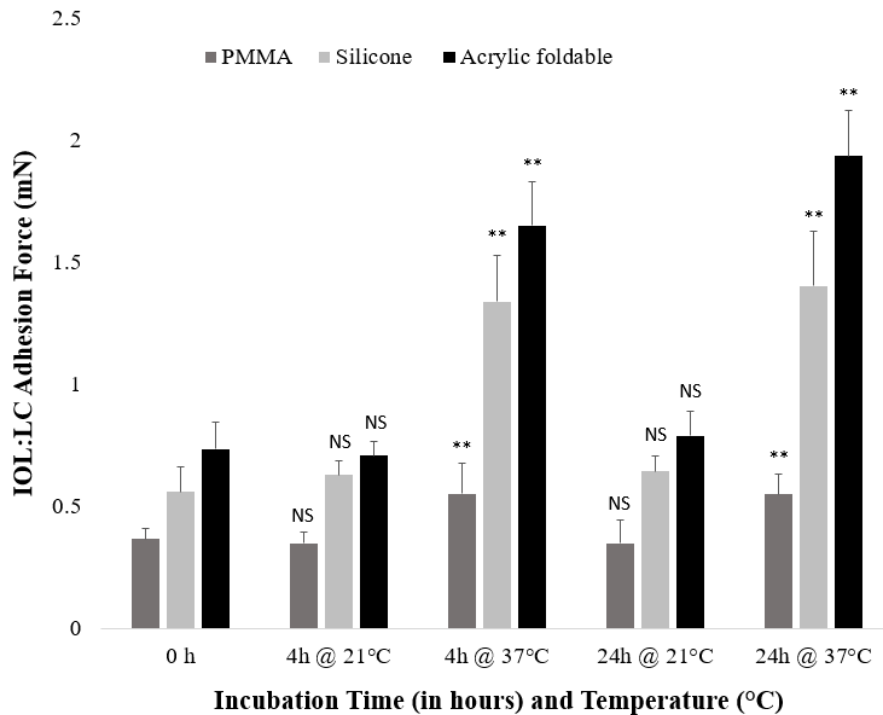


Figure 2.4. IOL: LC adhesion force for PMMA, silicone and acrylic foldable IOLs at different incubation time (0, 4 and 24 hours) and temperatures (21 °C and 37°C) (n = 10).

2.3.2. Effect of temperature and hydration time on surface hydrophobicity

Since hydration time and temperature have been shown to influence hydrophobicity of some materials (Bertrand et al., 2014); (Miyata and Yaguchi, 2004) and IOL surface hydrophobicity has been found to influence IOL: LC interactions (Li et al., 2013b; Zhao et al., 2017a), subsequent studies were carried out to investigate the potential role of IOLs' surface hydrophobicity in temperature and hydration time-dependent IOL: LC adhesion force. To find

the answer, contact angle measurements were collected for acrylic foldable, silicone and PMMA IOLs before and after 24-hour incubation at both 21 °C and 37 °C (Fig. 2.5). First, at T=0 prior to incubation, the hydrophobicity of all test IOLs was in the following order: Silicone > PMMA > acrylic foldable. At T=24 hours, there was slight reduction (~7-8%) in surface hydrophobicity in all three IOLs at 21 °C. Similar slight reduction of surface hydrophobicity was also observed in PMMA and silicone IOLs at 37 °C. Rather surprisingly, we observed a drastic and significant reduction (~ 49%) in surface hydrophobicity in acrylic foldable IOLs at 37 °C (Fig. 2.5). These results show that body temperature has significant influence on the surface hydrophilicity of acrylic foldable IOLs, but minor influence on PMMA and silicone IOLs. Using two-way ANOVA analyses, we also find that both IOL material type and incubation times have significant influence on contact angle at both 21°C and 37°C.

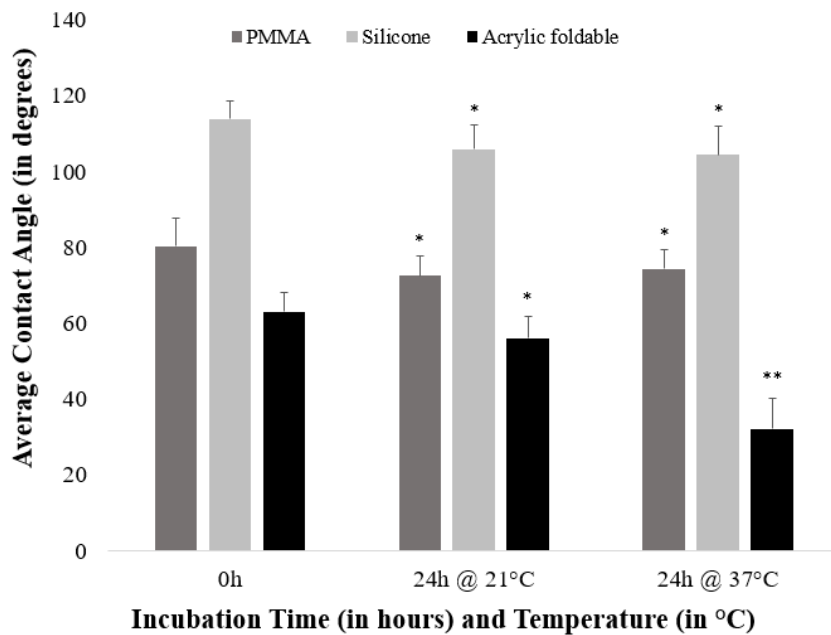


Figure 2.5. Change in surface contact angle as a function of incubation time and temperature. Contact angle measurements for PMMA, silicone and acrylic foldable test IOLs were carried out at 0 and 24 hours post hydration in BSS at different temperatures (21 °C and 37 °C) (n=10).

2.3.3. Effect of temperature and hydration time on surface roughness

Subsequent studies were carried out to determine the influence of incubation time and temperature on the surface roughness of IOLs. At T=0, we observed that there were large differences in surface roughness between different IOLs in the following order: PMMA > Silicone > Acrylic foldable IOLs. There was slight, but not statistically significant, changes in surface roughness with time (Fig. 2.6). Furthermore, similar surface roughness was found in all groups at 21 °C and 37 °C. In other words, temperature changes and incubation time do not seem to affect the surface roughness of these IOL groups. Using two-way ANOVA test with replicates, we find that IOL materials, but not incubation time, have significant effect on surface roughness at both 21°C and 37°C.

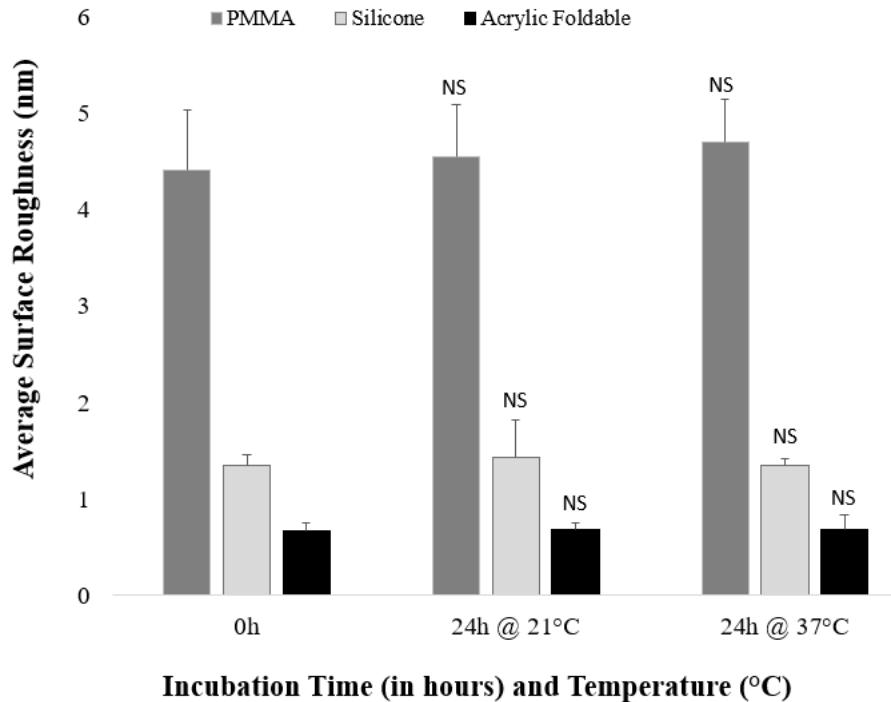


Figure 2.6. Change in surface Roughness as a function of incubation time and temperature in BSS. Surface Roughness measurement on PMMA, silicone and acrylic foldable test IOLs was carried out at 0 and 24 h post hydration in BSS at 21 °C and 37 °C for (n=10).

2.3.4. Examination of “no space no cell” hypothesis in vitro

To examine the “No space, No cell” hypothesis at a physiological condition, IOLs were placed inside the gelatin mold and placed in a 37 °C incubator for 24 hours with dye added after incubation. The amount of dye occupying the area under optic of the IOL is a quantification of the visual cue used to mimic cell infiltration and confirm the role that adhesion force plays in limiting the space between the IOL and posterior capsule. Baseline images for each IOL were collected and compared to images of samples after incubation (Fig. 2.7A). Results for baseline images indicated as $T_{inc}=0$ h, show Blue Dextran occupying the inside optic of the different IOL materials. Total average percent of dye penetration was ~ 10.26% for Acrylic foldable IOLs, ~16.53% for Silicone IOLs, and ~ 42.37% for PMMA IOLs (Fig. 2.7B). Images captured after gelatin mold was incubated for 24 hours showed a significant decrease in the total percent of Blue Dextran penetration at the IOL: LC interface for all materials by compared with T0 using paired t-test (Fig. 2.7A). The total percent of dye occupying the IOL: LC interface after 24-hour incubation was observed to be 3.16% for Acrylic foldable IOLs, 12.85% for Silicone IOLs, and 27.32% for PMMA IOLs (Fig. 2.7B). Two-way ANOVA test at 95% CI also determined that, at 37 °C, the average dye penetration percentages (%) are influenced by both IOL material properties and incubation time.

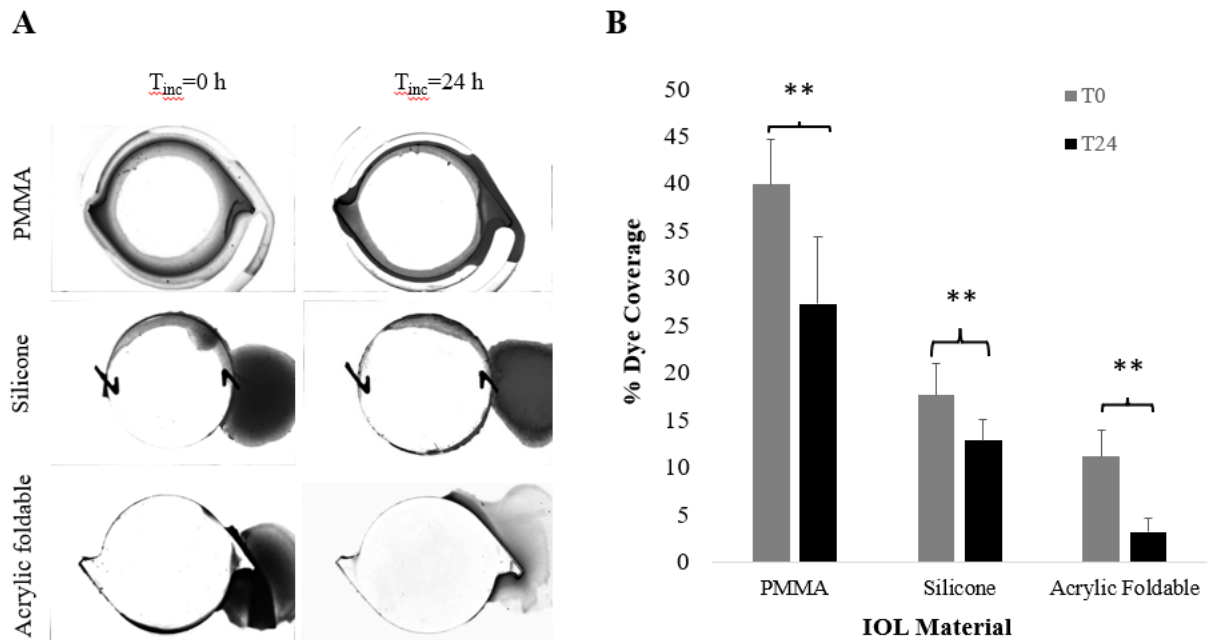


Figure 2.7. Photographs collected using the IOL: LC imaging system depicting visualization of dye penetration at IOL: LC interface at 37°C. (A) Representative images and percentage of dye coverage at IOL: LC interface for PMMA, silicone and acrylic foldable IOLs. (n = 10) (B) Paired t-test analysis of changes in dye penetration percentages by compared with 0 hour of the same IOL materials.

2.4 Discussion

Our study has found that the interactions between IOL: LC are significantly enhanced at body temperature – 37 °C in comparison with ambient temperature – 21 °C. The increase of temperature was found to increase the IOL: LC adhesion forces of all IOLs and to reduce the surface hydrophobicity of acrylic foldable IOLs. However, in this study, we found that temperature has insignificant effect on the surface roughness of IOLs. The increase of adhesion force may be associated with the increase of surface hydrophilicity post IOL implantation. Such relationship is supported by several early observations, which have indicated a relationship

between IOLs surface hydrophilicity and its adhesion force to ECM (Bertrand et al., 2014); (Miyata and Yaguchi, 2004). The mechanism governing temperature- and incubation time-dependent increase of surface hydrophilicity requires further studies and has yet to be determined. However, many previous studies support such observations. For example, a study showed that, under hydration, the surface hydrophobicity of 3 different hydrophobic polymers - Benz R&D's Benz IOL 25 (a copolymer of 2-hydroxyethyl methacrylate (HEMA) and ethoxyethyl methacrylate (EEMA)), Benz R&D's Benz HF1 (A copolymer of EEMA and ethoxyethyl acrylate (EEA) and PhysIOL.s.a's GF (A polymer blend of ethylene glycol phenyl ether acrylate (EGPEA), HEMA and poly(propylene glycol) dimethacrylate (PPGDMA) decreased owing to dynamic surface changes resulting from reorganization of the polar hydroxyl groups in the aqueous environment accompanied by likely variation in surface roughness and swelling of material in the aqueous medium (Bertrand et al., 2014). Other studies also suggest that a dynamic surface transformation under hydration and temperature increase may be responsible for the increase in surface hydrophilicity of the acrylic foldable lens (Bertrand et al., 2014); (Miyata and Yaguchi, 2004). Finally, a separate study also found that Alcon's MA60BM, a hydrophobic acrylic, increased its equilibrium water content and hydrophilicity at elevated temperatures (Miyata and Yaguchi, 2004). These results suggest that, after implantation, an acrylic foldable IOL increases its water uptake and surface hydrophilicity and leads to strong adhesion force with LC. In fact, implanted soft acrylic IOLs such as Alcon's Acrysof are increasing difficult to explant if the procedure is not conducted within a few weeks of surgery owing to their strong adhesion with the lens capsule post cataract surgery (Ursell et al., 1998). The mean adhesion force for PMMA group lenses was observed to be the lowest with minimal influence by temperature and hydration time among all studied materials. PMMA IOL is

reported to have high incidence of PCO in the clinic (Gift et al., 2009; Ram et al., 2014; Rønbeck et al., 2009b; Rønbeck and Kugelberg, 2014b) and is known to have minimal adhesion to lens capsule post implantation as demonstrated by various *in vitro* and *ex vivo* investigations (Oshika et al., 1998b, 1998c; Wejde et al., 2003b). The Silicone IOLs reported higher adhesion forces than the PMMA IOLs which is in agreement with clinical observations for these materials (Wejde et al., 2003b). These higher forces for the Silicone IOLs can be attributed to the presence of functional moieties on its surface that possess a high affinity for collagen (a major constituent of the gelatin capsule) (Rønbeck and Kugelberg, 2014c; Vasavada and Praveen, 2014).

Previous studies have shown that PMMA material IOLs have significantly more surface irregularities than silicone and acrylic IOLs (Lombardo et al., 2009). Further, both acrylic and silicone IOLs have been reported to have smooth surfaces with lowest surface roughness for acrylic IOLs (Mukherjee et al., 2012)(Yang et al., 2017). In fact, many studies have concluded that higher surface roughness of an IOL biomaterial leads to higher PCO growth as surface irregularities could increase the number of inflammatory cells adhering to the IOL optic surface and result in tissue formation (Katayama et al., 2007c)(Tanaka et al., 2005). Our results support this conjecture as lowest *Sa* measurements were reported for the acrylic foldable group (best clinical PCO outcomes), followed by silicone and PMMA (worst clinical PCO outcomes) at body temperature. Therefore, the reported consistent increase in adhesion force between the acrylic foldable IOLs and simulated LC may be attributed to its smooth surface, and water uptake characteristics under hydration. On the contrary, the small increase in adhesive forces for silicone material may be due to its relatively smooth surface and the presence of functional moieties on its surface that possess a high affinity for Collagen (Rønbeck and Kugelberg, 2014c; Vasavada and Praveen, 2014). Lastly, PMMA IOLs are reported to have minimal capsule

adhesion, a hard brittle surface (Linnola et al., 2003c; Oshika et al., 1998c) and high surface irregularities (Lombardo et al., 2006; Mukherjee et al., 2012; Yang et al., 2017). As a result, PMMA IOLs do not bind tightly to the lens capsule resulting in low IOL: LC adhesion forces and thus high PCO incidence.

Our results show that IOL material properties affect their adhesiveness to the simulated LC. Our results agree with previous observations which show that the adhesiveness of an IOL with the lens capsule is inversely proportional to the rate of PCO formation post-implantation in clinic (Linnola, 1997; Linnola et al., 2003)(Katayama et al., 2007c)(Nagata et al., 1998; Oshika et al., 1998b, 1998c; Wejde et al., 2003b). It should be noted that, in addition to surface adhesiveness, the geometry of IOL posterior optic edge has been shown to influence PCO rates (Buehl et al., 2007, 2005; Cheng et al., 2007; Eldred et al., 2014; Haripriya et al., 2017; Maddula et al., 2011; Mylonas et al., 2013; Nishi, 1999a; Nishi et al., 2000, 1998b; Wormstone, 2020; Wormstone and Eldred, 2016c). For example, round-edged IOLs are reported to have higher PCO rates owing to their inability to create a ‘barrier effect’ to prevent infiltration and proliferation of LECs (Buehl et al., 2005; Cheng et al., 2007; Maddula et al., 2011; Nishi et al., 2001, 2000). Furthermore, by testing the PCO progression of different materials with both round-edged and sharp-edged IOLs in pigmented rabbits, several studies found that there was no significant difference in the observed IOL PCO rates between IOLs with sharp posterior edges, irrespective of the IOL’s material composition (Nishi, 1999a, 1999b; Nishi et al., 2004b, 2000, 1998b, 1998a; Nishi and Nishi, 2002). It is believed that the presence of a sharp posterior optic edge creates a capsular bend or angle at the IOL-LC interface leading to firm binding of the lens capsule to the rectangular sharp optic edge thereby inhibiting the migration of LECs, and eventually reducing extent of PCO formation (Nishi, 1999a). On the other hand, round edged lenses fail to form a

capsular bend at the IOL-LC interface that leads to firm binding with the lens capsule (Nishi et al., 1998b). Interestingly, in another retrospective and comparative 2-year follow-up study that compared Nd: YAG procedure rates for 3 IOLs with different degree of edge sharpness in following order: Hoya PY60AD > Acrysof SN60WF > HOYA FY60AD showed lowest Nd: YAG rates for the Acrysof SN60WF IOL (Morgan-Warren and Smith, 2013) . It was concluded that while IOL edge sharpness contributes to the reduced PCO rates, the variation in the material constitution of these IOLs can potentially influence their susceptibility to PCO development independent of edge sharpness (Morgan-Warren and Smith, 2013). While surface hydrophilicity and roughness are the focus of this investigation, our results do not exclude the potential influence of IOL edge profile on the adhesion force of IOLs which will be evaluated in a future study.

It is worth nothing that previous studies have suggested that ocular temperature can vary from 30 – 37 °C depending on several factors such as patient age, ambient temperature, intraocular position, aqueous humor flow, cataract surgery induced trauma etc. (Jakobsson et al., 2015; Lucia et al., 2016; Modrzejewska et al., 2020; Nazaretyan et al., 2018; Walker et al., 2014). While the results from this study show significant differences in the performance characteristics of IOL materials at body temperature, the potential influence of ocular temperature fluctuation on the IOL: LC interactions should be investigated in the future.

Overall, our results support a general hypothesis that time, temperature and hydration of IOL materials, specifically, hydrophobic acrylic foldable IOLs such as Alcon’s Acrysof affect the physical and chemical properties of an IOL and the reduction of surface hydrophobicity at body temperature may influence IOL: LC interactions (Fig. 2.8) and subsequent PCO formation. This assumption is also supported by many previous observations. First, IOL material properties are

found to influence the speed of the capsule bending (Nishi et al., 1998b). For instance, using Optical Coherence tomography, studies have found that the capsule-IOL contact was much faster (10 days) for the Acrysof lens as opposed to a Silicone lens (~15 days) (Sacu et al., 2005a). Rapid adhesion of IOL materials after IOL implantation can potentially seal off the interfacial space and prevent cell infiltration i.e. ‘No space, No cell’ (Pearlstein et al., 1988). This assumption supports our results that there is an inverse relationship between adhesive force and dye penetration ratios. Specifically, the results of IOL adhesion force were in the following sequence: Acrylic foldable IOL > Silicone IOL > PMMA IOL while the dye penetrations results was in the following sequence: PMMA IOL > Silicone IOL > Acrylic foldable IOL. It is also worth nothing that while our model initially assumes perfect contact between the IOL and capsule during the fabrication of the simulated capsules, capsule shrink wrapping of the IOL is governed by cell driven events post implantation and can be influenced by the posterior optic edge geometry and haptic design of the IOL (Nishi, 1999a; Nishi et al., 2000, 1998b; Wormstone, 2020; Wormstone and Eldred, 2016b). This is addressed by utilizing specific capsules generated from the test IOL itself. Our adhesion force and dye penetration results have indirectly shown that different IOL materials bind to the surface of the IOL capsules differently. Further, our results determined by IOL: LC adhesion force and dye penetration are a measure of the IOL: LC surface interactions and gap closure as a function of time. A direct measure of IOL: LC interface using this model for different IOL materials and designs as a function of time should be studied in the future.

The results of this work provide several major substantiations that are essential to the pathogenesis of IOL-mediated PCO formation. Specifically, we showed that body temperature may alter the material properties, such as surface hydrophobicity of some IOLs by dynamic

surface transformations. By reducing its hydrophobicity, an acrylic foldable IOL such as Alcon’s Acrysof lens develops strong adhesion force with LCs. Finally, the tight interaction between IOLs and LCs mediated by IOL material’s bioadhesiveness and design would reduce the space available for cell migration or infiltration, and, perhaps, PCO formation. Our studies have also lent strong support that future *in vitro* or *ex vivo* studies should be carried at body temperature to better mimic the IOL: LC interactions and to assess their potential influence in PCO formation.

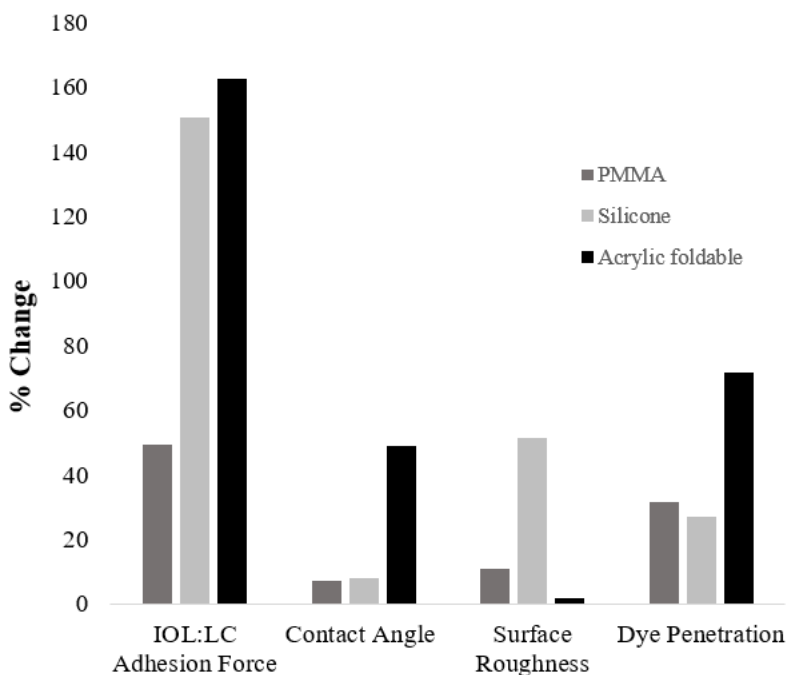


Figure 2.8. Percentage change in average IOL: LC adhesion force, contact angle, surface roughness and dye penetration for PMMA, silicone and acrylic foldable IOLs at 37°C.

2.5 Conclusion

Here we report a potential effect of temperature-dependent changes in surface properties of IOLs on their influence on IOL: LC adhesion forces using a newly established *in vitro* system. The overall results suggest that, at body temperature, the decrease of surface hydrophobicity may be

responsible for the significant increase of adhesive force between acrylic foldable and LC. Such increase of adhesive force significantly reduced the extent of dye penetration in this study and, perhaps, reduces cell infiltration and PCO formation in the clinic. While the influence of IOLs' edge profile on IOL: LC interactions has yet to be determined, our results provide new evidence to support the potential role of temperature, hydration time, surface hydrophobicity and IOL material properties on affecting the incidence of IOL-induced PCO.

CHAPTER 3

Role of Fibronectin and IOL surface modification in IOL: Lens Capsule Interactions

3.1 Introduction

Cataract is the second most common cause of blindness in the world affecting ~ 27 million people in the United States alone (Pérez-Vives, 2018a). Surgical removal of the cataractous lens followed by the implantation of an artificial Intraocular Lens (IOL) is performed to treat cataract induced visual impairment (Eldred et al., 2019). While surgical intervention followed by IOL implantation initially restores vision in patients, some patients develop Posterior Capsule Opacification (PCO) leading to secondary vision loss. Despite intensive research efforts, the potential influence of IOL design and surface properties on PCO incidence rates is not totally clear.

The surface hydrophobicity, surface roughness and posterior optic edge geometry of IOLs have all been indicated to affect PCO formation (Boulton and Saxby, 1998; Katayama et al., 2007c; Kim et al., 2001; Linnola et al., 2003b, 2000d; Oshika et al., 1998c; Ursell et al., 1998b; Versura, 1999b; Xu et al., 2016b, 2016a). It has been proposed that a strong adhesion of the IOL to the lens posterior capsule (PC) leaves less or no space for cells to grow or infiltrate into i.e. ‘No space, No cell’, a theory which has been used to describe the different rates of PCO for various older IOLs (Pearlstein et al., 1988c). It has also been suggested that the physical pressure caused by the tight binding between the IOL and the PC may squeeze out the LECs present in the capsule space and cause their atrophy (Linnola et al, 1997). Linnola proposed the ‘Sandwich Theory’ that states that bioactive IOL materials allow a single lens epithelial cell to bond both to the IOL and the PC which forms a ‘sandwich’ pattern comprised of the IOL, the cell monolayer, and the PC (Linnola 1997). It is believed that a tightly packed sandwich structure may lead to reduced epithelial proliferation and PCO formation (Linnola 1997). These hypotheses suggest that a strong interaction between IOL and PC reduce PCO formation by suppressing lens LEC

responses (infiltration and proliferation). While these hypotheses are in good agreement with clinical observations, it is not clear how IOL material properties would affect IOL: PC interactions and PCO incident rates. This study was designed to find the answers for these questions.

Various ECM proteins like fibronectin, vitronectin, fibrinogen, and transferrin have been found to accumulate between the capsule and IOL in various animal studies (Kochounian et al., 1994) (Saika et al., 1993; Shizuya Saika, 1997). It is believed that ECM proteins may act as mediators of IOL adhesion to the PC (Saika et al., 1993; Shizuya Saika, 1997). On the other hand, a study has shown that within hours of cataract surgery, the implanted IOL adsorbs a complex protein biofilm which may determine the subsequent cellular and tissue reactions to the IOL (Kochounian et al., 1994). Among all ECM proteins, fibronectin, a major glycoprotein of the extracellular matrix, is believed to impact the degree of IOL-induced PCO formation owing to its affinity for collagen, an essential material constituent of the lens capsule (Linnola et al., 2000b). The breakdown of the blood–aqueous barrier after cataract surgery increases the amount of soluble fibronectin in the aqueous humor that interacts with the implanted IOL’s surface and affects cellular responses (Linnola et al., 2003a). Fibronectin contains several functional domains, such as I6II1-II2-I7-I8-I9 modules, which have been shown to promote its binding to collagen and the cell surface (Shimizu et al., 1997a; Sottile et al., 2007a). This collagen and cell surface binding property of fibronectin may facilitate the binding between an IOL and the PC (Linnola et al., 2000e) and the progression of PCO (Linnola 1997). It should be noted that a significant amount of fibronectin and vitronectin were found to accumulate on the hydrophobic soft acrylates *ex vivo* (Linnola et al., 2000a), that are clinically known to show low rates of PCO (Linnola et al., 2000a; Nishi et al., 2004b; Pérez-Vives, 2018; Rönbeck et al., 2009a; Rønbeck

and Kugelberg, 2014; Ursell et al., 1998). Coincidentally, among different commonly used IOL materials such as hydrophobic acrylate, polymethyl methacrylate and silicone, hydrophobic acrylates IOLs are found to have a high affinity for fibronectin (Linnola et al., 2003a). While many *in vitro* and *ex vivo* studies have examined the interaction of fibronectin with various IOL materials, the potential role of adsorbed fibronectin on influencing IOL:PC adhesion force and PCO progression has yet to be directly investigated.

IOL surface physical and chemical properties have been shown to affect their protein adsorption and cell adherence capability (Johnston et al., 1999; Tan et al., 2017). Since the accumulation of extracellular matrix proteins and cells may contribute to PCO formation (Saika, 2004), many surface modification techniques have been investigated to study their ability to reduce the PCO potential of IOLs. In fact, surface modification of IOL materials to increase their surface hydrophilicity has been extensively studied. For example, hydrophilic coatings such as Poly (ethylene glycol) (PEG), Poly (ethylene glycol) methyl acrylate (PEGMA) and PEG-like thin coatings such as Di(ethyleneglycol) dimethyl ether (Digylme) are used to modify various biopolymers and are associated with reduced inflammatory responses (Lee et al., 2007; Ribeiro et al., 2009a; Tognetto et al., 2003; Xu et al., 2016c). While hydrophilic IOLs are known to adsorb less protein and are associated with lower levels of cell adherence (Tan et al., 2017), their PCO performance in the clinic is inferior when compared to hydrophobic IOLs (Zhao et al., 2017b). Thus, to capitalize on this anti-fouling property of hydrophilic IOLs and the superior PCO performance of the hydrophobic IOLs, researchers have engineered and studied hydrophobic acrylates coated with hydrophilic coatings in PCO rabbit models (Lee et al., 2007; Xu et al., 2016c). These studies have reported lower initial PCO rates when compared to non-

coated controls but the possible influence of these hydrophilic coatings on effecting IOL: PC interactions and long-term clinical PCO potential has not been fully studied yet.

To investigate the influence of adsorbed fibronectin and IOL surface modification on IOL:PC interactions, we first assessed the effect of fibronectin on IOL: PC adhesion force using a PCO predictive *in vitro* model and commercially available IOLs, including acrylic foldable, PMMA and silicone IOLs. The influence of fibronectin adsorption on potential cell infiltration and PCO formation was then assessed using a macromolecular dye imaging system. Furthermore, in order to study the influence of surface coating on IOL: PC interactions, acrylic foldable IOLs were coated with Digylme (DG) by modifying previously established vapor plasma deposition techniques (Johnston et. al., 2005; Menizes et al., 2012). The Digylme-coated IOLs were then used to investigate the ability of the surface coating to alter IOL surface properties, its fibronectin affinity, IOL: PC adhesion force, and cell infiltration potential.

3.2 Materials and Methods

3.2.1. Intraocular Lenses

Three commercially available IOLs (hydrophobic acrylic foldable (hereafter referred to as ‘acrylic foldable’), PMMA, and silicone IOLs) were used in this investigation. The acrylic foldable IOLs had a 6.0 mm biconvex optic, a sharp rectangular posterior edge and planar haptics with an overall length of 13.0 mm (Alcon’s SN60WF, Alcon Research, Fort Worth, Texas) with a dioptric power of 21.0D. The PMMA group consisted of single piece IOLs with a 5.5 mm PMMA optic, round posterior edge and multiflex haptics with an overall length of 13.0 mm (Alcon’s MTA4U0, Alcon Research, Fort Worth, Texas) with a dioptric power of 23.5D. The Silicone group was comprised of three-piece posterior chamber biconvex silicone 6.0 mm

optics that had a round edged profile and blue PMMA mod C haptics with an overall length of 13.0 mm (Allergan's AMO Array SA40N, Allergan Inc, Irvine, California) with dioptric powers between 10.0 D and 26.0 D.

3.2.2. Surface modification of acrylic foldable IOLs

To investigate the role of surface hydrophilicity on IOL: PC interactions, Diglyme-treated acrylic foldable IOLs were included in the study. For that, some of the acrylic foldable IOLs were surface modified with Diethylene glycol dimethyl ether (Diglyme) (hereafter referred to as DG-acrylic foldable). Diglyme coating was achieved by a plasma deposition process utilizing a vapor deposition plasma chamber (Nordson March PD-1000; Nordson Electronics Solutions, CA, USA) using a modified procedure (Menzies et al., 2012). Briefly, the surface of the IOLs was first treated with oxygen plasma under low pressure (200 mTorr) at 200 W for 5 min, followed by treatment with Argon gas at 250 mTorr at 100W for 1 min. Finally, diglyme deposition was achieved by treating the functionalized IOLs under a pressure of 250 mTorr at 40W for 20 min.

3.2.3. Preparation of Simulated Lens Capsules

Simulated PCs were created to possess a spherical cup shaped structure that closely mimics the 3D morphology, structure and mechanical integrity of the human capsular bag using previously established procedures (Jaitli and Roy et al, 2021a). To reduce their degradation in culture condition, all simulated PCs were gently cross-linked with glutaraldehyde as previously described (Dardelle et al., 2011; Jaitli et al., 2021a). Briefly, the gelatin solution crosslinked using 0.25% glutaraldehyde (Sigma Aldrich, #G6257, grade II, 25% in water) was poured into acrylic petri-dishes immediately prior to the placement of IOLs. Next, IOLs with haptics intact were taped onto small thin circular lightweight support materials to ensure the IOL stayed afloat through the solidification process at 4°C for 1 hour. IOLs were then gently peeled from the

gelatin surfaces with the help of thin forceps to create a capsule as described recently (Jaitli et al., 2021b)

3.2.4. Surface characterization of various treated IOLs

The influence of diglyme coating and adsorbed fibronectin on the surface properties of all test IOLs was characterized by measuring their surface contact angle. For fibronectin coated samples, IOLs were incubated with 500 μ L of human fibronectin solution (0.2 mg/mL) for 24 hours at room 37 °C prior to the surface characterization. Fibronectin solution concentration was utilized based on the previous studies (Carole A Cooke et al., 2006; Linnola et al., 2003c). Contact Angle measurements of all IOLs were made using the Video Contact Angle (VCA) Optima system (AST Product Inc., Billerica, MA) by following the manufacturer's instructions. The contact angle was calculated using the Sessile Drop method with an accuracy of $\pm 0.5^\circ$ as described earlier (Cunanan et al., 1998; Jung et al., 2017a)

3.2.5. Surface Coating and Fibronectin Adsorption on IOL: PC force and cell infiltration

All test IOLs and PC assemblies were incubated in a temperature-controlled chamber at $37\pm 1^\circ\text{C}$ for 24 hours prior to the study. In some groups, human fibronectin (Sigma-Aldrich, Lot # SLCG9672) was dissolved in Balanced Salt solution (BSS, Alcon BSS irrigation solution ALC-0065079515). Two μ L of human fibronectin solution (with 1, 10, 100, and 1000 $\mu\text{g/mL}$) or BSS (as control) was added onto the surface of the simulated PCs prior to the placement of the test IOLs. The amounts of fibronectin for this study were selected in accordance with published literature that have assessed the impact of fibronectin on surface properties of IOLs (Schroeder et al., 2009a) that are within the physiological fibronectin levels observed in human intraocular fluid (Probst et al., 2004). One group also contained 2 μ L of Bovine Serum Albumin (BSA,

Sigma-Aldrich, Lot # 078K0730) dissolved in BSS (1000 µg/mL). After incubation for 24 hours at 37 °C, the adhesion force of the IOL:PC was then measured using a microforce tester as described previously (Jaitli et al., 2021b). Further studies were carried out to assess the influence of fibronectin adsorption and surface coating on cell infiltration at the IOL: PC interface using a macromolecular dye imaging model (also called a simulated cell infiltration model) as described recently (Jaitli et al., 2021b). Briefly, after IOL:PC incubation for 24 hours, blue dextran dye solution (10µL at 5 mg/mL, Sigma-Aldrich D575) was then added at the edge of IOL-filled molds and the molds were then imaged to visualize and quantify the extent of dye penetration (or simulated cell infiltration) at the interspace between IOL and PC. All images were analyzed using ImageJ software. The area of the regions of the IOL not covered with blue dextran dye solution was calculated and compared with the total area of the IOL. The percentage of dye free or cell free area was then calculated using the formula [(area of dye free region/area of total IOL)*100].

3.2.6. Statistical analyses

All statistical data analysis was conducted utilizing the Minitab 19 Statistical Software Package. Two-sample t-test @ 95% Confidence Interval (CI) were conducted to determine statistically significant differences between the two groups (BSS and Fibronectin) for each material. Furthermore, one-way ANOVA test with appropriate post-hocs @ 95% Confidence Interval (CI) were performed to determine the statistically significant differences between the IOL material and its interaction with fibronectin protein.

3.3 Results

3.3.1. Effect of Fibronectin on IOL: PC adhesion force for acrylic foldable IOLs

Since fibronectin has been shown to be adsorbed onto acrylic foldable IOLs (Schroeder et al., 2009b), acrylic foldable IOLs (Alcon's Acrysof SN60WF) were used as the test subjects to assess the influence of fibronectin on IOL: PC adhesion force. First, different concentrations of fibronectin were added on a simulated PC prior to the IOL placement. After incubation for 24 hours at 37 °C, we found that there was a significant increase of adhesion force (2.346 ± 0.149 mN) in the 1000 µg/mL (or 2 µg/capsule) treated group when compared with the BSS control group (1.408 ± 0.158 mN) (Figure 3.1). On the other hand, there was no statistically significant difference between 1 µg/mL (1.243 ± 0.176 mN), 10 µg/mL (1.421 ± 0.187 mN), and 100 µg/mL (1.304 ± 0.120 mN) and the BSS control. To compare the adhesion force of fibronectin to another protein, similar concentration of BSA was also tested for adhesion force. The supplement of BSA (2 µg per capsule) showed no statistically significant difference (1.481 ± 0.084 mN) when compared to BSS control. A classic one-way ANOVA with Tukey's test (CI, $\alpha=95\%$) was performed to analyze the overall influence of FN on IOL:PC adhesion force. These results indicate that fibronectin present between the acrylic foldable IOL and the PC at 2 µg/capsule may significantly increase IOL: PC adhesion force. Thus, to further assess the role of fibronectin in mediating IOL: PC adhesion, subsequent studies were conducted in the presence of absence of fibronectin at 2 µg/capsule.

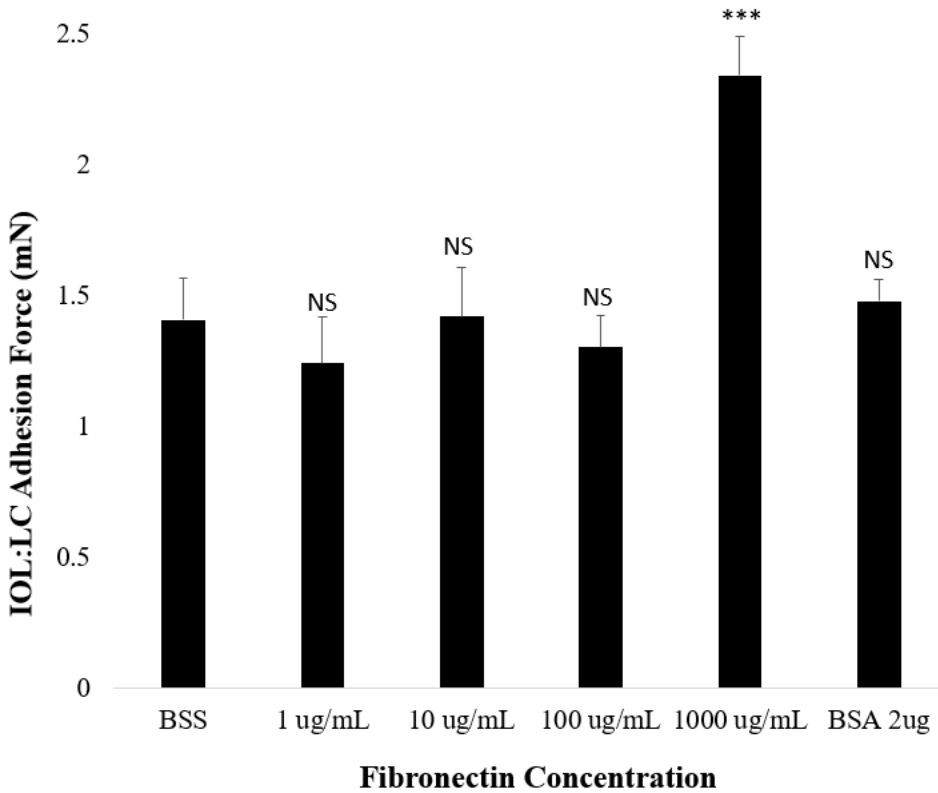


Figure 3.1. IOL: PC adhesion force as a function of fibronectin concentration after incubation of acrylic foldable IOLs @ 37°C for 24 hours. Data presented as mean ± SD (N=10).

3.3.2. Effect of Fibronectin on IOL: PC adhesion for different materials

We then investigated whether fibronectin would increase the adhesion force of PCs to IOLs made of other materials, such as PMMA IOLs and silicone IOLs. To find the answer, PMMA and silicone IOLs with simulated capsules were injected with 2µL of BSS (as control) or fibronectin solution (2 µg/capsule) and then incubated for 24 hours @ 37°C prior to adhesion force measurement. As expected, we found that fibronectin adsorption significantly increased the adhesion force of acrylic foldable IOLs (without vs. with fibronectin adsorption = 1.408 ± 0.158 vs 2.346 ± 0.149 mN). Rather surprisingly, we found that the presence of fibronectin slightly reduced the adhesion force of PMMA IOLs (without vs. with fibronectin adsorption = $0.409 \pm$

0.06 mN vs 0.334 ± 0.081 mN) and silicone IOLs (without vs. with fibronectin adsorption = 1.136 ± 0.153 mN vs 1.114 ± 0.112 mN) (Fig. 3.2). However, influence of FN on IOL: PC adhesion force of PMMA and silicone IOLs was not statistically significant based on a two-sample t-test when comparing the adhesion force of BSS with FN of each IOL material. Also, a one-way ANOVA on ranks with Dunn's test (95% CI) was performed to analyze the overall influence of fibronectin on IOL: PC adhesion force for different IOL materials. The results show that both IOLs materials and fibronectin presence have significant influence on the IOL: PC adhesion force.

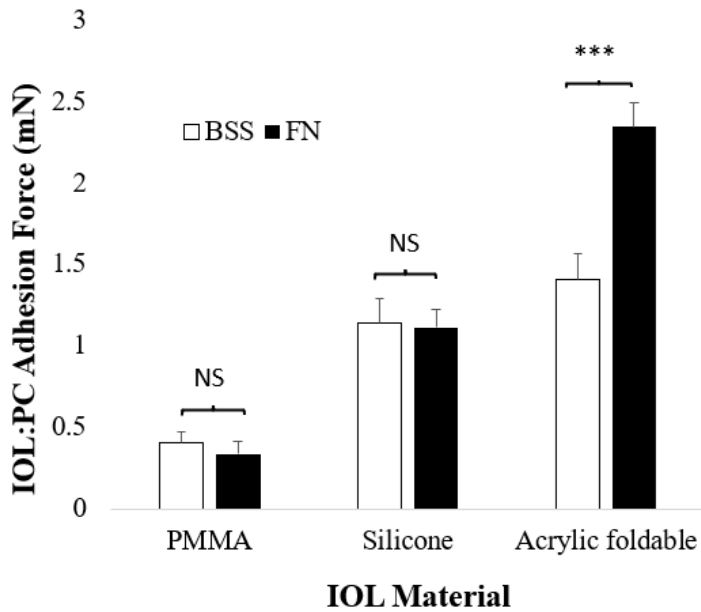


Figure 3.2. IOL: PC adhesion force of different IOL materials – Acrylic foldable, PMMA and Silicone - with either BSS (as control) or fibronectin (FN) solution (2 uL of 1 mg/mL FN in BSS) at IOL: PC interface and then incubated at 37°C for 24 hours. Data presented as mean \pm SD (N=10).

3.3.3. Simulated cell infiltration for different IOL materials in presence of

Fibronectin

High adhesion force between an IOL and the PC is believed to reduce cell infiltration at the IOL: PC interface. Thus, subsequent studies were carried out to assess the influence of fibronectin on cell infiltration at the IOL: PC interface using a simulated cell infiltration model. As shown in the representative images (Fig. 3.3A), we observed that, regardless of fibronectin presence, the extent of simulated cell infiltration among different IOL materials were in the following order PMMA > Silicone > Acrylic foldable (Fig. 3.3B). Further analyses show that the presence of fibronectin slightly increased the extent of cell infiltration in PMMA (% cell free area with vs. without fibronectin = 70.64 ± 6.656 % vs 72.68 ± 7.020 %) and silicone IOL (% cell free area with vs. without fibronectin = 82.02 ± 5.131 % vs 87.15 ± 2.206 %), although using a two-sample t-test, the differences shown between with and without fibronectin are not statistically significant for Silicone and PMMA. On the other hand, the presence of fibronectin was found to significantly reduce the extent of cell infiltration in acrylic foldable IOLs (% cell free area with vs. without fibronectin = 98.42 ± 0.576 % vs 96.84 ± 1.407 %). Further analyses using a Welch's one-way ANOVA with Games-Howell test (95% CI) showed that fibronectin has an overall significant effect on cell infiltration.

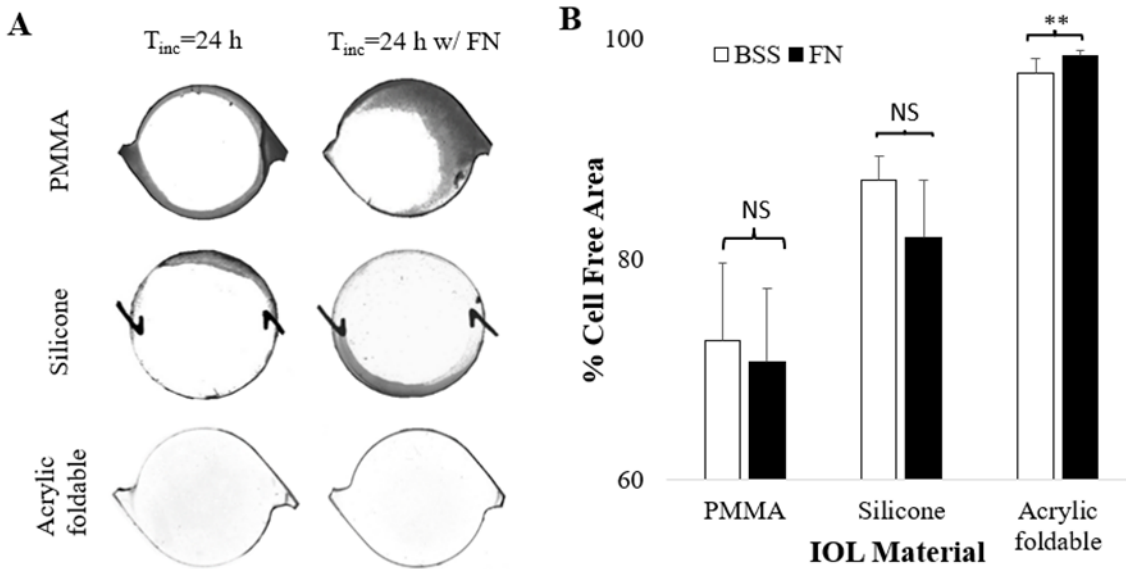


Figure 3.3. Simulated cell infiltration study for different IOL materials with either BSS (as control) or fibronectin (FN) solution (2 uL of 1 mg/mL FN in BSS) at IOL: PC interface and then incubated at 37°C for 24 hours. Data presented as mean \pm SD (N=10). (A) Representative images of simulated cell free regions for PMMA, silicone and acrylic foldable IOLs. (B) Paired t-test analysis of changes in simulated cell free areas at IOL: PC interface with and without the presence of FN (N=10).

3.3.4. Influence of surface coatings and fibronectin on surface hydrophilicity

Surface coatings have been shown to influence protein and, perhaps, fibronectin adsorption (Johnston et al., 2005; Lee et al., 2007; Menzies et al., 2012; Tognetto et al., 2003; Xu et al., 2016b, 2016a) and surface hydrophobicity/hydrophilicity of an IOL material is known to influence IOL: PC interactions (Li et al., 2013; Zhao et al., 2017). Thus, subsequent studies were carried out to understand the influence of a hydrophilic coating and fibronectin adsorption on the surface properties of IOLs. To find the answer, we first measured the surface hydrophobicity of acrylic foldable IOLs modified with Diglyme (DG-acrylic foldable) and acrylic foldable

controls. We observed that there is a statistically significant difference in the surface contact angles between DG-acrylic foldable and controls, in the absence of fibronectin using two-sample t-test (Fig. 3.4), as the Diglyme coating increased the surface hydrophilicity of acrylic foldable IOLs. Interestingly, the presence of fibronectin significantly reduced the surface hydrophobicity indicated by a decrease in surface contact angle of the acrylic foldable IOL from $72.7 \pm 1.2^\circ$ to $25.7 \pm 1.4^\circ$, but not for DG-acrylic foldable IOLs with reported contact angles of $37.6 \pm 0.8^\circ$ and $35.1 \pm 2.7^\circ$ for control and FN groups respectively. These results indicate that the Diglyme coating may reduce fibronectin adsorption and thus diminish the effect of adsorbed fibronectin on surface hydrophilicity. One-way ANOVA on ranks with Dunn's test confirmed that both surface coating and fibronectin adsorption have significant impact on surface contact angles.

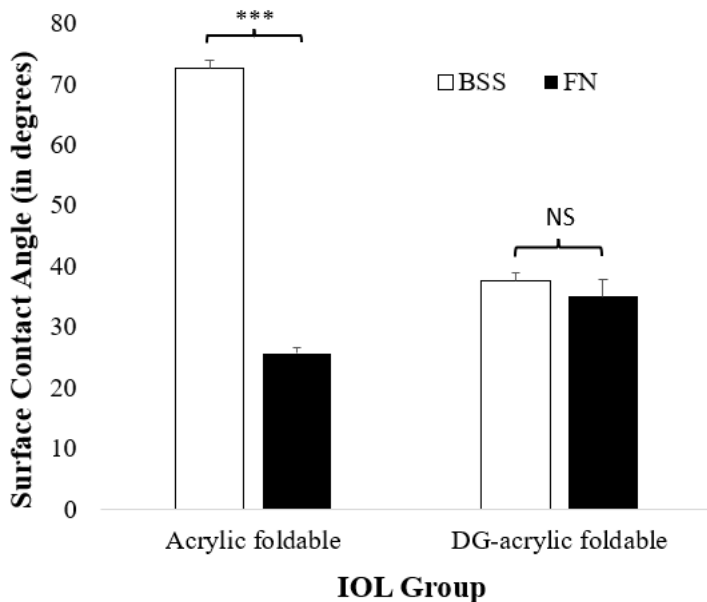


Figure 3.4. Surface contact angle of acrylic foldable and diglyme modified acrylic foldable (DG-acrylic foldable) incubated with either BSS (as control) or fibronectin (FN) solution (2 μ L of 1 mg/mL FN in BSS) at IOL: PC interface for 24 hours @ 37°C. Data presented as mean \pm SD (N=10).

3.3.5. Effect of Surface Coatings on IOL: PC adhesion force

A subsequent study was carried out to investigate whether surface coatings affect the IOL: PC adhesion force. To test that, we compared the adhesion force of acrylic foldable IOLs modified with Diglyme (DG-acrylic foldable) and acrylic foldable IOLs (as controls). Interestingly, we found that surface coatings had no statistically significant influence on the adhesion force (acrylic foldable control, 0.737 ± 0.111 mN; DG-acrylic foldable, 0.654 ± 0.146 mN) after only 5 minutes of incubation (Fig. 3.5). As expected, after incubation for 24 hours @ 37°C, the adhesion force for the acrylic foldable IOLs: PCs increased significantly from 0.737 ± 0.111 mN to 1.934 ± 0.185 mN. On the other hand, the change in IOL: PC adhesion force of DG-acrylic foldable IOLs with increasing incubation time was statistically insignificant according to a two-sample t-test (from 0.654 ± 0.146 mN to 0.785 ± 0.164 mN) (Fig. 3.5). These results confirm that surface properties affect the IOL: PC interaction and DG coating diminishes the increase of adhesion force of IOL: PC. A classic one-way ANOVA with Tukey's test also showed that both material coating and incubation time have significant influence on the IOL: PC adhesion forces.

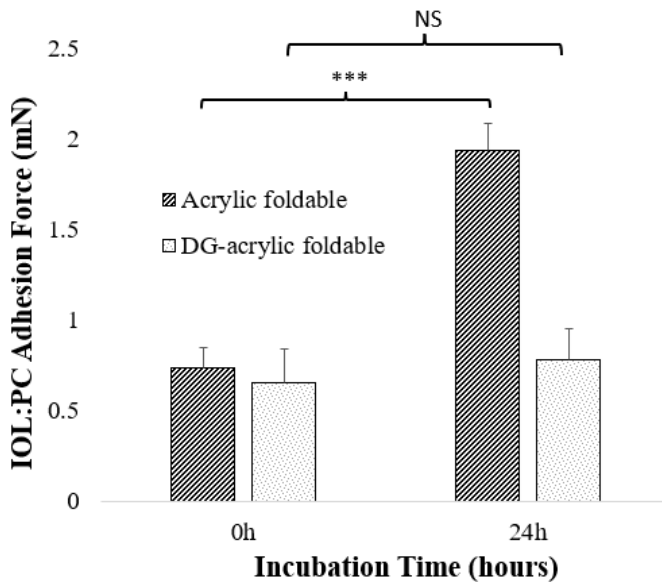


Figure 3.5. Influence of surface coatings on IOL: PC adhesion force of acrylic foldable and DG-modified acrylic foldable IOLs after incubated for different periods of time (0 and 24 hours) @ 37 °C.

We then investigated whether DG coatings and fibronectin presence would alter the adhesion force of IOL: PC. DG coating actually reduced the adhesion force (acrylic foldable control, 2.283 ± 0.149 mN; DG-acrylic foldable, 0.632 ± 0.131 mN) (Fig. 3.6). Furthermore, and in agreement with earlier findings, the presence of fibronectin significantly increased the adhesion force of the acrylic foldable controls with the PC (Fig. 3.6). On the other hand, the presence of fibronectin slightly, but not statistically significantly, reduced the IOL: PC adhesion force of Digylme coated acrylic foldable IOLs (Fig. 3.6). A one-way ANOVA with Tukey's test confirmed that both surface coating and fibronectin presence have significant influence on the IOL: PC adhesion forces.

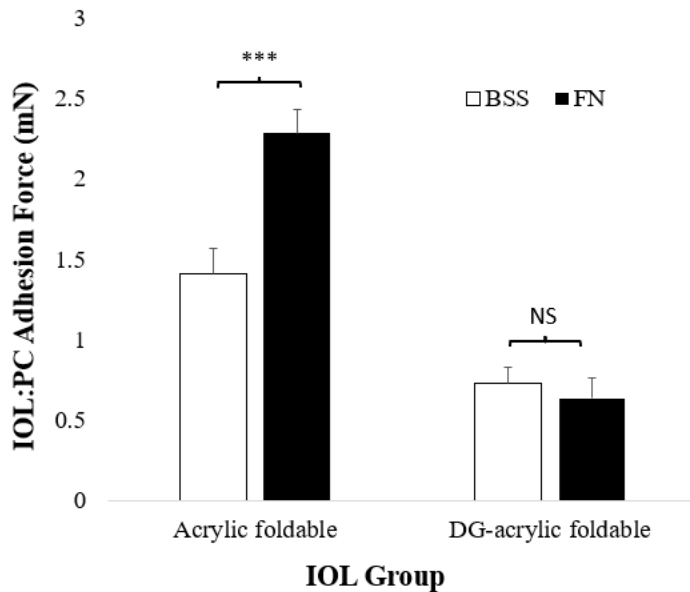


Figure 3.6. IOL: PC adhesion force of acrylic foldable and DG-modified acrylic foldable IOLs with or without the presence of FN (2 uL of 1 mg/mL FN in BSS vs. BSS) at IOL: PC interface @ 37°C for 24 hours.

3.3.6. Simulated cell infiltration for acrylic foldable-DG IOLs

Subsequent studies were carried out to assess the influence of surface coating and fibronectin adsorption on cell infiltration using a simulated cell infiltration model. As expected, and as shown in the representative images (Fig. 3.7A), the presence of fibronectin significantly reduced the cell infiltration at the acrylic foldable IOL: PC (control) assemblies (% cell free area in the presence vs. absence of fibronectin = $98.42 \pm 0.58\%$ vs. $96.84 \pm 1.41\%$) (Fig. 3.7B). On the other hand, a two-sample t-test showed that the presence of fibronectin had no statistically significant influence on the cell infiltration at DG-acrylic foldable IOL: PC assemblies (% cell free area with vs. without fibronectin = $25.05 \pm 12.15\%$ vs. $21.13 \pm 10.15\%$). Also, a one-way ANOVA on ranks with Dunn's test showed that surface coating and fibronectin presence have significant influence on cell infiltration at the IOL: PC interface.

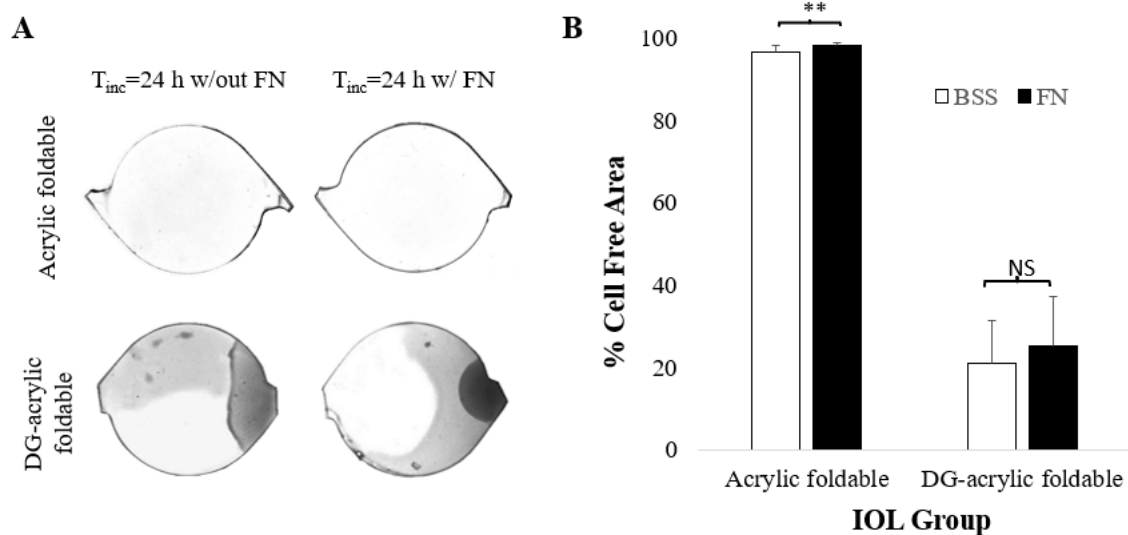


Figure 3.7. (A) Extent of simulated cell infiltration at IOL: PC interface with or without the presence of FN (2 μ L of 1 mg/mL FN in BSS vs. BSS) at IOL: PC interface incubated for 24 hours. Data presented as mean \pm SD (N=10). (B) Paired t-test analysis of changes in the extent of simulated cell (dye) infiltration in different conditions.

3.3.7. Relationship between IOL materials, IOL: PC adhesion force and simulated cell infiltration rates.

To determine the overall relationship between the IOL: PC adhesion force and cell infiltration, all test results were plotted and then compared (Fig. 3.8). The overall results show that the strong adhesion forces are associated with low cell infiltration rate. In fact, there is a very good linear relationship between adhesion force and cell infiltration rates among all commercially available IOLs. Furthermore, the presence of fibronectin has a different effect on the IOL: PC adhesion force and cell infiltration rate. In the case of acrylic foldable IOLs, the presence of fibronectin increases the IOL: PC adhesion force and slightly decreases cell infiltration rates. The trend suggests that fibronectin adsorption may reduce PCO incidence associated with acrylic foldable IOLs. On the other hand, and in the case of other IOLs (PMMA IOLs, silicone IOLs, and DG-acrylic foldable IOLs), the presence of fibronectin decreases the IOL: PC adhesion force and increases cell infiltration rate. The results suggest that fibronectin adsorption may in fact increase PCO incidence associated with the IOLs.

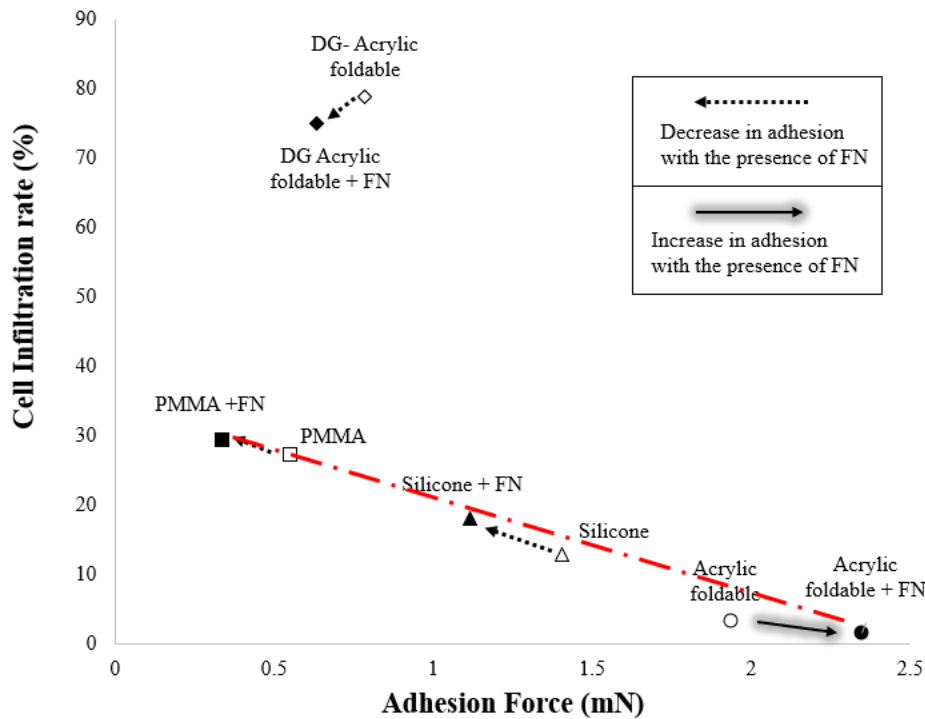


Figure. 3.8. Relationship between the IOL: PC adhesion force and cell infiltration at IOL: PC interface among all tested IOLs, including PMMA, silicone, acrylic foldable and DG-acrylic foldable with and without the presence of fibronectin (FN) after 24h of incubation at 37°C.

3.4. Discussion

Our study has shown that the influence of fibronectin adsorption on IOL: PC interaction varies among different IOLs. We found that fibronectin adsorption increased the hydrophilicity of acrylic foldable IOLs but had no influence on the hydrophilicity of PMMA IOLs and silicone IOLs. The findings are consistent with an earlier observation (Schroeder et al., 2009b). It is possible that the increase in hydrophilicity of the IOL surface resulting from fibronectin adsorption may increase the adhesiveness or adhesion force of IOLs and PCs via hydrophilic interactions (Schroeder et al., 2009; Yang et al., 2017) and/or fibronectin: collagen binding (Shimizu et al., 1997b; Sottile et al., 2007b). In fact, the results from many previous studies

suggest that the increased binding between acrylic foldable IOLs and PCs is responsible for the lowest rates of PCO in the clinic (Vanslyke et al., 2018; Linnola, 1997; Linnola et al., 2003b, 2000b; Oshika et al., 1998b, 1996; Rönbeck et al., 2009b; Rønbeck and Kugelberg, 2014b; Ursell et al., 1998b). These findings support that this new *in vitro* system can predict the PCO outcome and, can potentially aid future development of new IOL materials without relying on extensive cell culture and animal studies.

Our results indicate that adsorbed fibronectin may improve the binding of acrylic foldable IOLs and the PC. Studies have shown that fibronectin adsorption on acrylic foldable IOLs may lead to the formation of a sandwich-like structure (capsule/fibronectin/cell layer/fibronectin/IOL surface) (Linnola, 1997b). Such a bond between PC: IOL may be responsible for the low PCO rates in eyes with acrylic foldable IOLs compared to other types of IOLs (Linnola et al., 2000b; Wormstone et al., 2021). The sandwich theory suggests that cells may affect the interaction between the IOL and the PC by adhering to the IOL material as well as the PC, increasing the interaction between the IOL and the capsule (Linnola, 1997b). However, a recent study to examine the sandwich theory suggest that the initial growth of the cells in the PC may not be avoided by a strong interaction between the IOL edge and the capsule (Wormstone et al., 2021). But over time, when the posterior and the anterior capsules fuse together, the sandwich theory becomes more effective, preventing further growth of cells and PCO progression (Wormstone et al., 2021). In another study, it was concluded that the cell interaction with the IOL surface is limited (Eldred et al., 2019a) . Furthermore, given the choice between the lens capsule and an IOL, the cells are more likely to grow in the lens capsule in an environment supporting cell proliferation and adhesion, than on the surface of a synthetic IOL (Eldred et al., 2019a). Such potential influence of LECs on the IOL: PC adhesion force is beyond the scope of

this work and will be investigated in our future studies. In accordance with previous studies, among all tested IOLs (hydrophobic acrylic foldable, PMMA and silicone and DG-acrylic foldable), acrylic foldable IOLs were found to accumulate the largest amount of fibronectin (Linnola et al., 2003b; Linnola et al., 2000c, 2000b) and are associated with the highest degree of IOL: PC adhesion (Linnola, 1997; Linnola et al., 2000b, 2000c). It is likely that the IOL design, such as the optic size and round vs. sharp edge may have an impact on the adhesion force. Since studies conducted thus far have been focused on deciphering the role of different IOL materials in mediating IOL: PC interactions, the influence of IOL design on IOL: PC adhesion forces should be examined in future studies. While fibronectin was investigated here, we are aware that other extracellular matrix proteins, such as vitronectin, laminin, and collagen type IV, may also be adsorbed onto the IOL surface (Linnola et al., 2003b). The influence of other ECM proteins on IOL: PC interaction should be investigated in the future.

Our studies have also found that IOL: PC adhesion force for both PMMA and silicone IOLs did not change in the presence of fibronectin. These observations support findings in literature that indicated reduced fibronectin adsorption on both of these IOLs *in vitro* (Carole A. Cooke et al., 2006; Linnola et al., 2000a; Thom et al., 2019; Tortolano et al., 2015). These observations are further substantiated in *ex vivo* histological studies that showed insignificant amounts of fibronectin on the lens capsule and the IOL for both PMMA and silicone IOLs (Linnola et al., 2000b, 2000c). Our simulated cell infiltration study further confirmed that the adhesion of both PMMA and silicone IOLs with the lens capsule is in fact unaffected by the presence of fibronectin by reporting insignificant changes in the areas free of simulated cell infiltration when compared with control groups that contained no fibronectin. These results suggest that the

reduction of fibronectin presence in aqueous humor may be used as an alternative strategy to delay or diminish PCO formation following IOL implantation.

The influence of surface modified acrylic foldable IOLs- DG-acrylic foldable IOLs was examined on fibronectin adsorption and IOL: PC interactions. Our study showed that DG coating significantly reduced IOL: PC adhesion force and also alleviated the influence of adsorbed fibronectin on IOL: PC interactions. While the causes for the low adhesion forces of the Diglyme group are yet to be determined, the high surface hydrophilicity and low protein adsorption and cell affinity of Diglyme group may be responsible (Nisol et al., 2018; Ribeiro et al., 2009; Welch et al., 2016;). In fact, a study based on plasma polymerized Diglyme films on PMMA for creating biocompatible hydrophilic polymer surfaces showed a remarkable decrease in the surface contact angle with increased surface hydrophilicity (Cley et al., 2003). Another study that tested the intensities of protein fouling on Diglyme coated surfaces using negatively and positively charged proteins showed negligible protein adsorption on the surface (Muir et al., 2008). Overall results suggest that a hydrophilic coating, such as diglyme, may increase PCO incidence rate by diminishing fibronectin adsorption, reducing the IOL: PC adhesion force, and permitting a large extent of cell infiltration at the IOL: PC interface. Conversely, high fibronectin affinity materials or coating may be synthesized and used to produce new IOLs with low PCO potential.

3.5. Conclusion

Here we report a potential effect of fibronectin adsorption and hydrophilic coatings in altering surface properties of IOLs and their influence on IOL: PC adhesion forces and PCO potential using a newly established *in vitro* system. The overall results suggest that fibronectin adsorption

increases the adhesion force of acrylic foldable IOLs and the PC. Such strong IOL: PC adhesion force of acrylic foldable IOLs may be responsible for reducing the extent of cell infiltration and the incidence rate of PCO. However, fibronectin would have either no effect or an adverse effect on the IOL: PC interactions of other commercial IOLs, such as PMMA IOLs and silicone IOLs. In the case of surface modification, we find that a hydrophilic coating, such as Diglyme, could produce an adverse effect by increasing PCO potential via reduced fibronectin adsorption, and weakening the adhesion force resulting in increased cell infiltration at the IOL: PC interface. The overall results, at least in the case of acrylic foldable IOLs, provide major substantiations to support an interesting interplay among various key factors, and that high fibronectin affinity and hydrophobic surface characteristics may increase IOL: PC adhesiveness, lessen cell infiltration and, thus, reduce PCO incidence in the clinical setting.

CHAPTER 4

A 3D In vitro Model for Assessing Intraocular Lens: Posterior Lens Capsule Interactions and their Influence on Lens Epithelial Cell Responses

4.1. Introduction

Posterior Capsule Opacification (PCO) is a postoperative complication of intraocular lens (IOL) implantation.(Jaitli et al., 2021d; Kurosaka et al., 2002; Mencucci et al., 2015b) PCO, accompanied with the formation of unwanted extracellular matrix under and around the lens, may impair vision and render the treatment useless.(Cooksley et al., 2021b; Linnola, 1997c; Mencucci et al., 2015b; Wang et al., 2017) PCO occurs in 50% of adult cases and 100% of pediatrics up to 5 years after surgery.(Konopińska et al., 2021b; Linnola, 1997c; Vasavada et al., 2011) While neodymium: yttrium aluminum garnet (Nd: YAG) laser capsulotomy procedure can ablate the central posterior capsule (PC) and associated cells to restore vision, this procedure is expensive and comes with its complications.(Khambhiphant et al., 2015; Wang et al., 2017) Hence, it is important that new IOLs can be designed with low PCO potential. However, PCO is a complex mechanism and the factors of IOL design affecting its progression are not fully understood.

It is well established that PCO is characterized by the migration and proliferation of residual lens epithelial cells (LEC) on the posterior lens capsule (PLC) or from the anterior and equator of the capsule into the space under and sometimes around the IOL.(Cooksley et al., 2021b; Linnola, 1997c) The cells either differentiate abnormally and deposit extracellular matrix such as collagen that impedes vision or they may form large and clustered wedl or bladder cells that also cause opacification.(Konopińska et al., 2021b) Interestingly, clinical reports show that the severity of these cell responses differ by IOL type.(Katayama et al., 2007a; Ursell et al., 1998c) Thus, several hypothesis have been proposed to explain how IOL design would affect PCO formation.(Cooksley et al., 2021b; Jaitli et al., 2021d; Linnola, 1997c) One of the most well recognized hypothesis, the “No space, no cell” hypothesis, states that full contact between the

IOL and the PLC will yield insufficient space for LEC immigration and proliferation at the interface (Schematic 4.1).(Assia et al., 1999; Nishi et al., 2007) In fact, this hypothesis is supported by the results from several early studies (Table 4.3). First, studies have reported that IOLs with low PCO incidence such as polyacrylic IOLs have tight binding to the capsular bag and in vitro PLC,(Jaitli et al., 2021a; Katayama et al., 2007a; Oshika et al., 1998d; Wejde et al., 2003c) while IOLs with high PCO incidence such as silicone and PMMA IOLs have low binding to the lens capsule *in vitro*.(Katayama et al., 2007a; Oshika et al., 1998d) In addition, Optical Coherence Tomography post-operatively revealed that the severity of PCO is directly related to the space at the interface between an IOL and PC (Table 4.3).(Hayashi et al., 2002; Moreno-Montañés et al., 2008; S.-S. Yu et al., 2021) While there is a good relationship between IOL:PC affinity and PCO potential, there is insufficient evidence to support that IOL:PC binding and closure would hinder the migration and proliferation of LECs at IOL:PC interface which was the objective of the investigation.

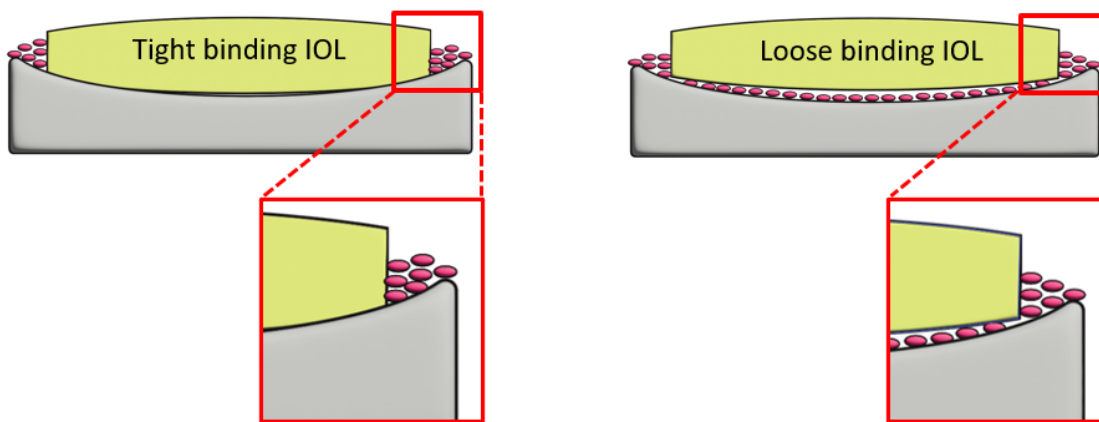


Figure 4.1. A schematic for “No Space, No Cell” hypothesis.

Metric	Acrylic	Silicone	PMMA
PCO Incidence in vivo	11.75%	33.5%	43.65%
Distance at IOL: PLC interface in vivo	26 μm	49.33 μm	98.66 μm

Table 4.1. Quantitative evidence supporting the “No space, no cell” hypothesis. Distance at IOL: PLC interface is directly proportional to PCO incidence.

To find the answer as part of our early investigation, we have realized that there is no suitable *in vitro* model to simulate LEC responses at the 3D IOL: PC interaction. Specifically, almost all *in vitro* models have been established on a flat platform such as culture plates, collagen membrane, or PDMS films where LECs are seeded, and their responses assessed.(Haeussler, 2011; Kurosaka et al., 2002; Mencucci et al., 2015b; Sun et al., 2014; Wang et al., 2017) Furthermore, to better simulate the PLC environment, the testing substrates can be coated with various lens capsule extracellular matrix (ECM) such as collagen type IV or laminin.(Haeussler, 2011; Mencucci et al., 2015b) Although these systems allow the assessment of direct interactions between LECs, substrates (or ECM), and IOLs, these models omit the structure and geometry of the Posterior Capsule. In other words, most of these models can be used to assess how only the substrates and IOL affect LEC proliferation and migration. Therefore, due to their 2D design, these models are unable to simulate IOL: PC interactions, including the proper *in vivo* IOL and PC closure mechanism which is consequential to IOL performance in response to LEC proliferation and infiltration.

To satisfy the need for an *in vitro* model capable of assessing the IOL: PLC interplay in 3D, a 3D simulated PLC *in vitro* model was recently developed. (Jaitli et al., 2021d, 2021a) In this model, PLC was made of crosslinked gelatin in either flat form or with a small indentation to assess the

interactions between IOLs and PLC by measuring the adhesion force using a micro-adhesion measurement apparatus.(Jaitli et al., 2021d, 2021a) The results generated from these studies showed that there is a good inverse relationship between the adhesion force and clinical PCO performance.(Jaitli et al., 2021d, 2021a) Despite of these exciting advancements, this model cannot be used to explore how IOL:PLC binding affinity would impact LEC capability of initiating PCO formation because it cannot recreate the IOL:PLC closure mechanism.

The closure mechanism of IOLs and PLC has been studied using Optical Coherence Tomography, a non-invasive imaging system (Table 4.2). Monitoring the IOL:PLC early interactions has shown that the PLC would gradually undergo “shrink wrapping” around the IOL which results in a capsular bend that limits infiltration depending on the IOL implanted.(Hayashi et al., 2002; Nishi et al., 2002) An important step in the capsular bend formation is the first contact between the IOL and PLC which starts from edge of IOLs around day 3 after placement,(Sacu et al., 2005b) and may spread toward the center of the IOL by the second week .(Hayashi et al., 2002) Such edge to center closure mechanism of the IOL on the PLC is believed to be the gatekeeper of initial LEC responses and thus required to accurately test the “No space, no cell” hypothesis.(Hayashi et al., 2002; Sacu et al., 2005b; M. Yu et al., 2021) To accurately simulate this interplay, the geometry, specifically degree of curvature of the simulated PLC must be similar to that of the native PLC after lens phacoemulsification. Currently, no in vitro model possesses this feature.

To simulate such a 3D IOL: PLC interaction, we intended to create a simulated PLC that mimics human PLC geometry. For that, we discovered that the normal geometry of human lens posterior capsule includes a curvature degree that ranges from 80° to 100° (Table 4.2).(Cabeza-Gil et al., 2021; Hecht, 1987; Oyster, 1999) Using a 3D print that possessed dimensions closely

resembling the human PLC as an imprint, we produced a simulated PLC with similar curvature to the native PLC. First, we examined whether IOL: PLC interactions were simulated effectively by evaluating IOL adhesion force to the simulated PLC and by measuring the space present at the IOL: PLC interface. We then quantified the space available at the edge of the IOL: PLC interface using a contrast enhancer to simulate LEC infiltration. Finally, LECs were then introduced to the system to study how the potential influence of IOL: PLC interactions affects LEC infiltration and proliferation at the interface.

Metric	Human Lens Capsule
Equatorial diameter	9-10 mm
Radius of curvature of PLC	8-10 mm
Curvature Degree of PLC	80-100°

Table 4.2. Dimensions of the native posterior lens capsule.



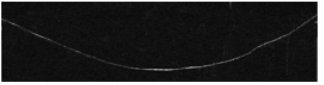
Dimensions	Mold #1	Mold #2	Mold #3
OCT Image			
Equatorial diameter	10 mm	10 mm	12 mm
Radius of curvature of PLC	17 mm	9 mm	6.5 mm
Curvature Degree of PLC	42°	80°	100°

Table 4.3. Potential Curvatures for simulated PLC and their dimensions measured using OCT.

4.2. Materials and methods

4.2.1. Intraocular Lenses

Three commercially available IOLs were used in this investigation. Acrylic foldable IOLs were a single piece with 6.0 mm biconvex optic and planar haptics, with an overall length of 13.0 mm, with a dioptric power of 21.0D (Alcon's SN60WF, Alcon Research, Fort Worth, Texas). The Polymethyl methacrylate (PMMA) IOLs were a single piece, 5.5 mm biconvex PMMA round posterior edge optic with an overall length of 13 mm and a dioptric power of 23.5D (Alcon's MTA4U0, Alcon Research, Fort Worth, Texas). The Silicone IOLs were a three-piece, posterior chamber biconvex silicone 6.0 mm optics with round edged profile and blue PMMA mod C haptics with an overall length of 13.0 mm and a dioptric power of 20.0D (Allergan's AMO Array SA40N, Allergan Inc, Irvine, California).

4.2.2. Fabrication and characterization of 3D simulated PLC

To investigate IOL and PLC interaction, we first produced a simulated PLC which possesses physical characteristics as the human lens capsule. Based on various publications, we have concluded that the human lens capsule should possess an equatorial diameter between 9 to 10 mm, a posterior radius of curvature between 8 to 10 mm, and a degree of curvature ranging from 80° to 100° (Table 2). To achieve this goal, we fabricated multiple simulated PLC using 3D prints with different dimensions. Briefly, gelatin was crosslinked to form the simulated PLC as previously published with minor modifications.(Jaitli et al., 2021d, 2021a) The 3D prints were used to create different curvatures in the gelatin by placing the 3D print on the molten gelatin during the crosslinking process. After the gelatin was fully crosslinked, the 3D print was carefully removed to expose the simulated PLC area. Next, the physical features of the simulated

PLCs were characterized using OCT imaging (Table 3). The simulated PLC with dimensions closest to the Human Lens Capsule was chosen for subsequent studies.

4.2.3. Adhesion Force Measurements

To confirm that our simulated PLC could mimic human PLC and IOL physical interactions, IOL adhesion force measurements were carried out using a previously established custom-made adhesion force apparatus (Jaitli et al., 2022, 2021a). To do this, an Acrylic, PMMA or Silicone IOL fitted with a 3-D printed pinhole structure on its anterior surface was placed on the simulated PLC. A flat and clear light weighted washer with inner and outer dimensions of 6.5 mm and 2.7 mm was placed on the IOL to prevent detachment when adding media. Next, 1 mL of Dulbecco's Minimum Essential Media (DMEM) was pipetted on the simulated PLC and the IOL: PLC assembly was incubated in a temperature-controlled chamber at 37 ± 1 °C for 24 hours. After 24 hours, the IOL adhesion force was measured.

4.2.4. OCT Imaging of IOL: PLC Closure Mechanism

Next, the closure mechanisms of the three IOLs to the simulated PLC was evaluated using an Optical Coherence Tomography system purchased from Thorlabs. First, an IOL was placed on the simulated PLC with a clear washer on top then the assembly was immersed in 1 mL of media. At different time points, the IOL: PLC assembly was imaged using OCT. The OCT had an imaging field of view adjusted for a depth of 2 mm and a lateral size of 8 mm to allow enough penetration to visualize the entire IOL: PLC interface. The image was taken across the origin points of the haptic on the optic body to ensure consistency. After imaging, the IOL: PLC distance, area, and percentage of IOL in contact with the PLC were measured using Image J analysis software.

4.2.5. IOL: PLC Interface Barrier Testing

After evaluating the closure mechanism of IOLs on the simulated PLC, their interface was tested for an opening at the IOL: PLC barrier that is too small to be visualized by OCT. This was done by measuring the Contrast Agent Enhancer (CAE) intensity at the IOL: PLC interface. First, the IOLs were placed on the simulated PLC and incubated at 37°C to initiate IOL: PLC closure. After different time points of incubation, 10 µL of the CAE was pipetted onto the edge of the IOL: PLC interface and OCT images were taken. Using ImageJ analysis software, the intensity of CAE at the IOL: PLC interface was measured then divided by the area at the interface. The higher the intensity/area, the larger the space at the edge of the IOL: PLC interface, and the higher the chances of LEC infiltration.

4.2.6. Assessment of IOL: PLC affinity on simulated LEC infiltration

To test the “No space, no cell” hypothesis, the influence of IOL: PLC affinity on available space at the interface was tested by simulating LEC infiltration using a contrast enhancer agent. The IOL: PLC systems were incubated for 0, 24 and 48 hours then contrast enhancer agent was placed at the edge of the IOL: PLC interface and its infiltration into the IOL: PLC space was visualized using OCT imaging. The percentage of area infiltrated by the contrast enhancer at each time point was measured.

4.2.7. Assessment of IOL: PLC affinity on LEC infiltration

To directly test the “No space, no cell” hypothesis, Human Lens Epithelial Cell Line B-3 (CRL-11421) purchased from the American Type Culture Collection (ATCC; Manassas, USA) was used. First, the influence of IOL: PLC affinity on LEC infiltration was determined. To achieve this, 10 µL of Human Lens Epithelial Cells (LECs) (10, 000 cells/µL) were seeded on the edge of the IOL: PLC interface. After LEC attachment, the IOL: PLC system was cultured in DMEM supplemented with 10% Fetal Bovine Serum (FBS) and 1% Penicillin-Streptomycin (PenStrep)

as previously described.(Wang et al., 2017) Over 5 days, microscopic images and OCT images of the IOL: PLC edge were taken to assess LEC infiltration. The cell distribution in each IOL: PLC system was measured and compared.

4.2.8. Assessment of IOL: PLC affinity on LEC proliferation

After testing the influence of IOL: PLC affinity on LEC infiltration, LEC proliferation at the IOL: PLC interface was assessed since the “No space, no cell” hypothesis postulates LECs may cease to proliferate if IOL: PLC binding is high, leaving little to no space. To test this theory, 100 μL of LECs (1000 cells/ μL) were seeded on the simulated PLC and allowed to attach. The excess media was discarded followed by IOL placement on the simulated PLC. After IOL: PLC interactions for 4 hours, the system was covered with cell culture media and LEC proliferation was monitored over time by taking microscopic images of the IOL: PLC interface. The cell density over time was measured.

4.2.9. Assessment of LEC metabolic activity at IOL: PLC interface

Next, the metabolic activity of LECs at the IOL: PLC interface was assessed because the “No space, no cell” hypothesis maintains that high binding IOLs that leave no space at the IOL: PLC interface will cause the contact inhibition of LECs present. This experiment was carried out on day 7 of proliferation experiments using Ki-67 antibody to stain LECs that were metabolically active, thus indirectly identifying contact inhibited LECs.

4.2.10. Statistical Analyses

Statistical analyses were carried out on R studio with a confidence interval of 95% for all tests. Welch’s ANOVA with Games-Howell test were done to determine significant statistical differences in adhesion force of Acrylic, PMMA, and Silicone IOLs. One-way ANOVA and Tukey’s test were carried out to statistically analyze differences in IOL: PLC distance, IOL: PLC

contact, and IOL: PLC Area at each time point. One-way ANOVA with Dunnett's and Games-Howell tests were used to determine the influence of IOL: PLC interactions on LEC infiltration by comparing mean cell density in the three groups at fixed distances along the infiltration path. Similarly, One-way ANOVA combined with Tukey's and Games Howell tests were used to determine whether the IOL: PLC interactions had a significant effect on LEC proliferation at fixed time points

4.3. Results

4.3.1. Physical interactions between IOLs and simulated PLC

The IOL adhesion force and the distance at the IOL: PLC interface between IOLs and our simulated PLC were first evaluated to ascertain whether our model could recreate in vivo IOL and Human Lens Capsule physical interactions. As expected, all IOLs had different adhesion force to the simulated PLC (Fig 4.2A). Acrylic IOL with low PCO incidence had a high adhesion force which was predicted by the "No space, no cell" hypothesis. We also found, in consistent with in vivo studies, Acrylic IOL had the smallest IOL: PLC distance and PMMA IOL had the largest IOL: PLC distance (Fig 4.2B). This result supports the notion that strong affinity between IOL: PLC will pull the IOL closer to the PLC, thus reducing the space at the interface. To test this notion, the closure process of the IOLs to the simulated PLC was characterized over time. As a matter of fact, the higher the IOL adhesion force to the simulated PLC, the faster the IOL met the simulated PLC (Fig 4.3). Overall, our results show our simulated PLC effectively recreated IOL and Human Lens Capsule interactions. Additionally, the results support our hypothesis that strong IOL: PLC binding force will influence IOL: PLC closure. However, the influence of IOL: PLC affinity on LEC infiltration is still unclear.

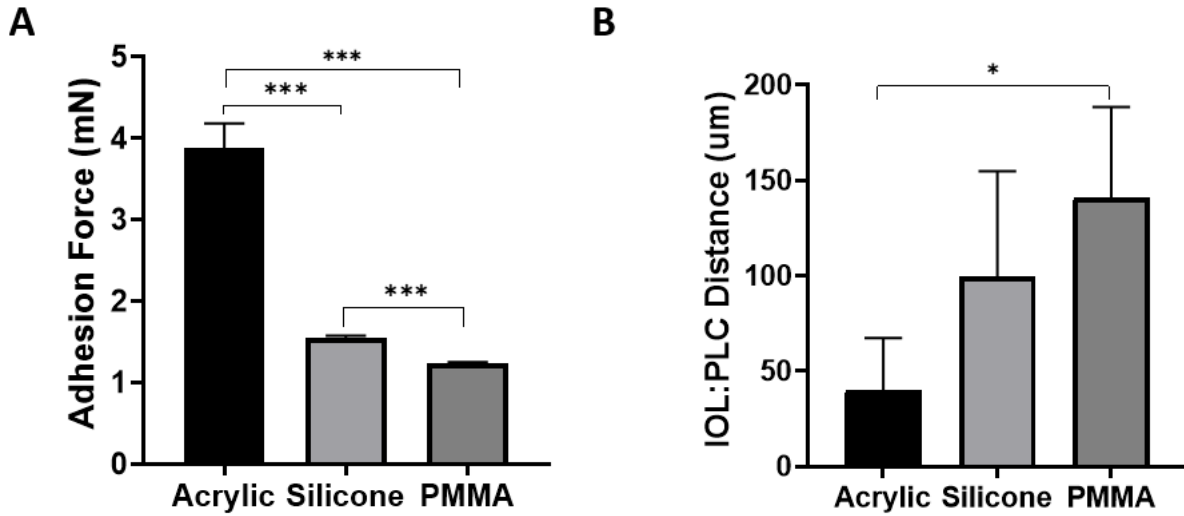


Figure 4.2. Physical interactions between IOL and simulated PLCs. A) Adhesion force of different IOLs to the simulated PLC. B) The distance between the IOL and simulated PLC.

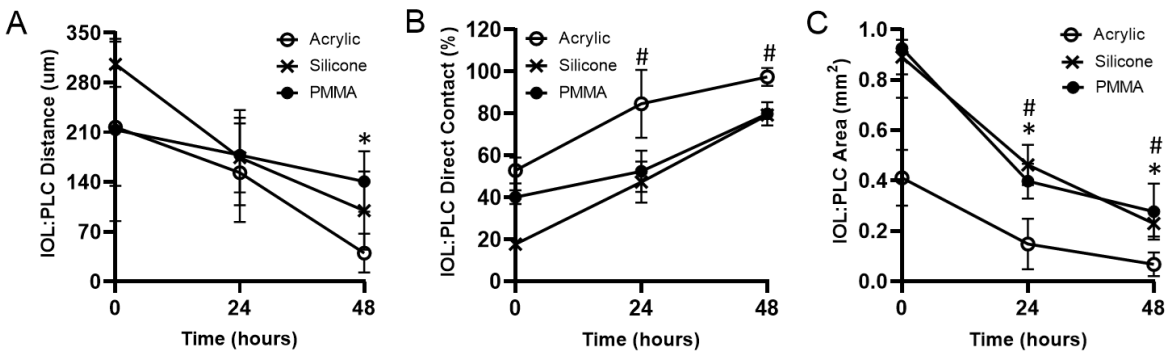


Figure 4.3. The rate of IOL: PLC closure. A) Distance of IOLs from simulated PLC. B) Percent of IOLs in direct contact with simulated PLC. C) Area between IOLs and simulated PLC. Statistical analysis was done using One-way ANOVA at each timepoint with Tukey's post-hoc test and an alpha of 0.05. '*' represents statistical significance of Acrylic vs PMMA, '#' represents statistical significance of Acrylic vs Silicone, '\$' represents statistical significance of Silicone vs PMMA.

4.3.2. The influence of IOL: PLC affinity on simulated cell infiltration

Thereafter, we tested the hypothesis that strong IOL: PLC affinity will limit cell infiltration. This was done by simulating LEC infiltration using a contrast enhancer agent. As expected, we found that large amounts of the contrast agent infiltrated the PMMA IOL: PLC interface whereas Acrylic IOL: PLC interface had low infiltration (Fig 4.4). Interestingly, the longer the IOL was incubated with the PLC, the lower the amount of contrast enhancer that infiltrated the IOL: PLC interface for all IOLs. However, Acrylic IOL with a higher affinity for the PLC had the lowest amount of contrast enhancer at its IOL: PLC interface at all time points. This result supports the hypothesis that tight binding will reduce the infiltration of the IOL: PLC interface. Although the performance of the IOL: PLC systems against LEC infiltration was indicated, it is unclear whether how these IOL: PLC interactions will affect LEC responses.

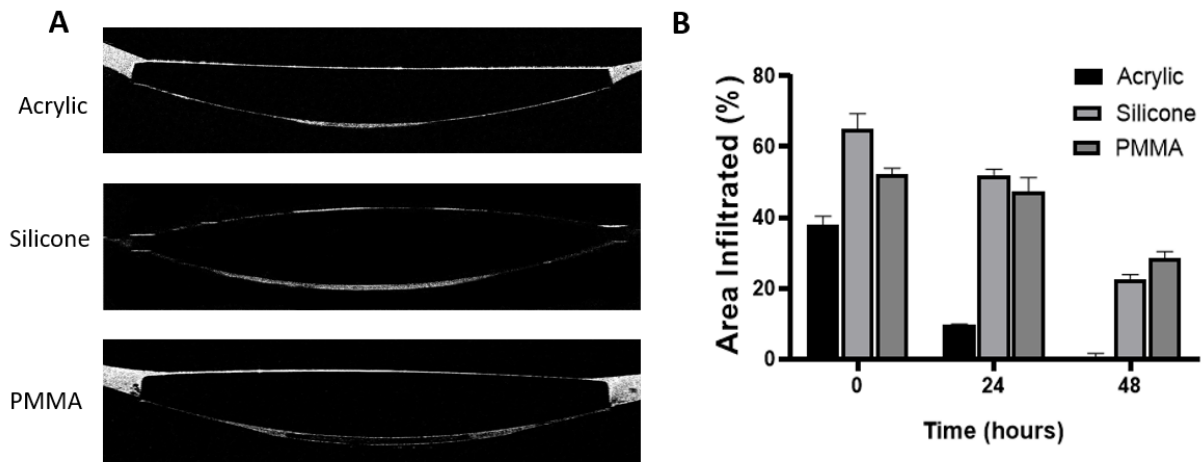


Figure 4.4. Evaluation of IOL: PLC closure by infiltration of a contrast enhancer. A) Images of contrast agent infiltration in Acrylic, PMMA and silicone IOLs. B) Percentage area at IOL: PLC interface infiltrated by contrast agent.

4.3.3. The influence of IOL: PLC affinity on LEC infiltration

To understand how IOL: PLC affinity affects LEC infiltration, LECs were seeded on the edge of the PLC and their attempted infiltration was assessed. Using OCT, we could visualize LECs on the edge and at the surface of the Acrylic IOL but there were no LECs at the Acrylic IOL: PLC interface (Fig 4.5A). On the other hand, LECs could be seen at the Silicone and PMMA IOL: PLC interface. Quantification of LEC distribution from the LEC seeding point towards the IOL: PLC interface showed a large density of LECs infiltrated the PMMA IOL: PLC interface whereas Acrylic IOL: PLC interface was minimally infiltrated (Fig 4.5B). This result directly supported the hypothesis that the high binding of Acrylic IOL to the PLC prevents LEC infiltration, and low binding of PMMA IOL to the PLC allows LEC infiltration. Technically, this experiment only tested the influence of IOL: PLC affinity on LEC infiltration. The effect of IOL: PLC binding on LEC proliferation was not determined.

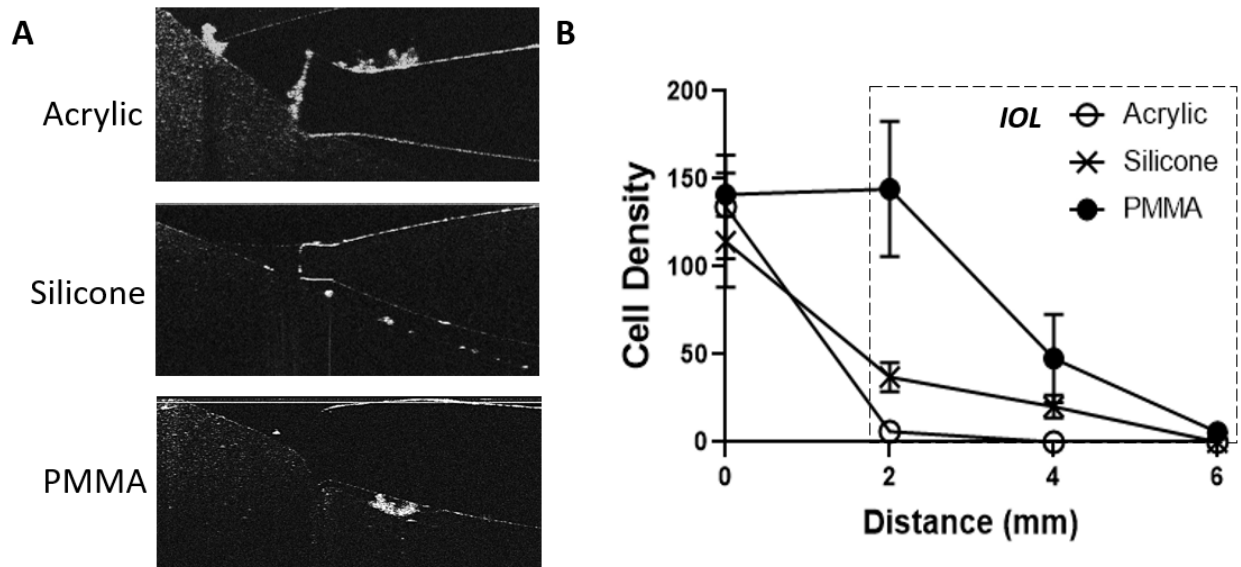


Figure 4.5. Evaluation of IOL: PLC closure's influence on LEC infiltration. A) OCT images showing LEC's attempt to infiltrate the IOL: PLC interface. B) Quantitative representation of LEC infiltration from the simulated PLC to the IOL: PLC interface. (Dotted box represents area covered by IOL).

4.3.4. The influence of IOL: PLC affinity on LEC proliferation

Thus, another experiment was designed to test the influence of IOL: PLC affinity on LEC proliferation. Here, the LECs were seeded at the IOL: PLC interface and their cell density was measured over time. As expected, LECs freely proliferated in PMMA IOL: PLC interface while LEC cell density did not significantly increase in the Acrylic IOL: PLC interface (Fig 4.6). This result supports our hypothesis that strong IOL: PLC affinity leaves no space for LECs to proliferate. However, the cellular mechanism behind the behavior of LECs at the interface was not clear.

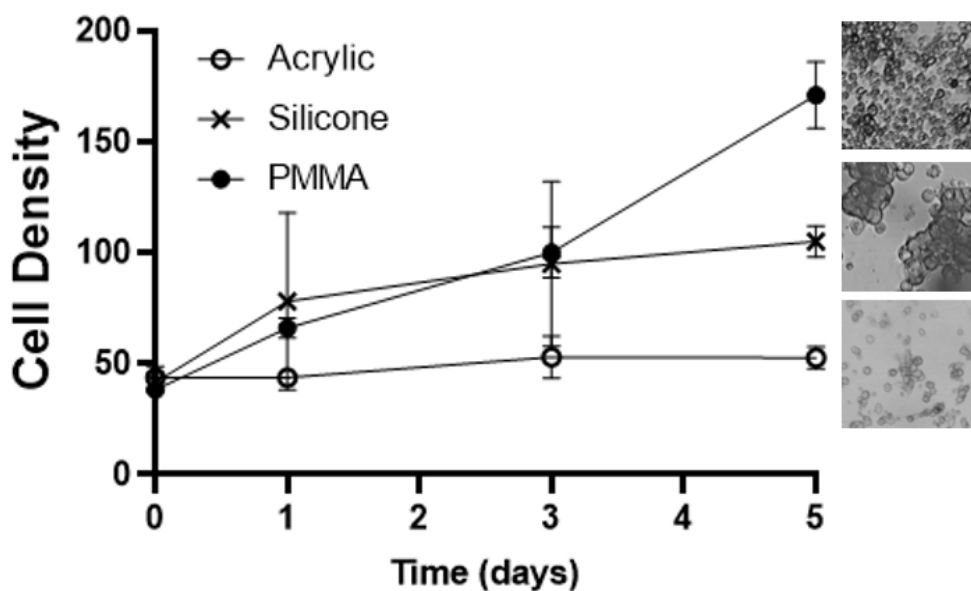


Figure 4.6. Evaluation of LEC proliferation at IOL: PLC interface. Cell density at IOL: PLC interface over time with microscope images of ROIs of LECs in Acrylic, PMMA and Silicone groups at day 5.

4.3.5. The influence of IOL: PLC affinity on LEC metabolic activity

The LEC metabolic activity was evaluated to understand the mechanism governing LEC proliferation in only low binding PMMA and Silicone IOL: PLC interfaces. Ki-67 antibody was used to tag LECs that were metabolically active thus indirectly identifying contact inhibited LECs. Interestingly, LECs present at the Acrylic IOL: PLC interface had the lowest percentage of metabolically active cells. This indicates that Acrylic IOL's strong binding with the PLC caused LECs to become contact inhibited hence no proliferation at the interface occurred. On the other hand, PMMA IOL: PLC binding was loose so LECs were not prompted to become contact inhibited. Overall, our results support the hypothesis that strong IOL: PLC affinity will prevent LEC infiltration and proliferation, hence will reduce the chances of PCO formation.

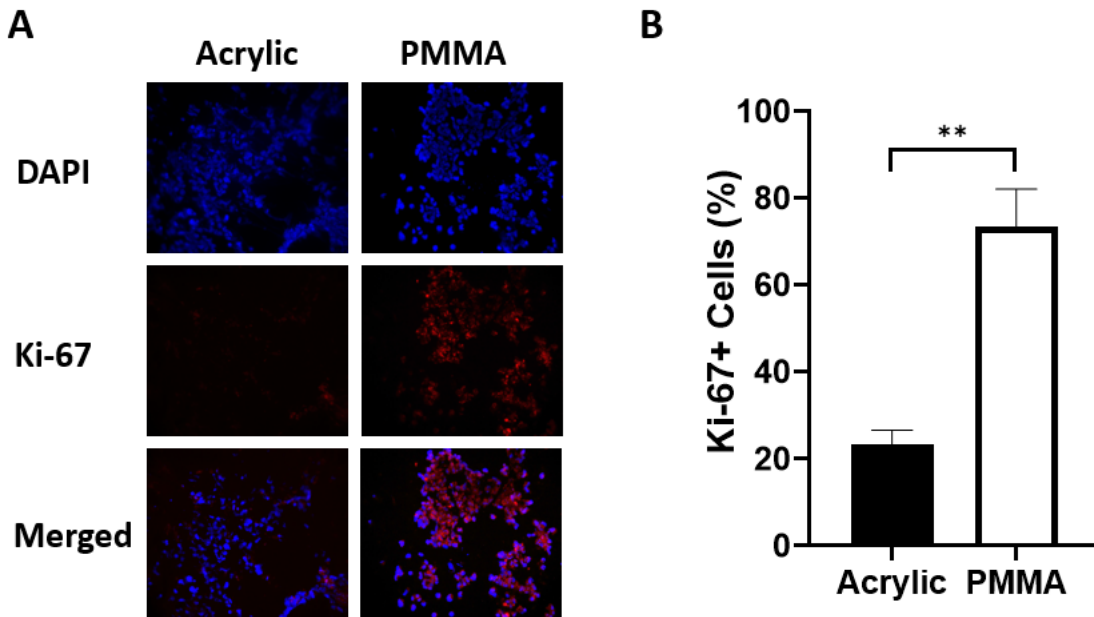


Figure 4.7. Metabolic activity of LECs at the IOL: PLC interface. A) Images of LECs stained with ki-67 antibody and counterstained with DAPI B) Percentage of metabolically active cells.

4.4. Discussion

A novel gelatin-based 3D in vitro posterior lens capsule was developed to test the “No space, no cell” hypothesis by studying the influence of IOL and PC interactions on cell responses. Although this work was a first of its kind, it was based on previous efforts to understand the role of IOL adhesion force on PCO formation using a similar simulated PLC with minor modifications.(Jaitli et al., 2022, 2021d, 2021a) In this current work, the previous system was altered to simulate the edge-to-center closure mechanism of IOLs to the PLC by introducing curvature to the geometry of the simulated PLC. Thus, allowing the direct assessment of the interactions between the IOL and PLC on LEC responses.

Optical Coherence Tomography (OCT) was utilized to visualize the interactions between the IOL and the simulated PLC. This technology has been used to assess the time taken for different IOLs to fully contact the PLC after surgical placement. It has been documented that the closure time of IOLs differ based on IOL material and design,(Hayashi et al., 2002; Nishi et al., 2002) and that IOLs with PCO have more space at the IOL: PC interface.(S.-S. Yu et al., 2021) However, the direct relationship between these variables and LEC responses had not been previously characterized. Hence, using our system, we sought out to simulate the closure mechanism of the IOL to the PC, and to determine the influence of space at the IOL: PC interface on LEC infiltration, proliferation, and epithelial-to-mesenchymal transition. First, we optimized the geometry of our simulated PLC to allow an edge-to-center closure of the IOL to the PC. Next, we found that the closure time of IOLs was related to the PCO incidence. Acrylic IOL with a low PCO incidence achieved the fastest closure time whereas PMMA IOL with a high PCO incidence was the slowest to contact the simulated PLC. In fact, while other IOLs completely covered the PLC, PMMA failed to completely enclose with the simulated PLC,

leaving a gap at the center even after five to seven days of incubation. Although this result supports the “No space, no cell” hypothesis, studies carried out on in vivo closure times have shown conflicting results.(Hayashi et al., 2002) This could be explained by differences in surgical technique and style of measurement. Nevertheless, there was a strong inverse relationship between PCO incidence and closure time.

In addition to assessing the relationship between PCO incidence and IOL closure mechanism, its direct influence on LEC responses was also a major motivation for this study. Since cell behavior differs with substrate type, the seeding density was optimized for the two major cell studies, infiltration, and proliferation. Results showed cells were able to survive and proliferate normally, so the optimum seeding density for both experiments were chosen to maximize cell behavior within a 7-day time frame. Interestingly, infiltration studies revealed what was expected, Acrylic with no space at its IOL: PC interface and high adhesion force succumbed to the least LEC infiltration, followed by silicone then PMMA. Additionally, a linear relationship curve showed a strong relationship between cell infiltration and adhesion force, which supports the “no space, no cell” hypothesis. Our results are in parallel with clinical findings since LEC infiltration is one of the precursors to PCO, and LEC infiltration was directly proportional to IOL PCO incidence. Similarly, proliferation studies showed a similar trend where cell density was inversely proportional to closure space and adhesion force, but directly proportional to PCO incidence. And as a first for in vitro studies, our system was able to study the ability of IOLs to induce contact inhibition in LECs. Finally, Epithelial-to-Mesenchymal Transition potential was also assessed which has been attempted in other in vitro studies. However, those studies carried out this experiment by culturing the cells on the IOL. Thus, IOLs that did not support cell attachment such as silicone could not be evaluated for its influence on EMT. Our results showed that IOLs

with less contact with the simulated PLC induced a greater percentage of LECs to differentiate towards a fibroblastic lineage, which has been documented as a fibrosis-type PCO precursor cell activity.

Although OCT and cell culture results supported the “no space, no cell” hypothesis and were parallel with PCO incidence, the studies carried out on the simulated PC possessed some limitations. First, the material base of the simulated PC consists of gelatin, a derivative of Collagen type I whereas the native PC is a basement membrane mostly comprised of Collagen type IV and laminin networks.(Danysh and Duncan, 2009c) Considering Acrylic IOLs bind strongly to laminin,(Katayama et al., 2007a) and that the presence of fibronectin can increase Acrylic IOL adhesion force to a simulated PC,(Jaitli et al., 2022) introducing ECM native to the lens capsule and its environment to our system may be necessary to accurately assess their effect on IOL adhesive force and cell responses. Second, cell culture experiments were carried out entirely with Human lens epithelial cell line B-3 (HLE B-3). HLE B-3 are commonly used for in vitro models in PCO migration and proliferation studies.(Mencucci et al., 2015b; Sun et al., 2014; Wang et al., 2017) This cell line has also been utilized for studying IOL effects on Epithelial to Mesenchymal transition.(Awasthi and Wagner, 2006; Sun et al., 2014) However, this cell line has not been employed to study ECM production that contributes to opacification. Other cell lines and primary lens epithelial cells should be tested to increase the system’s reliability. Third, this system predicts the PCO potential of IOLs in a short-term study that takes days whereas PCO takes months to years to fully form. Although it is well established that that acute LEC responses often lead to long term PCO formation,(Cooksley et al., 2021b; Konopińska et al., 2021b) further studies are needed to make such a connection. Finally, this system lacks active responses of the native PC such as shrink-wrapping and capsular bending.

Future modifications are necessary to equip the simulated PC with these capabilities. However, in addition to simulating IOL and PC physical interactions, this system has several benefits. Materials needed to create this in vitro model are accessible, inexpensive and the fabrication method is fast and reproducible. Our simulated PC is the first in vitro system capable of predicting PCO frequency of IOLs which could reduce the need for animal studies. Furthermore, this system allows several methods of testing the PCO potential of IOLs such as dye penetration studies, cell studies, and adhesion force studies. Ultimately, the capabilities of this system as a PCO predictor tool have not been exhausted.

4.5. Conclusion

A 3D in vitro model capable of simulating IOL and PC interactions for PCO assessment has been developed. Commercial IOLs were used in this study to correlate results to clinical outcomes. The results were consistent with PCO incidence and with several in vivo reports.(Cooksley et al., 2021b; Dawes et al., 2012b; Jaitli et al., 2021d; Wang et al., 2017; Wejde et al., 2003c) Our findings provide direct evidence to support the “No space, No cell” hypothesis and that this simulated PC has the potential to improve our collective knowledge of PCO formation, and the ability to predict the PCO potential of current and future IOLs.

CHAPTER 5

Conclusions and Future Direction

5.1. Conclusions

This research effort focused on using a 3D *in vitro* system to study IOL: Lens Capsule interactions, considering different parameters that might affect this interaction, like temperature, incubation time, ECM proteins and lens epithelial cells.

In Chapter 2, a potential effect of temperature-dependent changes in surface properties of IOLs and their influence on IOL: LC adhesion forces was studied using a newly established *in vitro* system. The overall results suggested that, at body temperature, the decrease of surface hydrophobicity may be responsible for the significant increase of adhesive force between acrylic foldable and PC. Such increase of adhesive force significantly reduced the extent of dye penetration in this study and, perhaps, may reduce cell infiltration and PCO formation in the clinic. Therefore, our results provided new evidence to support the potential role of temperature, hydration time, surface hydrophobicity and IOL material properties on affecting the incidence of IOL-induced PCO.

In Chapter 3, a potential effect of fibronectin adsorption and hydrophilic coatings in altering surface properties of IOLs and their influence on IOL: PC adhesion forces and PCO potential was studied using our 3D *in vitro* system. The overall results suggested that fibronectin adsorption increased the adhesion force of acrylic foldable IOLs and the PC. Such strong IOL: PC adhesion force of acrylic foldable IOLs may be responsible for reducing the extent of cell infiltration and the incidence rate of PCO. However, fibronectin would have either no effect or an adverse effect on the IOL: PC interactions of other commercial IOLs, such as PMMA IOLs and silicone IOLs. In the case of surface modification, we found that a hydrophilic coating, such as Diglyme, could produce an adverse effect by increasing PCO potential via reduced fibronectin adsorption, and weakening the adhesion force resulting in increased cell infiltration at the IOL:

PC interface. The overall results, at least in the case of acrylic foldable IOLs, provided major substantiations to support an interesting interplay among various key factors, and that high fibronectin affinity and hydrophobic surface characteristics may increase IOL: PC adhesiveness, lessen cell infiltration and, thus, reduce PCO incidence in the clinical setting.

In Chapter 4, the IOL: PC model was further analyzed in the presence of LECs. At first, the percentage contact of IOL's posterior side with the fabricated curved capsule was studied over time. The LEC proliferation and infiltration studies gave us a 3D view of the cell activity in different IOL materials like hydrophobic acrylic, PMMA and silicone. The IOL: PC interface with cells, and the time taken by the IOLs to achieve complete contact with the PC was observed using OCT imaging system. The overall results suggested that hydrophobic acrylic had the strongest adhesion with the capsule, resulting in minimal cell infiltration, whereas, PMMA had the lowest adhesion with maximum cell penetration.

5.2. Future Direction

The conducted research effort mostly emphasized on analyzing multiple factors affecting IOL: PC interactions. But a lot of parameters effecting this interaction can be improved.

Improving the capsule material is perhaps the first thing that can be focused on. The current material used for fabricating the simulated PCs is gelatin, crosslinked with an optimized concentration of glutaraldehyde. For creating a non-toxic environment for the cells, the crosslinked gelatin was repeatedly washed with culture medium to remove excess unbound glutaraldehyde. But glutaraldehyde may still be toxic for the cells in long term culture. Moreover, by repeatedly washing the gel also compromised the mechanical integrity of the gel

and often lead to gel degradation after a period of seven days. To overcome these problems, other crosslinkers may be explored in the future.

A lot of research has been conducted on corneal crosslinking using photo-crosslinked riboflavin on collagen. Riboflavin uses UV light as the crosslinker, which may be a better alternative to chemical crosslinking. Riboflavin crosslinked with gelatin can also be explored and eventually optimized as a suitable crosslinker for our capsule fabrication. Riboflavin is a vitamin which is often ingested as a supplement, hence is non-toxic if used within a reasonable range of concentration. A better alternative to gelatin can also be explored. Although gelatin is derived from collagen I, the native human lens capsule is majorly made of collagen IV. Hence, the capsule can be modified with certain amounts of collagen I and/or collagen IV in the future to create a better simulated 3D capsule. Collagen may also crosslink better with riboflavin and help us to better simulate the IOL: PC interactions.

The IOL design is one of the most important aspects that can be studied. Previously published research show that a square-edged IOLs have a better clinical PCO performance than round-edged IOLs. Our studies have mostly been done using square-edged IOLs. The same can be studied using round edged IOLs to analyze if the IOL edge design would affect LEC infiltration in our simulated 3D model.

One of the shortcomings of our IOL: PC research model was the lack of a positive control sample for most of our studies including adhesion force and cell activity. Rabbit lens capsules have been used in the past by other researchers to study IOL: PC interactions. A rabbit capsule model can be developed by attempting to securely attach the posterior lens capsule of the rabbit lens to our simulated capsule. This can be an excellent ex-vivo model to be referred to as a positive control for our recently developed IOL: LEC: PC model.

The rabbit capsule also contains the ECM proteins naturally found in the lens capsule like fibronectin, vitronectin, laminin and collagen IV, which can give us a better idea of the role of proteins in IOL: capsule interaction. In our previous studies, we have examined the role of fibronectin in improving the interaction between IOL and PLC. The other important proteins like vitronectin, laminin and collagen IV can also be studied to better understand the contribution of different proteins in IOL: PLC interactions.

REFERENCES

- Aliancy, J., Werner, L., Ludlow, J., Nguyen, J., Masino, B., Ha, L., Mamalis, N., 2018. Long-term capsule clarity with a disk-shaped intraocular lens. *J Cataract Refract Surg* 44, 504–509. <https://doi.org/10.1016/j.jcrs.2017.12.029>
- Artaria, L.G., Ziliotti, F., Ziliotti-Mandelli, A., 1994. Long-term results after silicon intraocular lens implantation. *Klin Monbl Augenheilkd* 204, 268–270. <https://doi.org/10.1055/s-2008-1035532>
- Assia, E.I., Blumenthal, M., Apple, D.J., 1999. Effect of expandable full-size intraocular lenses on lens centration and capsule opacification in rabbits. *J Cataract Refract Surg* 25, 347–356. [https://doi.org/10.1016/S0886-3350\(99\)80082-0](https://doi.org/10.1016/S0886-3350(99)80082-0)
- Awasthi, N., Wagner, B.J., 2006. Suppression of human lens epithelial cell proliferation by proteasome inhibition, a potential defense against posterior capsular opacification. *Invest Ophthalmol Vis Sci* 47, 4482–4489. <https://doi.org/10.1167/iovs.06-0139>
- Bellucci, R., 2013. An introduction to intraocular lenses: Material, optics, haptics, design and aberration, in: *Cataract*. S. Karger AG, pp. 38–55. <https://doi.org/10.1159/000350902>
- Bertrand, V., Bozukova, D., Svaldo Lanero, T., Huang, Y.S., Schol, D., Rosière, N., Grauwels, M., Duwez, A.S., Jérôme, C., Pagnouille, C., De Pauw, E., De Pauw-Gillet, M.C., 2014. Biointerface multiparametric study of intraocular lens acrylic materials. *J Cataract Refract Surg* 40, 1536–1544. <https://doi.org/10.1016/j.jcrs.2014.01.035>
- Boulton, M., Saxby, L., 1998. Adhesion of IOLs to the posterior capsule. *Br J Ophthalmol*. <https://doi.org/10.1136/bjo.82.5.468>
- Buehl, W., Findl, O., Menapace, R., Sacu, S., Kriechbaum, K., Koepl, C., Wirtitsch, M., 2005. Long-term effect of optic edge design in an acrylic intraocular lens on posterior capsule opacification. *J Cataract Refract Surg*. <https://doi.org/10.1016/j.jcrs.2004.09.053>
- Buehl, W., Menapace, R., Findl, O., Neumayer, T., Bolz, M., Prinz, A., 2007. Long-term Effect of Optic Edge Design in a Silicone Intraocular Lens on Posterior Capsule Opacification. *Am J Ophthalmol*. <https://doi.org/10.1016/j.ajo.2007.02.017>
- Cabeza-Gil, I., Grasa, J., Calvo, B., 2021. A numerical investigation of changes in lens shape during accommodation. *Sci Rep* 11, 1–12. <https://doi.org/10.1038/s41598-021-89145-z>
- Cehade, M., Elder, M.J., 1997. Intraocular lens materials and styles. *Aust N Z J Ophthalmol*. <https://doi.org/10.1111/j.1442-9071.1997.tb01512.x>
- Cheng, J.W., Wei, R.L., Cai, J.P., Xi, G.L., Zhu, H., Li, Y., Ma, X.Y., 2007. Efficacy of Different Intraocular Lens Materials and Optic Edge Designs in Preventing Posterior Capsular Opacification: A Meta-Analysis. *Am J Ophthalmol*. <https://doi.org/10.1016/j.ajo.2006.11.045>
- Cley, C., Rita, P., Algatti, M.A., n.d. STUDY OF HYDROPHOBIC / HYDROPHILIC PROPERTIES OF PLASMA POLYMERIZED DIGLYME FILMS OF INTEREST IN BIOMATERIALS INDUSTRY 453–454.
- Cooke, Carole A., McGimpsey, S., Mahon, G., Best, R.M., 2006. An In Vitro Study of Human Lens Epithelial Cell Adhesion to Intraocular Lenses with and without a Fibronectin Coating 47, 2–6. <https://doi.org/10.1167/iovs.05-1275>
- Cooke, Carole A., McGimpsey, S., Mahon, G., Best, R.M., 2006. An in vitro study of human lens epithelial cell adhesion to intraocular lenses with and without a fibronectin coating. *Invest Ophthalmol Vis Sci* 47, 2985–2989. <https://doi.org/10.1167/iovs.05-1275>

- Cooksley, G., Lacey, J., Dymond, M.K., Sandeman, S., 2021a. Factors affecting posterior capsule opacification in the development of intraocular lens materials. *Pharmaceutics* 13, 1–29. <https://doi.org/10.3390/pharmaceutics13060860>
- Cooksley, G., Lacey, J., Dymond, M.K., Sandeman, S., 2021b. Factors affecting posterior capsule opacification in the development of intraocular lens materials. *Pharmaceutics* 13, 1–22. <https://doi.org/10.3390/pharmaceutics13060860>
- Cumming, J.S., Ritter, J.A., 1994. The measurement of vitreous cavity length and its comparison pre- and postoperatively. *European Journal of Implant and Refractive Surgery* 6, 261–272. [https://doi.org/10.1016/S0955-3681\(13\)80226-2](https://doi.org/10.1016/S0955-3681(13)80226-2)
- Cunanan, C.M., Ghazizadeh, M., Buchen, S.Y., Knight, P.M., 1998. Contact-angle analysis of intraocular lenses. *J Cataract Refract Surg* 24, 341–351. [https://doi.org/10.1016/S0886-3350\(98\)80322-2](https://doi.org/10.1016/S0886-3350(98)80322-2)
- Danysh, B.P., Duncan, M.K., 2009a. The lens capsule. *Exp Eye Res.* <https://doi.org/10.1016/j.exer.2008.08.002>
- Danysh, B.P., Duncan, M.K., 2009b. The lens capsule. *Exp Eye Res.* <https://doi.org/10.1016/j.exer.2008.08.002>
- Danysh, B.P., Duncan, M.K., 2009c. The lens capsule. *Exp Eye Res* 88, 151–164. <https://doi.org/10.1016/j.exer.2008.08.002>
- Dardelle, G., Subramaniam, A., Normand, V., 2011a. Determination of covalent cross-linker efficacy of gelatin strands using calorimetric analyses of the gel state. *Soft Matter.* <https://doi.org/10.1039/c0sm01374a>
- Dardelle, G., Subramaniam, A., Normand, V., 2011b. Determination of covalent cross-linker efficacy of gelatin strands using calorimetric analyses of the gel state. *Soft Matter.* <https://doi.org/10.1039/c0sm01374a>
- Dawes, L.J., Illingworth, C.D., Michael Wormstone, I., 2012a. A fully human in vitro capsular bag model to permit intraocular lens evaluation. *Invest Ophthalmol Vis Sci* 53, 23–29. <https://doi.org/10.1167/iovs.11-8851>
- Dawes, L.J., Illingworth, C.D., Michael Wormstone, I., 2012b. A fully human in vitro capsular bag model to permit intraocular lens evaluation. *Invest Ophthalmol Vis Sci* 53, 23–29. <https://doi.org/10.1167/iovs.11-8851>
- Eldred, J.A., Spalton, D.J., Wormstone, I.M., 2014. An in vitro evaluation of the Anew Zephyr open-bag IOL in the prevention of posterior capsule opacification using a human capsular bag model. *Invest Ophthalmol Vis Sci* 55, 7057–7064. <https://doi.org/10.1167/iovs.14-15302>
- Eldred, J.A., Zheng, J., Chen, S., Wormstone, I.M., 2019a. An in vitro human lens capsular bag model adopting a graded culture regime to assess putative impact of iols on pco formation. *Invest Ophthalmol Vis Sci* 60, 113–122. <https://doi.org/10.1167/iovs.18-25930>
- Eldred, J.A., Zheng, J., Chen, S., Wormstone, I.M., 2019b. An in vitro human lens capsular bag model adopting a graded culture regime to assess putative impact of iols on pco formation. *Invest Ophthalmol Vis Sci* 60, 113–122. <https://doi.org/10.1167/iovs.18-25930>
- Findl, O., Buehl, W., Bauer, P., Sycha, T., 2010. Interventions for preventing posterior capsule opacification. *Cochrane Database of Systematic Reviews.* <https://doi.org/10.1002/14651858.CD003738.pub3>
- FW, M.R. & K., 1996. The extracellular matrix. In: Murray RK, Granner DK, Mayes PA & Rodwell VW (eds) *Harpersí Biochemistry*. Appleton & Lange, Stamford, Connecticut. UpToDate® 183, 667–673.

- Gift, B.W., English, R. V., Nadelstein, B., Weigt, A.K., Gilger, B.C., 2009. Comparison of capsular opacification and refractive status after placement of three different intraocular lens implants following phacoemulsification and aspiration of cataracts in dogs. *Vet Ophthalmol.* <https://doi.org/10.1111/j.1463-5224.2009.00667.x>
- Haeussler, D.J., 2011. The Effects of Hyaluronic Acid on Lens Epithelial Cell Migration 76.
- HariPriya, A., Chang, D.F., Vijayakumar, B., Niraj, A., Shekhar, M., Tanpreet, S., Aravind, S., 2017. Long-term Posterior Capsule Opacification Reduction with Square-Edge Polymethylmethacrylate Intraocular Lens: Randomized Controlled Study. *Ophthalmology.* <https://doi.org/10.1016/j.ophtha.2016.11.010>
- Hayashi, H., Hayashi, K., Nakao, F., Hayashi, F., 2002. Elapsed time for capsular apposition to intraocular lens after cataract surgery. *Ophthalmology* 109, 1427–1431. [https://doi.org/10.1016/S0161-6420\(02\)01112-0](https://doi.org/10.1016/S0161-6420(02)01112-0)
- Hecht, E., 1987. *Optics*, 2nd ed. Addison-Wesley.
- Huang, X.D., Yao, K., Zhang, Z., Zhang, Y., Wang, Y., 2010. Uveal and capsular biocompatibility of an intraocular lens with a hydrophilic anterior surface and a hydrophobic posterior surface. *J Cataract Refract Surg* 36, 290–298. <https://doi.org/10.1016/j.jcrs.2009.09.027>
- Hyeon, I.L., Mee, K.K., Jung, H.K., Hyun, J.L., Won, R.W., Jin, H.L., 2007. The efficacy of an acrylic intraocular lens surface modified with polyethylene glycol in posterior capsular opacification. *J Korean Med Sci* 22, 502–507.
- J Gonzalez-Martin-Moro, J J Gonzalez-Lopez, 2015. Posterior capsule opacification, capsular bag distension syndrome, and anterior capsular phimosis: A retrospective cohort study. *Arch Soc Esp Oftalmol* 90, 69–75.
- Jaitli, A., Roy, J., 2022. Role of fibronectin and IOL surface modification in IOL: Lens capsule interactions. *Exp Eye Res* 221. <https://doi.org/10.1016/j.exer.2022.109135>
- Jaitli, A., Roy, J., 2021. Effect of time and temperature-dependent changes of IOL material properties on IOL: Lens capsule interactions. *Exp Eye Res* 211, 108726. <https://doi.org/10.1016/j.exer.2021.108726>
- Jaitli, A., Roy, J., Chatila, A., Liao, J., Tang, L., 2022. Role of fibronectin and IOL surface modification in IOL: Lens capsule interactions. *Exp Eye Res* 221, 109135. <https://doi.org/10.1016/j.exer.2022.109135>
- Jaitli, A., Roy, J., Chatila, A., Liao, J., Tang, L., 2021a. Effect of time and temperature-dependent changes of IOL material properties on IOL: Lens capsule interactions. *Exp Eye Res* 211, 108726. <https://doi.org/10.1016/j.exer.2021.108726>
- Jaitli, A., Roy, J., McMahan, S., Liao, J., Tang, L., 2021b. An in vitro system to investigate IOL: Lens capsule interaction. *Exp Eye Res.* <https://doi.org/10.1016/j.exer.2020.108430>
- Jaitli, A., Roy, J., McMahan, S., Liao, J., Tang, L., 2021c. An in vitro system to investigate IOL: Lens capsule interaction. *Exp Eye Res.* <https://doi.org/10.1016/j.exer.2020.108430>
- Jaitli, A., Roy, J., McMahan, S., Liao, J., Tang, L., 2021d. An in vitro system to investigate IOL: Lens capsule interaction. *Exp Eye Res* 203, 108430. <https://doi.org/10.1016/j.exer.2020.108430>
- Jakobsson, G., Sundelin, K., Zetterberg, H., Zetterberg, M., 2015. Increased levels of inflammatory immune mediators in vitreous from pseudophakic eyes. *Invest Ophthalmol Vis Sci* 56, 3407–3414. <https://doi.org/10.1167/iovs.15-16837>
- Johnston, R.L., Spalton, D.J., Hussain, A., Marshall, J., 1999. In vitro protein adsorption to 2 intraocular lens materials, *J Cataract Refract Surg.*

- Jung, G.B., Jin, K.H., Park, H.K., 2017a. Physicochemical and surface properties of acrylic intraocular lenses and their clinical significance. *J Pharm Investig* 47, 453–460. <https://doi.org/10.1007/s40005-017-0323-y>
- Jung, G.B., Jin, K.H., Park, H.K., 2017b. Physicochemical and surface properties of acrylic intraocular lenses and their clinical significance. *J Pharm Investig* 47, 453–460. <https://doi.org/10.1007/s40005-017-0323-y>
- Katayama, Y., Kobayakawa, S., Yanagawa, H., 2007a. The Relationship between the Adhesion Characteristics of Acrylic Intraocular Lens Materials and Posterior Capsule Opacification 276–281. <https://doi.org/10.1159/000108121>
- Katayama, Y., Kobayakawa, S., Yanagawa, H., Tochikubo, T., 2007b. The relationship between the adhesion characteristics of acrylic intraocular lens materials and posterior capsule opacification. *Ophthalmic Res* 39, 276–281. <https://doi.org/10.1159/000108121>
- Katayama, Y., Kobayakawa, S., Yanagawa, H., Tochikubo, T., 2007c. The relationship between the adhesion characteristics of acrylic intraocular lens materials and posterior capsule opacification. *Ophthalmic Res* 39, 276–281. <https://doi.org/10.1159/000108121>
- Khambhiphant, B., Liumsirijarern, C., Saehout, P., 2015. The effect of Nd: YAG laser treatment of posterior capsule opacification on anterior chamber depth and refraction in pseudophakic eyes. *Clinical Ophthalmology* 9, 557–561. <https://doi.org/10.2147/OPTH.S80220>
- Kim, M.K., Park, I.S., Park, H.D., Wee, W.R., Lee, J.H., Park, K.D., Kim, S.H., Kim, Y.H., 2001. Effect of poly(ethylene glycol) graft polymerization of poly(methyl methacrylate) on cell adhesion: In vitro and in vivo study. *J Cataract Refract Surg* 27, 766–774. [https://doi.org/10.1016/S0886-3350\(00\)00701-X](https://doi.org/10.1016/S0886-3350(00)00701-X)
- Kochounian, H.H., Kovacs, S.A., Sy, J., Grubbs, D.E., Maxwell, W.A., 1994. Identification of Intraocular Lens-Adsorbed Proteins in Mammalian In Vitro and In Vivo Systems. *Archives of Ophthalmology*. <https://doi.org/10.1001/archophth.1994.01090150125034>
- Konopińska, J., Młynarczyk, M., Dmuchowska, D.A., Obuchowska, I., 2021a. Posterior capsule opacification: A review of experimental studies. *J Clin Med*. <https://doi.org/10.3390/jcm10132847>
- Konopińska, J., Młynarczyk, M., Dmuchowska, D.A., Obuchowska, I., 2021b. Posterior capsule opacification: A review of experimental studies. *J Clin Med* 10. <https://doi.org/10.3390/jcm10132847>
- Kurosaka, D., Obasawa, M., Kurosaka, H., Nakamura, K., 2002. Inhibition of lens epithelial cell migration by an acrylic intraocular lens in vitro. *Ophthalmic Res* 34, 29–37. <https://doi.org/10.1159/000048322>
- Kwon, C., Kim, Y., Jeon, H., 2017. Collective Migration of Lens Epithelial Cell Induced by Differential Microscale Groove Patterns. *J Funct Biomater* 8, 34. <https://doi.org/10.3390/jfb8030034>
- Li, Y., Wang, J., Chen, Z., Tang, X., 2013a. Effect of hydrophobic acrylic versus hydrophilic acrylic intraocular lens on posterior capsule opacification: Meta-analysis. *PLoS One*. <https://doi.org/10.1371/journal.pone.0077864>
- Li, Y., Wang, J., Chen, Z., Tang, X., 2013b. Effect of hydrophobic acrylic versus hydrophilic acrylic intraocular lens on posterior capsule opacification: Meta-analysis. *PLoS One*. <https://doi.org/10.1371/journal.pone.0077864>
- Lin, Q., Tang, J., Han, Y., Xu, X., Hao, X., Chen, H., 2017. Hydrophilic modification of intraocular lens via surface initiated reversible addition-fragmentation chain transfer

- polymerization for reduced posterior capsular opacification. *Colloids Surf B Biointerfaces* 151, 271–279. <https://doi.org/10.1016/j.colsurfb.2016.12.028>
- Linnola, R.J., 1997a. Sandwich theory: Bioactivity-based explanation for posterior capsule opacification. *J Cataract Refract Surg* 23, 1539–1542. [https://doi.org/10.1016/S0886-3350\(97\)80026-0](https://doi.org/10.1016/S0886-3350(97)80026-0)
- Linnola, R.J., 1997b. Sandwich theory: Bioactivity-based explanation for posterior capsule opacification. *J Cataract Refract Surg*. [https://doi.org/10.1016/S0886-3350\(97\)80026-0](https://doi.org/10.1016/S0886-3350(97)80026-0)
- Linnola, R.J., 1997c. Sandwich theory: Bioactivity-based explanation for posterior capsule opacification. *J Cataract Refract Surg* 23, 1539–1542. [https://doi.org/10.1016/S0886-3350\(97\)80026-0](https://doi.org/10.1016/S0886-3350(97)80026-0)
- Linnola, R.J., Sund, M., Ylönen, R., Pihlajaniemi, T., 2003a. Adhesion of soluble fibronectin, vitronectin, and collagen type IV to intraocular lens materials. *J Cataract Refract Surg* 29, 146–152. [https://doi.org/10.1016/S0886-3350\(02\)01422-0](https://doi.org/10.1016/S0886-3350(02)01422-0)
- Linnola, R.J., Sund, M., Ylönen, R., Pihlajaniemi, T., 2003b. Adhesion of soluble fibronectin, vitronectin, and collagen type IV to intraocular lens materials. *J Cataract Refract Surg* 29, 146–152. [https://doi.org/10.1016/S0886-3350\(02\)01422-0](https://doi.org/10.1016/S0886-3350(02)01422-0)
- Linnola, R.J., Sund, M., Ylönen, R., Pihlajaniemi, T., 2003c. Adhesion of soluble fibronectin, vitronectin, and collagen type IV to intraocular lens materials. *J Cataract Refract Surg* 29, 146–152. [https://doi.org/10.1016/S0886-3350\(02\)01422-0](https://doi.org/10.1016/S0886-3350(02)01422-0)
- Linnola, R.J., Werner, L., Pandey, S.K., Escobar-Gomez, M., Znoiko, S.L., Apple, D.J., 2000a. Adhesion of fibronectin, vitronectin, laminin, and collagen type IV to intraocular lens materials in pseudophakic human autopsy eyes. Part 2: Exploited intraocular lenses. *J Cataract Refract Surg* 26, 1807–1818. [https://doi.org/10.1016/S0886-3350\(00\)00747-1](https://doi.org/10.1016/S0886-3350(00)00747-1)
- Linnola, R.J., Werner, L., Pandey, S.K., Escobar-Gomez, M., Znoiko, S.L., Apple, D.J., 2000b. Adhesion of fibronectin, vitronectin, laminin, and collagen type IV to intraocular lens materials in pseudophakic human autopsy eyes. Part 1: Histological sections. *J Cataract Refract Surg*. [https://doi.org/10.1016/S0886-3350\(00\)00748-3](https://doi.org/10.1016/S0886-3350(00)00748-3)
- Linnola, R.J., Werner, L., Pandey, S.K., Escobar-Gomez, M., Znoiko, S.L., Apple, D.J., 2000c. Adhesion of fibronectin, vitronectin, laminin, and collagen type IV to intraocular lens materials in pseudophakic human autopsy eyes. Part 2: Exploited intraocular lenses. *J Cataract Refract Surg* 26, 1807–1818. [https://doi.org/10.1016/S0886-3350\(00\)00747-1](https://doi.org/10.1016/S0886-3350(00)00747-1)
- Linnola, R.J., Werner, L., Pandey, S.K., Escobar-Gomez, M., Znoiko, S.L., Apple, D.J., 2000d. Adhesion of fibronectin, vitronectin, laminin, and collagen type IV to intraocular lens materials in pseudophakic human autopsy eyes. Part 2: Exploited intraocular lenses. *J Cataract Refract Surg* 26, 1807–1818. [https://doi.org/10.1016/S0886-3350\(00\)00747-1](https://doi.org/10.1016/S0886-3350(00)00747-1)
- Linnola, R.J., Werner, L., Pandey, S.K., Escobar-Gomez, M., Znoiko, S.L., Apple, D.J., 2000e. Adhesion of fibronectin, vitronectin, laminin, and collagen type IV to intraocular lens materials in pseudophakic human autopsy eyes. Part 1: Histological sections. *J Cataract Refract Surg*. [https://doi.org/10.1016/S0886-3350\(00\)00748-3](https://doi.org/10.1016/S0886-3350(00)00748-3)
- Lombardo, M., Carbone, G., Lombardo, G., De Santo, M.P., Barberi, R., 2009. Analysis of intraocular lens surface adhesiveness by atomic force microscopy. *J Cataract Refract Surg* 35, 1266–1272. <https://doi.org/10.1016/j.jcrs.2009.02.029>
- Lombardo, M., De Santo, M.P., Lombardo, G., Barberi, R., Serrao, S., 2006. Analysis of intraocular lens surface properties with atomic force microscopy. *J Cataract Refract Surg* 32, 1378–1384. <https://doi.org/10.1016/j.jcrs.2006.02.068>

- Lucia, U., Grisolia, G., Dolcino, D., Astori, M.R., Massa, E., Ponzetto, A., 2016. Constructal approach to bio-engineering: The ocular anterior chamber temperature. *Sci Rep* 6, 1–6. <https://doi.org/10.1038/srep31099>
- M, R.S., R, V.A., Johar R, K.S., A, V. v, 2007. Post-operative capsular opacification.
- Maddala, S., Werner, L., Ness, P.J., Davis, D., Zaugg, B., Stringham, J., Burrow, M., Yeh, O., 2011. Pathology of 157 human cadaver eyes with round-edged or modern square-edged silicone intraocular lenses: Analyses of capsule bag opacification. *J Cataract Refract Surg*. <https://doi.org/10.1016/j.jcrs.2010.10.058>
- Mareo, N.D., Rotner, B.D., 1989. Relating the Surface Properties of Intraocular Lens Materials to Endothelial Cell Adhesion Damage, *Investigative Ophthalmology & Visual Science*.
- Mencucci, R., Favuzza, E., Boccalini, C., Gicquel, J.J., Raimondi, L., 2015a. Square-edge intraocular lenses and epithelial lens cell proliferation: Implications on posterior capsule opacification in an in vitro model. *BMC Ophthalmol* 15. <https://doi.org/10.1186/1471-2415-15-5>
- Mencucci, R., Favuzza, E., Boccalini, C., Gicquel, J.J., Raimondi, L., 2015b. Square-edge intraocular lenses and epithelial lens cell proliferation: Implications on posterior capsule opacification in an in vitro model. *BMC Ophthalmol* 15, 1–5. <https://doi.org/10.1186/1471-2415-15-5>
- Miyata, A., Yaguchi, S., 2004. Equilibrium water content and glistenings in acrylic intraocular lenses. *J Cataract Refract Surg* 30, 1768–1772. <https://doi.org/10.1016/j.jcrs.2003.12.038>
- Modrzejewska, A., Cieszyński, Ł., Zaborski, D., Parafiniuk, M., 2020. Infrared thermography for the analysis of ocular surface temperature after phacoemulsification. *Arq Bras Oftalmol* 83, 202–208. <https://doi.org/10.5935/0004-2749.20200035>
- Moreno-Montañés, J., Alvarez, A., Bes-Rastrollo, M., García-Layana, A., 2008. Optical coherence tomography evaluation of posterior capsule opacification related to intraocular lens design. *J Cataract Refract Surg* 34, 643–650. <https://doi.org/10.1016/j.jcrs.2007.11.035>
- Morgan-Warren, P.J., Smith, J. m. A., 2013. Intraocular lens-edge design and material factors contributing to posterior-capsulotomy rates: Comparing Hoya FY60AD, PY60AD, and AcrySof SN60WF. *Clinical Ophthalmology*. <https://doi.org/10.2147/OPHTH.S48824>
- Muir, B.W., Tarasova, A., Gengenbach, T.R., Menzies, D.J., Meagher, L., Rovere, F., Fairbrother, A., McLean, K.M., Hartley, P.G., 2008. Characterization of low-fouling ethylene glycol containing plasma polymer films. *Langmuir* 24, 3828–3835. <https://doi.org/10.1021/la702689t>
- Mukherjee, R., Chaudhury, K., Das, S., Sengupta, S., Biswas, P., 2012. Posterior capsular opacification and intraocular lens surface micro-roughness characteristics: An atomic force microscopy study. *Micron* 43, 937–947. <https://doi.org/10.1016/j.micron.2012.03.015>
- Mylonas, G., Prskavec, M., Baradaran-Dilmaghani, R., Karnik, N., Buehl, W., Wirtitsch, M., 2013. Effect of a single-piece and a three-piece acrylic sharp-edged IOL on posterior capsule opacification. *Curr Eye Res*. <https://doi.org/10.3109/02713683.2012.717242>
- Nagata, T., Minakata, A., Watanabe, I., 1998. Adhesiveness of AcrySof to a collagen film. *J Cataract Refract Surg*. [https://doi.org/10.1016/S0886-3350\(98\)80325-8](https://doi.org/10.1016/S0886-3350(98)80325-8)
- Nazaretyan, R.E., Zadorozhnyy, O.S., Umanets, M.M., Naumenko, V.A., Pasychnikova, N. V., Shafranskii, V. V., 2018. Intraocular temperature changes during vitrectomy procedure. *Oftalmol Zh*.

- Nibourg, L.M., Gelens, E., Kuijer, R., Hooymans, J.M.M., van Kooten, T.G., Koopmans, S.A., 2015. Prevention of posterior capsular opacification. *Exp Eye Res* 136, 100–115. <https://doi.org/10.1016/j.exer.2015.03.011>
- Nishi, O., 1999a. Posterior capsule opacification. Part 1: Experimental investigations. *J Cataract Refract Surg* 25, 106–117. [https://doi.org/10.1016/S0886-3350\(99\)80020-0](https://doi.org/10.1016/S0886-3350(99)80020-0)
- Nishi, O., 1999b. Preventing posterior capsule opacification by creating a discontinuous sharp bend in the capsule. *J Cataract Refract Surg*. [https://doi.org/10.1016/S0886-3350\(99\)80049-2](https://doi.org/10.1016/S0886-3350(99)80049-2)
- Nishi, O., Nishi, K., 2002. Preventive effect of a second-generation silicone intraocular lens on posterior capsule opacification. *J Cataract Refract Surg*. [https://doi.org/10.1016/S0886-3350\(02\)01430-X](https://doi.org/10.1016/S0886-3350(02)01430-X)
- Nishi, O., Nishi, K., Akura, J., 2002. Speed of capsular bend formation at the optic edge of acrylic, silicone, and poly(methyl methacrylate) lenses. *J Cataract Refract Surg* 28, 431–437. [https://doi.org/10.1016/S0886-3350\(01\)01094-X](https://doi.org/10.1016/S0886-3350(01)01094-X)
- Nishi, O., Nishi, K., Akura, J., Nagata, T., 2001. Effect of round-edged acrylic intraocular lenses on preventing posterior capsule opacification. *J Cataract Refract Surg*. [https://doi.org/10.1016/S0886-3350\(00\)00644-1](https://doi.org/10.1016/S0886-3350(00)00644-1)
- Nishi, O., Nishi, K., Mano, C., Ichihara, M., Honda, T., 1998a. The inhibition of lens epithelial cell migration by a discontinuous capsular bend created by a band-shaped circular loop or a capsule-bending ring. *Ophthalmic Surg Lasers*. <https://doi.org/10.3928/1542-8877-19980201-07>
- Nishi, O., Nishi, K., Osakabe, Y., 2004a. Effect of intraocular lenses on preventing posterior capsule opacification: Design versus material. *J Cataract Refract Surg* 30, 2170–2176. <https://doi.org/10.1016/j.jcrs.2004.05.022>
- Nishi, O., Nishi, K., Osakabe, Y., 2004b. Effect of intraocular lenses on preventing posterior capsule opacification: Design versus material. *J Cataract Refract Surg*. <https://doi.org/10.1016/j.jcrs.2004.05.022>
- Nishi, O., Nishi, K., Sakanishi, K., 1998b. Inhibition of migrating lens epithelial cells at the capsular bend created by the rectangular optic edge of a posterior chamber intraocular lens. *Ophthalmic Surg Lasers*. <https://doi.org/10.3928/1542-8877-19980701-10>
- Nishi, O., Nishi, K., Wickström, K., 2000. Preventing lens epithelial cell migration using intraocular lenses with sharp rectangular edges. *J Cataract Refract Surg*. [https://doi.org/10.1016/S0886-3350\(00\)00426-0](https://doi.org/10.1016/S0886-3350(00)00426-0)
- Nishi, O., Yamamoto, N., Nishi, K., Nishi, Y., 2007. Contact inhibition of migrating lens epithelial cells at the capsular bend created by a sharp-edged intraocular lens after cataract surgery. *J Cataract Refract Surg* 33, 1065–1070. <https://doi.org/10.1016/j.jcrs.2007.02.022>
- Nisol, B., Watson, S., Meunier, A., Juncker, D., Lerouge, S., Wertheimer, M.R., 2018. Energetics of reactions in a dielectric barrier discharge with argon carrier gas: VI PEG-like coatings. *Plasma Processes and Polymers* 15. <https://doi.org/10.1002/ppap.201700132>
- Noble, B.A., Hayward, J.M., Huber, C., 1990. Secondary evaluation of hydrogel lens implants. *Eye (Basingstoke)* 4, 450–455. <https://doi.org/10.1038/eye.1990.57>
- Oshika, T., Nagata, T., Ishii, Y., 1998a. Adhesion of lens capsule to intraocular lenses of polymethylmethacrylate, silicone, and acrylic foldable materials: An experimental study. *British Journal of Ophthalmology* 82, 549–553. <https://doi.org/10.1136/bjo.82.5.549>

- Oshika, T., Nagata, T., Ishii, Y., 1998b. Adhesion of lens capsule to intraocular lenses of polymethylmethacrylate, silicone, and acrylic foldable materials: An experimental study. *British Journal of Ophthalmology* 82, 549–553. <https://doi.org/10.1136/bjo.82.5.549>
- Oshika, T., Nagata, T., Ishii, Y., 1998c. Adhesion of lens capsule to intraocular lenses of polymethylmethacrylate, silicone, and acrylic foldable materials: An experimental study. *British Journal of Ophthalmology* 82, 549–553. <https://doi.org/10.1136/bjo.82.5.549>
- Oshika, T., Nagata, T., Ishii, Y., 1998d. Adhesion of lens capsule to intraocular lenses of polymethylmethacrylate, silicone, and acrylic foldable materials: An experimental study. *British Journal of Ophthalmology* 82, 549–553. <https://doi.org/10.1136/bjo.82.5.549>
- Oshika, T., Suzuki, Y., Kizaki, H., Yaguchi, S., 1996. Two year clinical study of a soft acrylic intraocular lens. *J Cataract Refract Surg.* [https://doi.org/10.1016/S0886-3350\(96\)80278-1](https://doi.org/10.1016/S0886-3350(96)80278-1)
- Oyster, C.W., 1999. *The Human Eye: Structure and Function*. Oxford University Press.
- Pearlstein, C.S., Lane, S.S., Lindstrom, R.L., 1988a. The Incidence of Secondary Posterior Capsulotomy in Convex-Posterior vs. Contex-Anterior Posterior Chamber Intraocular Lenses. *J Cataract Refract Surg.* [https://doi.org/10.1016/S0886-3350\(88\)80020-8](https://doi.org/10.1016/S0886-3350(88)80020-8)
- Pearlstein, C.S., Lane, S.S., Lindstrom, R.L., 1988b. The Incidence of Secondary Posterior Capsulotomy in Convex-Posterior vs. Contex-Anterior Posterior Chamber Intraocular Lenses. *J Cataract Refract Surg.* [https://doi.org/10.1016/S0886-3350\(88\)80020-8](https://doi.org/10.1016/S0886-3350(88)80020-8)
- Pearlstein, C.S., Lane, S.S., Lindstrom, R.L., 1988c. The Incidence of Secondary Posterior Capsulotomy in Convex-Posterior vs. Contex-Anterior Posterior Chamber Intraocular Lenses. *J Cataract Refract Surg* 14, 578–580. [https://doi.org/10.1016/S0886-3350\(88\)80020-8](https://doi.org/10.1016/S0886-3350(88)80020-8)
- Pérez-Vives, C., 2018a. Biomaterial influence on intraocular lens performance: An overview. *J Ophthalmol* 2018. <https://doi.org/10.1155/2018/2687385>
- Pérez-Vives, C., 2018b. Biomaterial influence on intraocular lens performance: An overview. *J Ophthalmol* 2018. <https://doi.org/10.1155/2018/2687385>
- Ram, J., Jain, V.K., Agarwal, A., Kumar, J., 2014. Hydrophobic acrylic versus polymethyl methacrylate intraocular lens implantation following cataract surgery in the first year of life. *Graefe's Archive for Clinical and Experimental Ophthalmology.* <https://doi.org/10.1007/s00417-014-2689-0>
- Ribeiro, M.A., Ramos, A.S., Manfredini, M.I., Alves, H.A., Honda, R.Y., Kostov, K.G., Lucena, E.F., Ramos, E.C.T., Mota, R.P., Algatti, M.A., Kayama, M.E., 2009. Polyurethane coating with thin polymer films produced by plasma polymerization of diglyme. *J Phys Conf Ser* 167. <https://doi.org/10.1088/1742-6596/167/1/012056>
- Rønbeck, M., Kugelberg, M., 2014a. Posterior capsule opacification with 3 intraocular lenses: 12-year prospective study. *J Cataract Refract Surg.* <https://doi.org/10.1016/j.jcrs.2013.07.039>
- Rønbeck, M., Kugelberg, M., 2014b. Posterior capsule opacification with 3 intraocular lenses: 12-year prospective study. *J Cataract Refract Surg.* <https://doi.org/10.1016/j.jcrs.2013.07.039>
- Rønbeck, M., Kugelberg, M., 2014c. Posterior capsule opacification with 3 intraocular lenses: 12-year prospective study. *J Cataract Refract Surg.* <https://doi.org/10.1016/j.jcrs.2013.07.039>
- Rønbeck, M., Zetterström, C., Wejde, G., Kugelberg, M., 2009a. Comparison of posterior capsule opacification development with 3 intraocular lens types. Five-year prospective study. *J Cataract Refract Surg* 35, 1935–1940. <https://doi.org/10.1016/j.jcrs.2009.05.048>

- Rönbeck, M., Zetterström, C., Wejde, G., Kugelberg, M., 2009b. Comparison of posterior capsule opacification development with 3 intraocular lens types. Five-year prospective study. *J Cataract Refract Surg*. <https://doi.org/10.1016/j.jcrs.2009.05.048>
- Sacu, S., Findl, O., Linnola, R.J., 2005a. Optical coherence tomography assessment of capsule closure after cataract surgery. *J Cataract Refract Surg*. <https://doi.org/10.1016/j.jcrs.2004.04.057>
- Sacu, S., Findl, O., Linnola, R.J., 2005b. Optical coherence tomography assessment of capsule closure after cataract surgery. *J Cataract Refract Surg* 31, 330–336. <https://doi.org/10.1016/j.jcrs.2004.04.057>
- Saika, S., 2004. Relationship between posterior capsule opacification and intraocular lens biocompatibility. *Prog Retin Eye Res*. <https://doi.org/10.1016/j.preteyeres.2004.02.004>
- Saika, S., 1997a. Deposition of extracellular matrix on silicone intraocular lens implants in rabbits. *Graefe's Archive for Clinical and Experimental Ophthalmology* 235, 517–522. <https://doi.org/10.1007/BF00947010>
- Saika, Shizuya, 1997. Deposition of extracellular matrix on intraocular lenses in rabbits: An immunohistochemical and transmission electron microscopic study. *Graefe's Archive for Clinical and Experimental Ophthalmology* 235, 241–247. <https://doi.org/10.1007/BF00941766>
- Saika, S., 1997b. Deposition of extracellular matrix on silicone intraocular lens implants in rabbits. *Graefe's Archive for Clinical and Experimental Ophthalmology* 235, 517–522. <https://doi.org/10.1007/BF00947010>
- Saika, S., Kobata, S., Yamanaka, O., Yamanaka, A., Okubo, K., Oka, T., Hosomi, M., Kano, Y., Ohmi, S., Uenoyama, S., Tamura, M., Kanagawa, R., Uenoyama, K., 1993a. Cellular fibronectin on intraocular lenses explanted from patients. *Graefe's Archive for Clinical and Experimental Ophthalmology* 231, 718–721. <https://doi.org/10.1007/BF00919287>
- Saika, S., Kobata, S., Yamanaka, O., Yamanaka, A., Okubo, K., Oka, T., Hosomi, M., Kano, Y., Ohmi, S., Uenoyama, S., Tamura, M., Kanagawa, R., Uenoyama, K., 1993b. Cellular fibronectin on intraocular lenses explanted from patients. *Graefe's Archive for Clinical and Experimental Ophthalmology* 231, 718–721. <https://doi.org/10.1007/BF00919287>
- Saika, S., Yamanaka, A., Tanaka, S.I., Ohmi, S., Ohnishi, Y., Ooshima, A., 1995. Extracellular matrix on intraocular lenses. *Exp Eye Res* 61, 713–721. [https://doi.org/10.1016/S0014-4835\(05\)80022-3](https://doi.org/10.1016/S0014-4835(05)80022-3)
- Schroeder, A.C., Lingenfelder, C., Seitz, B., Grabowy, U., Spraul, C.W., Gatzoufas, Z., Herrmann, M., 2009a. Impact of fibronectin on surface properties of intraocular lenses. *Graefe's Archive for Clinical and Experimental Ophthalmology*. <https://doi.org/10.1007/s00417-009-1130-6>
- Schroeder, A.C., Lingenfelder, C., Seitz, B., Grabowy, U., Spraul, C.W., Gatzoufas, Z., Herrmann, M., 2009b. Impact of fibronectin on surface properties of intraocular lenses. *Graefe's Archive for Clinical and Experimental Ophthalmology*. <https://doi.org/10.1007/s00417-009-1130-6>
- Shepherd, J.R., 1989. Capsular opacification associated with silicone implants. *J Cataract Refract Surg* 15, 448–450. [https://doi.org/10.1016/S0886-3350\(89\)80069-0](https://doi.org/10.1016/S0886-3350(89)80069-0)
- Shiba, T., Mitooka, K., Tsuneoka, H., 2003. In vitro analysis of AcrySof intraocular lens glistening. *Eur J Ophthalmol* 13, 759–763. <https://doi.org/10.1177/1120672103013009-1004>

- Shimizu, M., Minakuchi, K., Moon, M., Koga, J., 1997a. Difference in interaction of fibronectin with type I collagen and type IV collagen. *Biochimica et Biophysica Acta - Protein Structure and Molecular Enzymology* 1339, 53–61. [https://doi.org/10.1016/S0167-4838\(96\)00214-2](https://doi.org/10.1016/S0167-4838(96)00214-2)
- Shimizu, M., Minakuchi, K., Moon, M., Koga, J., 1997b. Difference in interaction of fibronectin with type I collagen and type IV collagen. *Biochimica et Biophysica Acta - Protein Structure and Molecular Enzymology* 1339, 53–61. [https://doi.org/10.1016/S0167-4838\(96\)00214-2](https://doi.org/10.1016/S0167-4838(96)00214-2)
- Sottile, J., Shi, F., Rublyevska, I., Chiang, H.Y., Lust, J., Chandler, J., 2007a. Fibronectin-dependent collagen I deposition modulates the cell response to fibronectin. *Am J Physiol Cell Physiol* 293, 1934–1946. <https://doi.org/10.1152/ajpcell.00130.2007>
- Sottile, J., Shi, F., Rublyevska, I., Chiang, H.Y., Lust, J., Chandler, J., 2007b. Fibronectin-dependent collagen I deposition modulates the cell response to fibronectin. *Am J Physiol Cell Physiol* 293, 1934–1946. <https://doi.org/10.1152/ajpcell.00130.2007>
- Sun, C. bin, Teng, W. qi, Cui, J. tao, Huang, X. jun, Yao, K., 2014. The effect of anti-TGF- β 2 antibody functionalized intraocular lens on lens epithelial cell migration and epithelial-mesenchymal transition. *Colloids Surf B Biointerfaces* 113, 33–42. <https://doi.org/10.1016/j.colsurfb.2013.08.024>
- Tan, X., Zhan, J., Zhu, Y., Cao, J., Wang, L., Liu, S., Wang, Y., Liu, Z., Qin, Y., Wu, M., Liu, Y., Ren, L., 2017. Improvement of Uveal and Capsular Biocompatibility of Hydrophobic Acrylic Intraocular Lens by Surface Grafting with 2-Methacryloyloxyethyl Phosphorylcholine-Methacrylic Acid Copolymer. *Sci Rep* 7. <https://doi.org/10.1038/srep40462>
- Tanaka, T., Shigeta, M., Yamakawa, N., Usui, M., 2005. Cell adhesion to acrylic intraocular lens associated with lens surface properties. *J Cataract Refract Surg.* <https://doi.org/10.1016/j.jcrs.2004.11.050>
- Thom, H., Ender, F., Samavedam, S., Vivez, C.P., Gupta, S., Dhariwal, M., de Haan, J., O’Boyle, D., 2019. Effect of AcrySof versus other intraocular lens properties on the risk of Nd:YAG capsulotomy after cataract surgery: A systematic literature review and network meta-analysis. *PLoS One* 14. <https://doi.org/10.1371/journal.pone.0220498>
- Tortolano, L., Serrano, C., Jubeli, E., Saunier, J., Yagoubi, N., 2015. Interaction of intraocular lenses with fibronectin and human lens epithelial cells: Effect of chemical composition and aging. *J Biomed Mater Res A* 103, 3843–3851. <https://doi.org/10.1002/jbm.a.35528>
- Ursell, P.G., Spalton, D.J., Pande, M. v., 1997. Anterior capsule stability in eyes with intraocular lenses made of poly(methyl methacrylate), silicone, and AcrySof. *J Cataract Refract Surg.* [https://doi.org/10.1016/S0886-3350\(97\)80025-9](https://doi.org/10.1016/S0886-3350(97)80025-9)
- Ursell, P.G., Spalton, D.J., Pande, M. v., Hollick, E.J., Barman, S., Boyce, J., Tilling, K., 1998a. Relationship between intraocular lens biomaterials and posterior capsule opacification. *J Cataract Refract Surg* 24, 352–360. [https://doi.org/10.1016/S0886-3350\(98\)80323-4](https://doi.org/10.1016/S0886-3350(98)80323-4)
- Ursell, P.G., Spalton, D.J., Pande, M. V., Hollick, E.J., Barman, S., Boyce, J., Tilling, K., 1998b. Relationship between intraocular lens biomaterials and posterior capsule opacification. *J Cataract Refract Surg* 24, 352–360. [https://doi.org/10.1016/S0886-3350\(98\)80323-4](https://doi.org/10.1016/S0886-3350(98)80323-4)
- Ursell, P.G., Spalton, D.J., Pande, M. V., Hollick, E.J., Barman, S., Boyce, J., Tilling, K., 1998c. Relationship between intraocular lens biomaterials and posterior capsule opacification. *J Cataract Refract Surg* 24, 352–360. [https://doi.org/10.1016/S0886-3350\(98\)80323-4](https://doi.org/10.1016/S0886-3350(98)80323-4)

- Vanslyke, J.K., Boswell, B.A., Musil, L.S., 2018. Fibronectin regulates growth factor signaling and lens cell differentiation.
- Vasavada, A.R., Praveen, M.R., 2014. Posterior Capsule Opacification After Phacoemulsification. *Asia-Pacific Journal of Ophthalmology*.
<https://doi.org/10.1097/apo.0000000000000080>
- Vasavada, A.R., Praveen, M.R., Tassignon, M.J., Shah, S.K., Vasavada, Vaishali A., Vasavada, Viraj A., Van Looveren, J., De Veuster, I., Trivedi, R.H., 2011. Posterior capsule management in congenital cataract surgery. *J Cataract Refract Surg* 37, 173–193.
<https://doi.org/10.1016/j.jcrs.2010.10.036>
- Versura, P., 1999a. Adhesion mechanisms of human lens epithelial cells on 4 intraocular lens materials. *J Cataract Refract Surg* 25, 527–533. [https://doi.org/10.1016/s0886-3350\(99\)80050-9](https://doi.org/10.1016/s0886-3350(99)80050-9)
- Versura, P., 1999b. Adhesion mechanisms of human lens epithelial cells on 4 intraocular lens materials. *J Cataract Refract Surg* 25, 527–533. [https://doi.org/10.1016/s0886-3350\(99\)80050-9](https://doi.org/10.1016/s0886-3350(99)80050-9)
- Walker, B.N., James, R.H., Calogero, D., Ilev, I.K., 2014. Impact of environmental temperature on optical power properties of intraocular lenses. *Appl Opt*.
<https://doi.org/10.1364/ao.53.000453>
- Wang, G.Q., Dang, Y.L., Huang, Q., Woo, V.C.P., So, K.F., Lai, J.S.M., Cheng, G.P.M., Chiu, K., 2017. In Vitro Evaluation of the Effects of Intraocular Lens Material on Lens Epithelial Cell Proliferation, Migration, and Transformation. *Curr Eye Res* 42, 72–78.
<https://doi.org/10.3109/02713683.2016.1156133>
- Weed, B.C., Borazjani, A., Patnaik, S.S., Prabhu, R., Horstemeyer, M.F., Ryan, P.L., Franz, T., Williams, L.N., Liao, J., 2012. Stress state and strain rate dependence of the human placenta. *Ann Biomed Eng* 40, 2255–2265. <https://doi.org/10.1007/s10439-012-0588-2>
- Wejde, G., Kugelberg, M., Zetterström, C., 2003a. Posterior capsule opacification: Comparison of 3 intraocular lenses of different materials and design. *J Cataract Refract Surg* 29, 1556–1559. [https://doi.org/10.1016/S0886-3350\(03\)00342-0](https://doi.org/10.1016/S0886-3350(03)00342-0)
- Wejde, G., Kugelberg, M., Zetterström, C., 2003b. Posterior capsule opacification: Comparison of 3 intraocular lenses of different materials and design. *J Cataract Refract Surg* 29, 1556–1559. [https://doi.org/10.1016/S0886-3350\(03\)00342-0](https://doi.org/10.1016/S0886-3350(03)00342-0)
- Wejde, G., Kugelberg, M., Zetterström, C., 2003c. Posterior capsule opacification: Comparison of 3 intraocular lenses of different materials and design. *J Cataract Refract Surg* 29, 1556–1559. [https://doi.org/10.1016/S0886-3350\(03\)00342-0](https://doi.org/10.1016/S0886-3350(03)00342-0)
- Welch, N.G., Madiona, R.M.T., Easton, C.D., Scoble, J.A., Jones, R.T., Muir, B.W., Pigram, P.J., 2016. Chromium functionalized diglyme plasma polymer coating enhances enzyme-linked immunosorbent assay performance. *Biointerphases* 11, 041004.
<https://doi.org/10.1116/1.4967442>
- Werner, L., Mamalis, N., Pandey, S.K., Izak, A.M., Nilson, C.D., Davis, B.L., Weight, C., Apple, D.J., 2004. Posterior capsule opacification in rabbit eyes implanted with hydrophilic acrylic intraocular lenses with enhanced square edge. *J Cataract Refract Surg* 30, 2403–2409. <https://doi.org/10.1016/j.jcrs.2004.02.085>
- Wormstone, I.M., 2020. The human capsular bag model of posterior capsule opacification. *Eye (Basingstoke)* 34, 225–231. <https://doi.org/10.1038/s41433-019-0680-z>
- Wormstone, I. Michael, Damm, N.B., Kelp, M., Eldred, J.A., 2021a. Assessment of intraocular lens/capsular bag biomechanical interactions following cataract surgery in a human in vitro

- graded culture capsular bag model. *Exp Eye Res* 205, 108487.
<https://doi.org/10.1016/j.exer.2021.108487>
- Wormstone, I. Michael, Damm, N.B., Kelp, M., Eldred, J.A., 2021b. Assessment of intraocular lens/capsular bag biomechanical interactions following cataract surgery in a human in vitro graded culture capsular bag model. *Exp Eye Res* 205, 108487.
<https://doi.org/10.1016/j.exer.2021.108487>
- Wormstone, I.M., Eldred, J.A., 2016a. Experimental models for posterior capsule opacification research. *Exp Eye Res* 142, 2–12. <https://doi.org/10.1016/j.exer.2015.04.021>
- Wormstone, I.M., Eldred, J.A., 2016b. Experimental models for posterior capsule opacification research. *Exp Eye Res* 142, 2–12. <https://doi.org/10.1016/j.exer.2015.04.021>
- Wormstone, I.M., Eldred, J.A., 2016c. Experimental models for posterior capsule opacification research. *Exp Eye Res* 142, 2–12. <https://doi.org/10.1016/j.exer.2015.04.021>
- Wormstone, I. M., Wormstone, Y.M., Smith, A.J.O., Eldred, J.A., 2021. Posterior capsule opacification: What’s in the bag? *Prog Retin Eye Res*.
<https://doi.org/10.1016/j.preteyeres.2020.100905>
- Xia, J., Lu, D., Han, Y., Wang, J., Hong, Y., Zhao, P., Fang, Q., Lin, Q., 2021. Facile multifunctional IOL surface modification via poly(PEGMA-co-GMA) grafting for posterior capsular opacification inhibition. *RSC Adv* 11, 9840–9848.
<https://doi.org/10.1039/d1ra00201e>
- Xu, X., Tang, J.M., Han, Y.M., Wang, W., Chen, H., Lin, Q.K., 2016a. Surface PEGylation of intraocular lens for PCO prevention: An in vivo evaluation. *J Biomater Appl*.
<https://doi.org/10.1177/0885328216638547>
- Xu, X., Tang, J.M., Han, Y.M., Wang, W., Chen, H., Lin, Q.K., 2016b. Surface PEGylation of intraocular lens for PCO prevention: An in vivo evaluation. *J Biomater Appl* 31, 68–76.
<https://doi.org/10.1177/0885328216638547>
- Yang, N., Zhang, D.D., Li, X.D., Lu, Y.Y., Qiu, X.H., Zhang, J.S., Kong, J., 2017. Topography, Wettability, and Electrostatic Charge Consist Major Surface Properties of Intraocular Lenses. *Curr Eye Res* 42, 201–210. <https://doi.org/10.3109/02713683.2016.1164187>
- Yu, M., Huang, Y., Wang, Y., Xiao, S., Wu, X., Wu, W., 2021. Three-dimensional assessment of posterior capsule–intraocular lens interaction with and without primary posterior capsulorrhexis: an intraindividual randomized trial. *Eye* 1–7.
<https://doi.org/10.1038/s41433-021-01815-4>
- Yu, S.-S., Guo, Y.-W., Zhao, Y., Yuan, X.-Y., 2021. Anterior segment OCT application in quantifying posterior capsule opacification severity with varied intraocular lens designs. *Int J Ophthalmol* 14, 1384–1391. <https://doi.org/10.18240/ijo.2021.09.13>
- Zhao, Y., Yang, K., Li, J., Huang, Y., Zhu, S., 2017a. Comparison of hydrophobic and hydrophilic intraocular lens in preventing posterior capsule opacification after cataract surgery An updated meta-analysis. *Medicine (United States)*.
<https://doi.org/10.1097/MD.00000000000008301>
- Zhao, Y., Yang, K., Li, J., Huang, Y., Zhu, S., 2017b. Comparison of hydrophobic and hydrophilic intraocular lens in preventing posterior capsule opacification after cataract surgery An updated meta-analysis. *Medicine (United States)*.
<https://doi.org/10.1097/MD.00000000000008301>
- Ziebarth, N.M., Arrieta, E., Feuer, W.J., Moy, V.T., Manns, F., Parel, J.M., 2011. Primate lens capsule elasticity assessed using Atomic Force Microscopy. *Exp Eye Res*.
<https://doi.org/10.1016/j.exer.2011.03.008>

BIOGRAPHICAL INFORMATION

Joyita Roy grew up in a small town called Ranchi, located in the eastern side of India. Due to her interest in the field of biology, Joyita moved to New Delhi to pursue her undergraduate studies in Biotechnology at Amity University, Noida, in the year 2013.

Joyita was enrolled in a 5-year BS/MS program, during which she did five internships. One of her significant internships was at the Advanced Center for Treatment, Research and Education in Cancer (ACTREC), Navi Mumbai, where she studied the activity of the Akt molecule in IGF1R signaling pathway using A2780 ovarian epithelial cancer cells. She also learnt about cell culture and tissue culture techniques during her training, which influenced her to pursue a higher education in tissue engineering. Joyita graduated with her Bachelor and Master of Engineering degree in Biotechnology in May 2018, soon after which she moved to the United States with a goal to attain a PhD.

Joyita received a STEM scholarship from The University of Texas at Arlington and started her PhD in Biomedical Engineering, with specialization in Tissue Engineering. Joyita accepted a position in Dr. Liping Tang's lab and continued under his mentorship till she graduated. During the first three years of her program, she thoroughly enjoyed her time as a Teaching Assistant where her job was to teach the students how to digitally design biomedical implants and devices. After assisting different projects in the lab, Joyita started her thesis work on cataract research, focusing on Posterior Capsule Opacification, where she developed a novel 3D in vitro model to study the intraocular lens and lens capsule interactions on lens epithelial cell responses. By collaborating with other members of the lab and constant advise from Dr. Tang, Joyita was able to successfully complete her dissertation. Joyita feels extremely honored and fortunate that she was chosen to be a part of a research team with talented scientists and great minds. She is very

excited to use the skills she learned as a doctoral student in the next phase of her professional life.

In her personal life, Joyita has always been inclined towards music, art and dance. She has received years of professional training as a vocalist in Indian classical music and has performed at various musical events. She can play many musical instruments, with guitar being her favorite. Joyita has a passion for cooking and likes to try different cuisines, and also enjoys watching movies at the theater with her fiancé. She loves to spend time with her parents and little brother, go on family vacations and explore new places together.